NTNU

Norwegian University of
Science and Technology

Model for evaluating drilling efficiency based on the concept of Mechanical Specific Energy

Paal Vegar Berg
Øyvind Sæther Tveit

Petroleum Geoscience and Engineering
Submission date: June 2016
Supervisor: Pål Skalle, IPT
Co-supervisor: Isak Swahn, IPT
Sigve Hovda, IPT

Norwegian University of Science and Technology
Department of Petroleum Engineering and Applied Geophysics

Acknowledgement

This report is a master thesis in Drilling Engineering, at the department of Petroleum Engineering and Applied Geophysics (IPT) at the Norwegian University of Science and Technology (NTNU).

To begin with, we would like to express our sincere gratitude to our supervisor, Professor Pål Skalle, for his guidance and encouragement while working on this thesis. His knowledge within drilling engineering has been of utmost importance for us.

Secondly, we would like to thank Dr.Eng. Tommy Toverud for assistance on technical matters, especially with regard to programming of the agent.

We would also like to show our thankfulness to Professor Sigbjørn Sangesland and Assistant Professor Bjørn Astor Brechan.

Lastly, we would like to thank each other for the team-work and the dedication shown during this semester, and our fellow students for help and support throughout the period of the master thesis.

Paal Vegar Berg and Øyvind Sæther Tveit

Trondheim, June 2016

Sammendrag

For å utføre mer kostnads-effektive brønnoperasjoner, er systemer for å øke effektiviteten under boring ønskelig. Denne masteroppgaven undersøker muligheten ved å presentere ny informasjon som illustrerer effektiviten under boring, basert på allerede eksisterende data som er tilgjengelig for de fleste brønnoperasjoner.

Basert på ideen om Mekanisk Spesifikk Energi, presentert av Teale (1965), har det blitt gjort et forsøk på å korrigere og forbedre denne metoden til å bedre illustrere den faktiske boreeffektiviteten som foregår nedihulls. Gjennom arbeid med denne metoden ble det hovedsakelig identifisert tre svakheter. Den originale metoden tar ikke hensyn til hydraulisk energi, estimerer ikke faktisk energi tap, og tar ikke hensyn til formasjonens hardhet. Disse tre aspektene ble dermed utarbeidet, og står for de største endringene ved den nye metoden.

For å teste den nye metoden, og gjøre den kompatibel med de data som oftest er tilgjengelig, ble det utarbeidet en matematisk agent i MATLAB. Til nå har metoden blitt testet på data fra tre seksjoner av en brønn lokalisert i Nordsjøen. På grunn av begrenset tilgang på boredata var det vanskelig å trekke noen ordentlig konklusjon på modellens effektivitet, men noen mønster ble identifisert.

Resultatene viste at metodene identifiserer hoveddelen av arbeidet utført under boring som roterende energi. Ved å mer nøyaktig evaluere den faktiske energien som overføres til formasjonen, vil resultatet fra modellen være til større nytte for boremanskapet. Resultater viste også at å inkludere hydraulisk energi var nødvendig, da denne utgjorde for mye av samlet total energi til å bli neglisjert. Dette til tross for at metoden blir noe mer komplisert. En av de største utfordringene viste seg å være innhenting av informasjon som omhandlet endringer i effektivitet basert på formasjonshardhet. Dette problemet oppsto da metoden som ble brukt til å estimere tilført energi og formasjonshardhet var for avhengig av samme skalar, ROP. For framtidig arbeid vil en metode som baserer seg på UCS trolig være best egnet til å beregne hardhet. Framtidig arbeid bør også arbeide videre med metoder for å effektivt identifisere bakgrunnen til ineffektivitetene, da dette ikke er grundig nok gjennomgått i denne oppgaven.

Summary

Systems to increase efficiency during drilling is desirable in order to have more cost-effective well operations. This master's thesis studies the possibility to present new information real-time regarding the actual drilling efficiency, based on already existing data commonly available during most operations. Said data should not only help increase efficiency, but also help identify insufficiencies, and be used when evaluating if re-modelling of the drillstring is profitable to improve efficiency.

Based on the concept of Mechanical Specific Energy presented by Teale (1965), an attempt has been made to adjust and improve this method to present the actual drilling efficiency down-hole in a better way. During work with this method, three main insufficiencies were identified. The original method does not include hydraulic energy, does not estimate actual energy loss, and does not account for formation hardness. These three problems were the cause of the largest alterations.

To test the new method, and to make it compatible with the data usually available, a mathematical agent was modelled in Matlab. The method has so far been tested on drilling data from three sections of a well located in the North Sea. Due to a limited amount of available drilling data, no real conclusions could be made. Nevertheless, some patterns were identified.

Results show, that the current method identifies most of the work used for drilling progress as rotational energy. By more accurately evaluating the actual energy reaching the formation, the actual drilling efficiency will be of more use for the driller. Evaluation of hydraulic energy showed that while these extensions make the method more complicated, hydraulic energy contribution is too large to be considered negligible. Data regarding how the formation hardness affects the drilling efficiency was proven difficult to achieve, as the correlation between the method chosen to specify energy input and formation hardness were considered too large to be a reliable source of information. For future work, a method based on the Unconfined Compression Strength would probably prove more beneficial. Further work with this model should also focus on proper identification of sources of inefficiencies, as this was not thoroughly addressed in present thesis.

Contents

1 Introduction

In 2014, operating costs on the Norwegian shelf amounted to NOK 64 Billion, distributed over 78 producing fields. For an industry affected by low oil prices, new approaches and solutions are needed to face increasingly tougher competition in the market. The upheaval caused by the sudden drop in oil prices changed the premises of the market, and the focus went from producing as much as possible regardless of cost, to producing with as low cost as possible.

Currently, the most common method in the industry to identify optimal drilling parameters for efficiency is a drill-off test. The weakness of this method is the lack of adaption in accordance with further progress. This means that the results provided become less reliable as the operation progresses.

In the 60s, Teale (1965) introduced the term Mechanical Specific Energy (MSE) as a measure of drilling efficiency. MSE is defined as the ratio between input energy and volume of removed formation in a drilling process. Monitoring and adjusting the drilling process according to MSE is believed to increase efficiency and safety during drilling by providing a new source of information, based on already available data. A number of companies have had trial runs, many of which have shown promising results. In 2005, ExxonMobil decided to implement MSE in their global organisation, resulting in $54M saved, still maintaining their solid safety record (Hamrick 2011). The rest of the market have yet to follow, because while MSE has its advantages, there are still a few uncertainties linked to some of its aspects. The main downside of the current MSE concept seems to be lack of evaluation, i.e. evaluating MSE with regard to hydraulic specific energy, formation hardness, and loss of torque and drag along the drillstring.

Based on a theoretical study on the already existing models of MSE, this thesis aims at improving the MSE-method by accounting for the influence torque and hydraulic have on MSE. Eventually, it may prove to be an effective tool to help meet the demand for more cost-effective well operations. In order to achieve this, identification and evaluation of both the strengths and weaknesses of this method will be performed, in addition to focusing on limiting some of the problems faced today by the use of MSE. The main objective will be to solve the deficiency in information regarding formation hardness. This will make the driller more aware of the actual efficiency, but also make it easier to identify real sources of inefficiency.

The results will be used in the development of a new mathematical model for actual drilling efficiency, which will be implemented into a MATLAB-agent, and tested on data from a well in the North Sea. The future aim for the agent is to be compatible

with Real-Time Drilling Data (RTDD). This will enable it to serve as a tool for both optimizing input energy during the drilling processes, and for evaluating the profitability of re-modelling the drillstring, i.e. whether or not it is economically expedient to retract the drillstring to re-model the BHA.

2 Previously published knowledge

2.1 Drilling efficiency in general

Efficiency during drilling is an important part of cost saving measures. Drilling for petroleum purposes is a complex system, and relies on many different factors such as bit size, bit efficiency, torque, WOB, RPM, flowrate, mud rheology and formation hardness, etc. This makes the task of achieving and maintaining high ROP a challanging task, requiring more than just supplying the drillstring with sufficient power.

2.1.1 Current method to evaluate drilling efficiency

The most common method in the industry today is the trial-and-error concept, known as a drill-of test. This method is conducted by applying a number of different WOBs and RPMs, to see which combination the ROP responds to the best. Depending on the conditions, there are two different types, the active- and the passive method (Guerrero 2007).

The active method is best used for fast drilling conditions, and is conducted by starting drilling at the minimum recommended WOB. The weight is then increased by increments of 1000 kg until the ROP no longer responds positive to the added weight. This test is conducted for different RPMs, and constant flowrate.

The passive drill-off test is best used for slow drilling conditions. Here the driller starts at 80 percent of max WOB. The driller then locks the break and starts drilling at a constant RPM. At 80 percent of maximum recommended WOB, the drillstring will be compressed, but as the bit drills forward and no more drillstring is lowered into the well, the WOB will reduce. During further drilling, the compression stress will approach zero at the end of the drillstring. The test for this specific RPM is complete when the WOB goes towards zero due to the elongation of the string. This test is conducted for different RPMs, resulting in a continuous curve for ROP vs WOB, as shown in Fig. 1.

2.1.2 Founder point

As seen from Fig. 1, the curves at different RPMs follow a specific pattern consisting of three regions. At low values of WOB, the curve tends to be flat. At this point, the ROP does not respond to the additional energy input from increasing the WOB. The threshold compression strength of the formation has yet to be reached, and only rock fines and powder are produced (Pessier and Fear 1992). The second region is identified by a linear increase in ROP. In this region, the bit works at its maximum efficiency, and an increase in input energy results in a proportional increase in ROP. All systems

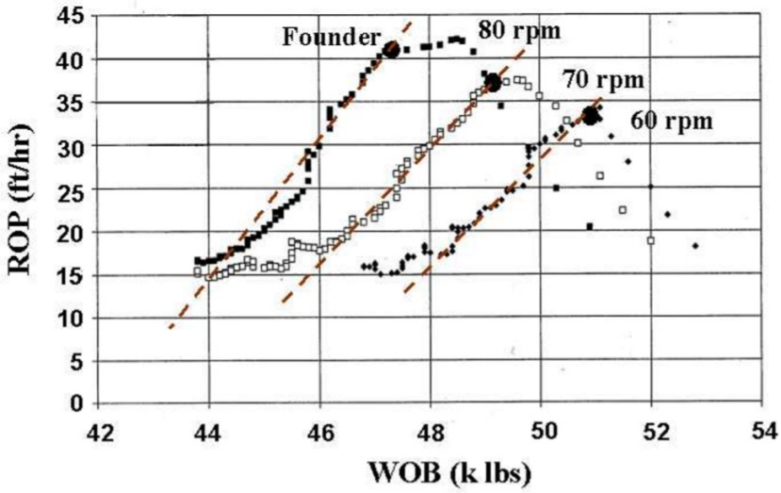

Figure 1: ROP vs. WOB on the resulting plot of a drill-off-test. The characterizing curves are shown for 80, 70 and 60 rpm (Dupriest and Koederitz 2005).

exhibit this type of curve, and every system has its limit. At one point, the curve starts to flatten out, and the increase in input energy no longer increases the ROP. This is known as the founder point of the system.

The founder point indicates that the system has reached its limit, and that increased input energy is hindered from being transferred to the formation by one of many factors. The founder point also indicates that the system has reached the highest possible ROP, and further increasing the input energy will bring the operation into region three; a region of drilling inefficiency. At this point, the driller needs to embrace this speed of progress as acceptable, or identify the cause of founder and recomplete the system accordingly. The most common reasons of founder are vibrations, bit balling and bottom hole balling.

It is important to understand that every system has its point of founder. By identifying and re-completing the limiting factor, the point at which the founder occurs will increase only until the next limiter appears. It is therefore important to identify not only the current cause of founder, but also the probable increase in efficiency that could be achieved by changing the system. Then evaluate the cost of recompleting the system versus the benefit of probable time saved. Fig. 2 illustrates how recompleting the system can affect the point of founder.

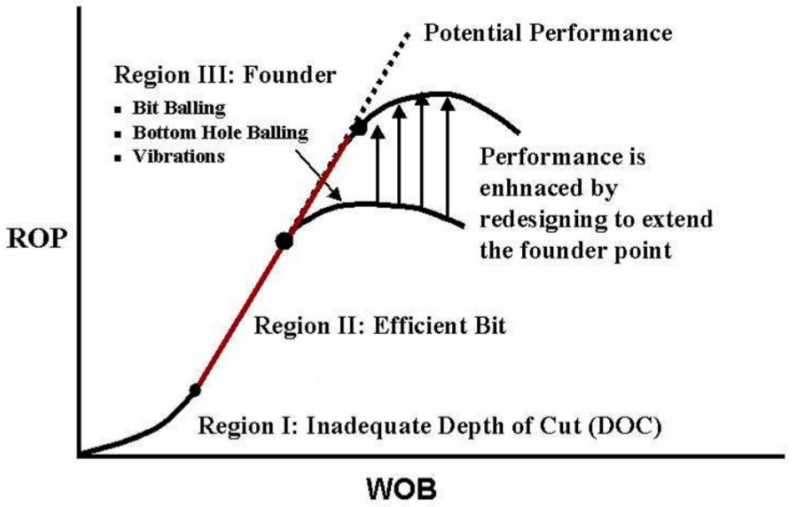

Figure 2: The three regions of efficiency during drilling (Dupriest and Koederitz 2005).

2.1.3 Causes of inefficiency

During work with drilling efficiency, more than 40 different categories of penetration limiters were identified (Dupriest 2006). Out of these 40 categories, only 4 categories were directly related to the bit. All these penetration limiters can be divided into two groups. The first group includes factors that limit input energy. These types of problems are usually caused by insufficient equipment, and are often too expensive to repair. This could be rig-limits such as insufficient rig top drive or rotary torque. The problem could also be caused by other limits, like insufficient drillstring make-up torque, weight of the drill-collars, bit durability, hole cleaning or directional targeting control. Stated problems limit the system to the second part of the drill-off curve, and the system will not reach a characteristic founder point, as it does not have, or is prevented from applying, sufficient energy.

The second category includes factors that create inefficiency or founder. These factors prohibit the energy from being properly transferred to the formation, causing a large portion of the input energy to go to waste. The most common problems are bit balling, bottom hole balling and vibrations.

Bit balling

Bit balling is a common issue when drilling in clay stone and shale formations, and will result in reduced efficiency for the drilling progress. Bit balling, as shown in Fig. 3, comes from the accumulation of materials within the cutting structure of the bit, and can happen at any time during drilling.

Figure 3: Accumulated materials within the cutting structure of the bit (Drillingformulas 2014).

Bit balling is commonly identified by reduced ROP, reduced torque and increased Standpipe Pressure (SPP) as the materials hinder the flow of fluid through the passage between the well-bore wall and the balled bit. The chance of bit balling can be limited by avoiding too high WOB, and too high hydrostatic pressure in the wellbore. If bit balling is expected, small junk slot area in PDC bit should be avoided. For rock bits, steel tooth bits are preferred. It is also important that the bit nozzles are not extended, and that the center jet is not blocked. The centre jet is important for efficiently flushing the accumulated materials (Drillingformulas 2014).

If the problem has already occurred, the operation should be stopped until the issue is resolved. The problem is most commonly solved by increasing RPM and mud flowrate, while simultaneously lowering the WOB. In some cases, pumping of a high viscosity pill might be necessary. A reduction in SPP indicates that the removal of debris has created a clear path.

Bottom hole balling

Another common problem is bottom hole balling. This problem is mostly experienced when hard formation bits grind, creating finer particles, which in turn clog the hole. This is commonly associated with the term chip hold down effect, where the particles broken loose from the formation are held in place by differential pressure, making them difficult to move. Fig. 4 shows a chip as it is held in place by the pressure exerted by the mud.

Bottom-hole balling is usually identified by reduced ROP and reduced torque, differing

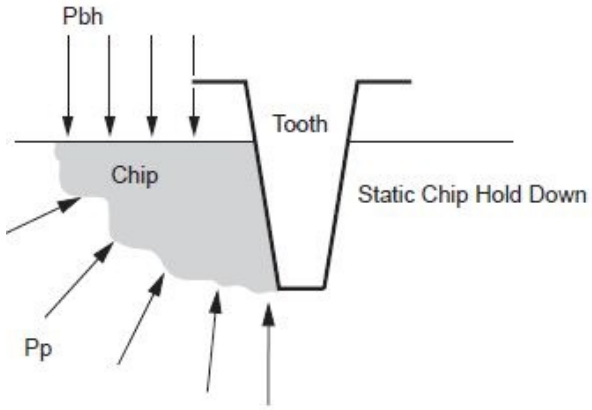

Figure 4: The chip is kept in place by the differential pressure between bottom hole pressure and pore pressure (Petroleumsupport 2015).

from bit balling by no change in stand-pipe pressure. Bottom hole balling could be avoided by increasing the hydraulic horsepower, and avoiding the use of an insert bit.

Vibrations

Vibrations in the drillstring is a common cause for drilling inefficiency. Vibrations usually occur when one or more of the following factors are present; lithological transitions, use of under-reamer, poor BHA design and/or poor parameter management (Abbott 2014), usually in combination with high WOB and relatively high RPM. The most common problems associated with vibrations are complications causing additional stress to both the wellbore and the drillstring (Ahmadi and Altintas 2011). This type of stress could cause severe fatigue and damage to the drillstring over time, resulting in tool failure and an additional re-trip. This is expensive for the operation in terms of both time and and cost. Continuous stress to the wellbore often results in reduced wellbore surface quality making additional obstacles during tripping and circulation.

Vibrations could be detected by reduced ROP, but are also some times measured by sensors tracking in real-time. Vibrations can be divided in to three different categories as illustrated in Fig. 5.

Axial vibrations, also known as bit bounce, are vibrations along the trajectory of the wellbore. This type of vibration mostly affects the bit cutters and the bearings (Slb 2010), but also prevent energy from being efficiently transferred to the formation.

Stick and Slip vibrations happens when a part of the drillstring intermittent gets stuck at high frequency, while the part of the drillstring above the stuck section keeps rotating.

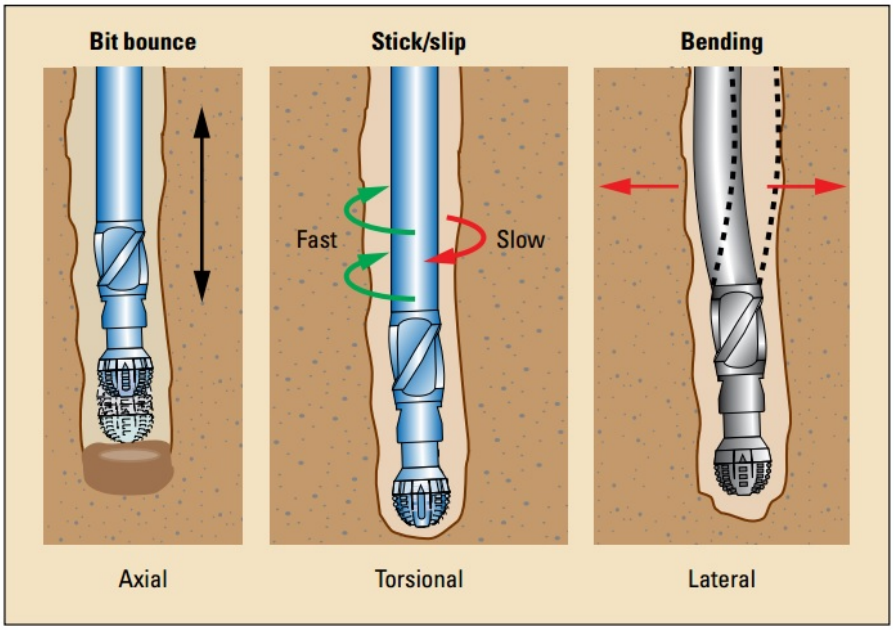

Figure 5: Three different types of vibrations acting on the drillstring (Slb 2010).

The drillstring then gather potential energy as the string itself gets twirled. At one point the torque becomes too high for the wellbore to hold, and the formation lets go of the drillstring. The drillstring will then rotate rapidly as the torsional energy is released. If the problem is not solved the drillstring will once again go stuck until enough energy once again is worked up. This type of vibrations cause fatigue to drill collar connections, but may also damage the bit.

The most harmful type of vibrations are the lateral vibrations. Here the drillstring move in a circular motion around the larger diameter of the wellbore. This type of behaviour damages the surface of the wellbore, but can also cause severe fatigue to the drillstring components. Lateral vibrations may come as backward whirl and forward synchronous, differencing at what direction the rotary motion against the wellbore occurs. This is illustrated in the Fig. 6.

When identifying vibrations as the problem, the driller should reduce WOB and stay below the critical RPM. If this does not help, the string-design should be re-evaluated.

2.2 Mechanical Specific Energy (MSE)

Teale (1965) introduced the concept of MSE. Specific energy, or energy density is defined to be a measure of the work done to remove one unit volume of material. The purpose

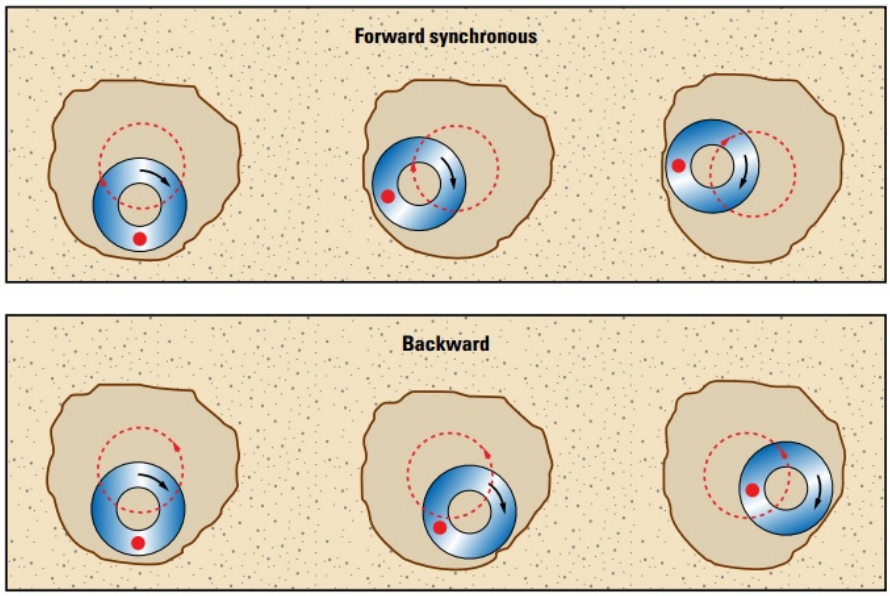

Figure 6: Lateral vibrations (Slb 2010).

of this method is to properly present information regarding the efficiency of the drilling process. While there has been a lot of research on the subject since then, the concept was not properly introduced to the market until ExxonMobil implemented a trial run in 2005 to improve their operation efficiency (Dupriest 2005). The outcome exceeded their expectations. By use of MSE on six of their rigs over a period of three months, the ROP was increased by 133 percent, and new field records were established on 10 of 11 wells. After one year, the concept was implemented in the entire global organisation. This resulted in several positive outcomes, substantial cost-savings for global operations being among those. During the next year the organisation reported to have saved $54 million, sat 50 new drilling records, while one of the most solid safety records in the industry was preserved (Hamrick 2011).

2.2.1 The model

MSE quantifies the ratio between the mechanical energy input from the rig, and the responding ROP. The formula derived by Teal is given as:

$$\text{MSE} = \frac{\text{Input energy}}{\text{Output ROP}} \tag{1}$$

From Eq. 1, one can conclude that a low MSE value is preferred, as it means that a large volume of rock is removed per unit energy input, something that indicates an

efficient operation. The mechanical input energy consist of two forces, the axial force and the rotational force. By definition, rotational work is given as torque, times the rotation angle, while the axial work is given as force, times distance. For the drilling process, the axial force is given as the WOB that pushes the cutting edges of the bit into the rock, and the rotational force that creates a circular motion that breaks free fragments of the rock of varying sizes. The volume removed per unit time may be expressed as the cross-sectional area of the bit times the ROP. Formulated in Eqs. 2 and 3 (Hamrick 2011):

$$\text{MSE} = \frac{\text{Vertical energy input per time}}{\text{Volume removed per time}} + \frac{\text{Rotational energy input per time}}{\text{Volume removed per time}} \tag{2}$$

Inserting expressions for all of the terms yields:

$$\text{MSE} = \frac{\text{WOB} \cdot \Delta h}{\text{Area} \cdot \Delta h} + \frac{2\pi \cdot \text{Torque} \cdot \#\text{Rotations per time}}{\text{Area} \cdot \Delta h} \tag{3}$$

Where Δh is change in measured depth per time.

Teale then derived the following formula based on commonly available real-time drilling data.

$$\text{MSE} = \frac{\text{WOB}}{\text{Area}} + \frac{2\pi \cdot \text{Torque} \cdot \text{RPM}}{\text{Area} \cdot \text{ROP}} \tag{4}$$

Other methods have also been presented. Based on the assumption that the parameters WOB, torque and ROP are interrelated to each other, and that the relationship between WOB and torque can be described as linear in a normal processing range, Hamrick (2011) worked on a theory of expressing MSE based solely on WOB and constants.

2.2.2 MSE efficiency formula

During drilling, much energy will be lost in the transaction between bit and formation. Even under perfect conditions, the bit will only be able to deliver 30-40 percent of the input energy into further progress (Dupriest 2005), illustrated in Fig. 7. This was also tested by (Pessier and Fear 1992), where comparing different bits in a full scale simulator proved that while a PDC-bit can drill with less WOB due to three to five times greater sliding friction than the roller cone bit, it experiences the same magnitude additional torque, and they both end up with an efficiency of close to 30 percent. Other reasons for this high loss of energy, are factors like friction between the bit components and unnecessary torque.

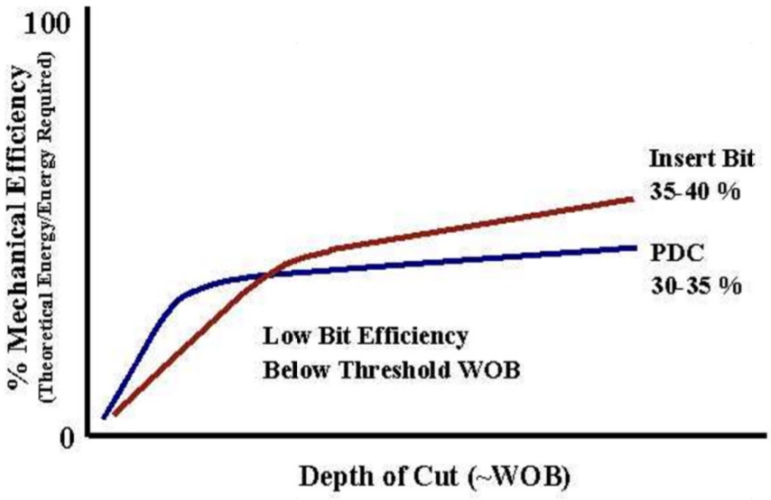

Figure 7: Bit efficiency vs. Depth of cut (Dupriest 2005).

Even though the bit efficiency factor is known to vary between 30 and 40 percent, the standardization is set to 35 percent for most operations. The MSE-efficient formula then becomes:

$$\text{MSE} = \text{Bit efficiency factor} \cdot \left(\frac{\text{WOB}}{\text{Area}} + \frac{2\pi \cdot \text{Torque} \cdot \text{RPM}}{\text{Area} \cdot \text{ROP}} \right) \tag{5}$$

While downhole data during drilling has become more common, the majority of drilling data is still measured from surface. This means that the energy delivered at the bit is not of the same scale as the energy supplied and measured. Common transmission losses are illustrated in Fig. 8.

Energy lost along the drillstring is usually approximated by simply adding an additional efficiency factor, i.e. a Loss efficiency factor. This factor is set on a scale from 0 to 1, and is meant to exclude the lost energy due to transmission losses along the well path, such as drag and vibrations. The MSE-efficient formula then becomes

$$\text{MSE} = \text{Total efficiency factor} \cdot \left(\frac{\text{WOB}}{\text{Area}} + \frac{2\pi \cdot \text{Torque} \cdot \text{RPM}}{\text{Area} \cdot \text{ROP}} \right) \tag{6}$$

Total efficiency is the product of Bit efficiency and Loss efficiency.

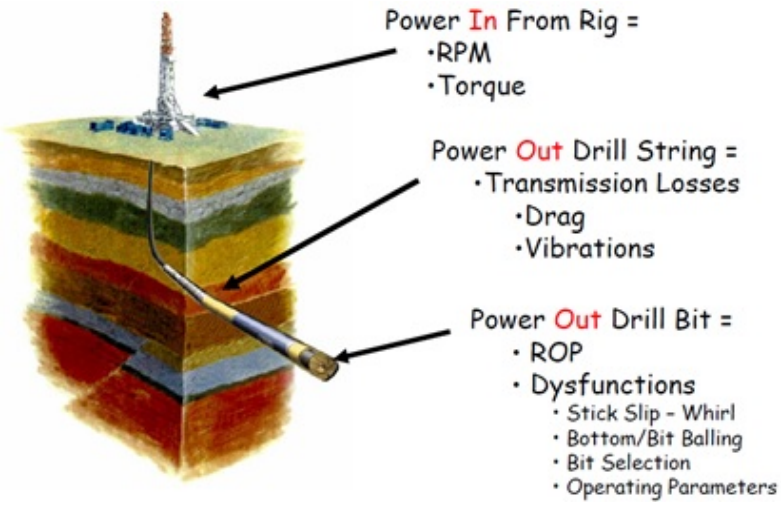

Figure 8: Transmission losses along the drillstring (Abbott 2014).

2.2.3 Application of MSE during operation

MSE is primarily used as a trending tool. This means that the specific value of the MSE curve is of less importance than the trend. As mentioned earlier, each section often starts with a drill-off test to identify the optimal parameters for this formation in combination with this drillstring setup. From this information, the driller can calculate the new-bit-MSE (Guerrero 2007). The new-bit-MSE is the optimal MSE available for this system, and should be identified at the start of the section. This is because, at this point, the bit is still sharp, and should be able to achieve optimal performance. The new-bit-MSE will then be the lowest possible MSE for this system, and all future drilling should be evaluated against this value.

When new-bit-MSE is identified, a trend-line should be established. The trend-line is assumed to increase linearly with elapsed time, as illustrated in Fig. 9. The need of higher mechanical input energy is mainly caused by three factors; bit dullness, formation compaction and additional drag due to increased well depth.

The driller should work to keep the MSE as close to the trend-line as possible, as this should be the optimal performance. If the MSE increases above this line, the problem needs to be identified and proper measures needs to be implemented. To identify the reason behind the occurring founder, all the parameters need to be evaluated. As mentioned in section 2.1.3, different causes of inefficiency affect different parameters, making it possible to diagnose the problem to a certain degree. In most cases, this problem may be solved by simply adjusting input parameters. Table 1 represent four different scenarios of inefficiency, where changes in different parameters are indications

of specific problems. Suggested counter-measures are also listed.

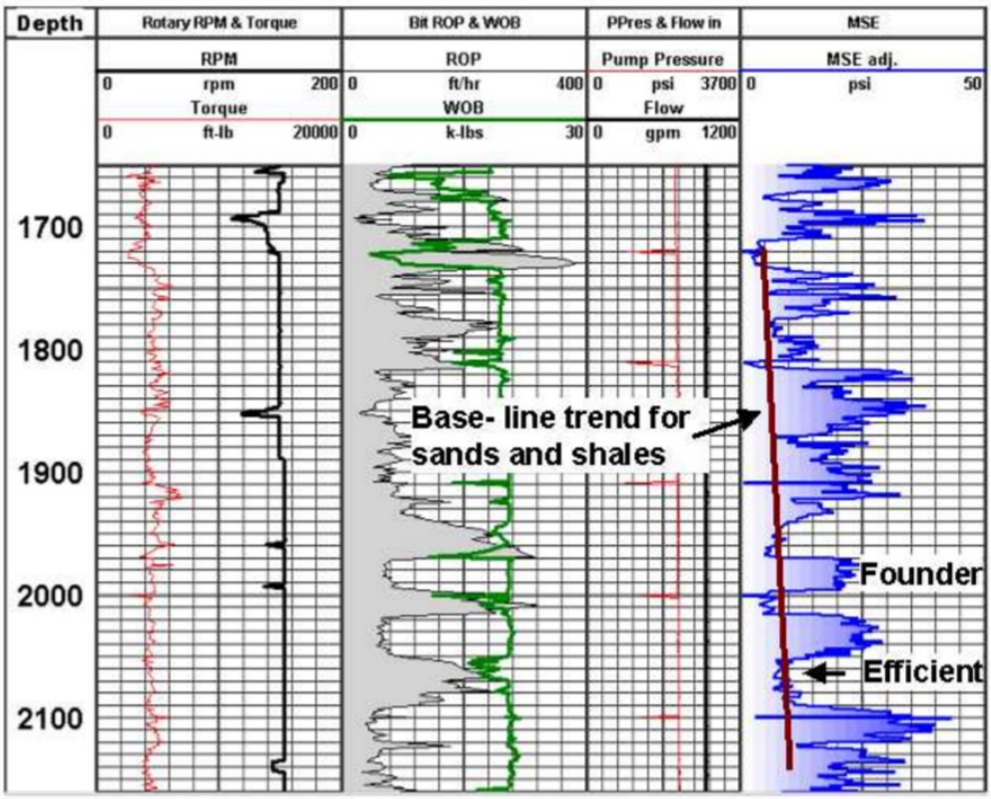

Figure 9: MSE vs. depth. New-bit trend-line indicated with red (Dupriest 2005).

Table 1: MSE troubleshooting. The different parameters and corresponding discrepancies for different scenarios (Krueger et al. 2012).

Parameters	**Scenario 1**	**Scenario 2**	**Scenario 3**	**Scenario 4**
RPM	Normal	Normal	Normal	Normal
Torque	Normal	Normal	Normal	Large variations
WOB	Normal	High	Normal	Large variations
Mud flow	Normal	Normal	Normal	Normal
Vibrations	Normal	Normal	Lateral	Impact-like torsional changes
MSE	High	Very high	High and varying	High and varying
Problem	Bit balling	Inadequate bottomhole cleaning	Lateral vibrations	DS Buckling
Action	Adjust hydraulics	Adjust hydraulics	Increase WOB, reduce RPM	Reduce WOB

Still, during optimal performance by the driller, ROP may not be as high as expected, and an increase of ROP is required. As explained in section 2.1.3, optimal ROP is not always possible to obtain through altering the input values of energy. If this problem arises, the entire system needs to be re-evaluated according to the identified cause. Re-evaluation should be done according to a cost-benefit evaluation, to determine if the lost time and resources to recomplete the system is worth the expected increase in ROP for the remaining part of the current section.

2.2.4 Input data for MSE

Since MSE mainly is a new way of displaying information based on already existing data, different parameters need to be available for use of this concept. During later years, a number of different MSE-methods have been derived to include different types of parameters. For the most common concept, the following parameters are required:

WOB	Weight On Bit [lbf]
RPM	Revolutions Per Minute [min^{-1}]
Torque	Rotational torque [in-lb] or [ft-lb]
Area	Cross-sectional area of bit [in^2] or [ft^2]
ROP	Rate Of Penetration [in/h] or [ft/h]

These are all the parameters needed to compute MSE. Still additional info should be available to take proper use of the method. Data regarding bit dulling and bit efficiency could help improve the accuracy of the bit efficiency factor. For evaluating loss along the drillstring, parameters like mud weight, downhole vibrations and friction should be available, or the problem could be avoided by measuring values downhole. At the start of each section, a drill-off test should be conducted. This provides vital information regarding the current optimal parameters, and could be used to set a trending curve for the rest of the operation as mentioned in the previous subchapter.

2.2.5 Cases with MSE

As mentioned in section 2.2, the concept of MSE was investigated by ExxonMobil in 2004, to see if it could be a useful tool for rig-site personnel. The pilot program included six rigs over a period of three months. MSE was used to evaluate drilling efficiency in real-time. The two biggest improvements recognized were easy identification of optimal drilling parameters, and providing quantitative data to cost-justify changes to

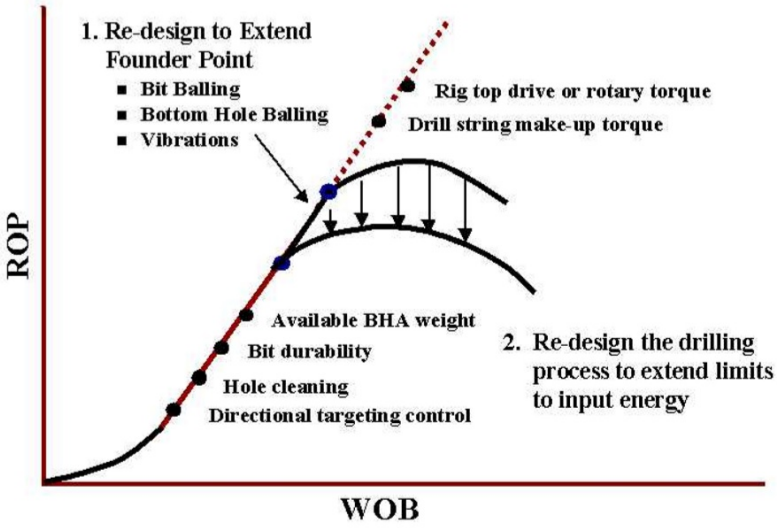

Figure 10: Potential efficiency. Shows how redesigning the system can postpone the founder-point (Dupriest 2005).

the drillstring design to postpone the founder point of the current system, as shown in Fig. 10.

During the program, MSE analysis justified changes in areas like BHA design, bit selection, make-up torque, directional target sizing and motor differential ratings. The program as a whole resulted in an increase of 133 percent for the average ROP, and field records were set on 10 out of 11 wells.

Amadi et al. (2012) released a paper with Schlumberger regarding MSE used for cost reduction through prediction of optimum ROP using historical drilling data. The calculations and illustrations were completed after the well was actually completed, so the gathered data was not used during operation. The investigated area reached across four formations labelled F4, F5, F6 and F7, from 7400 ft to 10600 ft. During the post-drilling investigation, UCS-logs were also available and used during examination, and is therefore available in the plot below. MSE was calculated at intervals of one foot, and reported at every ten feet, as shown in Fig. 11. Eq. 6 was used for MSE calculations. An efficiency factor of 0.125 was used in order to account for bit efficiency and lost energy.

The efficiency of the operation varies, visible as fluctuations in the black graph on the lower plot. At some points, including the area from 7500-8000 ft the MSE values are almost identical to the UCS values. At this point, the drilling is operating under optimal performance. During other parts of the operation, the efficiency is reduced.

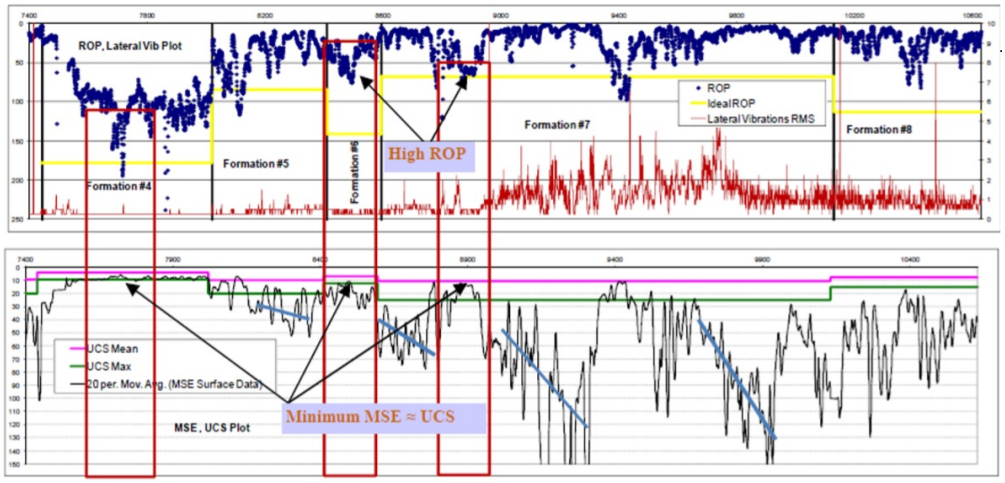

Figure 11: MSE vs. Depth. Hardness and other parameters are also presented in the same plot (Amadi et. al 2012).

This is often associated with a change in lithology, as the driller have to readjust the parameters to fit the new formation. At 9400-9800 ft there are clear efficiency problems related to the increase in vibrations. It is important to remember that the driller had neither MSE nor UCS data available during drilling.

Based on these data, actual performance during this section was evaluated against the ideal performance identified by the UCS-logs. To achieve optimal performance, i.e. all input energy is used for increased penetration rate, the driller would have to be able to keep MSE equal to UCS at all times. The comparison between actual ROP and ideal ROP is illustrated in the bar chart on Fig. 12.

Calculated from these values the operation spent just above 100 hours drilling. If the operation had been performed optimally, the entire interval could have been drilled in 33 hours. While this is not a probable scenario, the paper concluded that by active use of MSE the drilling progress could have been raised by 30 – 60 percent compared to best offset well performance. They also concluded that real use of MSE could provide additional data needed to make informed decisions regarding improvements of the drilling process, which in turn could help in the goal of cutting total cost.

2.2.6 Potential improvements

The strength of the MSE plot is that it more accurately illustrates the actual efficiency of the drilling process. As seen in the chapter above this information is crucial in cost-saving and cost-justification, and if utilized correctly could in turn save both time and cost. Additional advantages of the current MSE system is that it is simple to

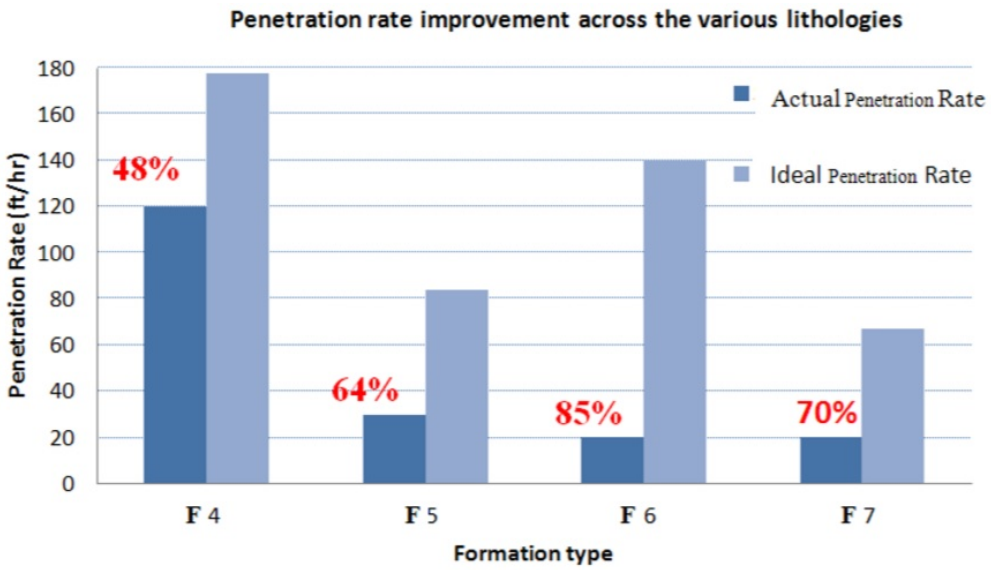

Figure 12: A bar chart showing the actual ROP vs. ideal ROP. The percent values in red are the reduction in ROP due to inefficient operation (Amadi et al. 2012).

use, easy to understand, and that it relies on common drilling variables like WOB and torque. This means that the method can be utilized for almost every drilling scenario without too much changes or additional costs.

The downside to the method is that it for some scenarios may be too simple. This means that valuable information is lost when making some of the simplifications, making it less reliable than required. Evaluation of the method shows that the biggest fault of the system is that it fails to take into consideration changes in the formation. Due to the nature of the MSE formula, it only considers the energy needed to remove a given volume of rock, not the additional energy needed to remove a hard formation compared to a softer formation. This lack of information makes it difficult for the driller to adjust input parameters accordingly. Each change in lithology will therefore cause a larger than necessary fluctuation in MSE, usually in a negative favour. This is well illustrated in Fig. 11.

Information about formation hardness could also help provide a clearer picture of the actual efficiency. An example could be a scenario where the bit encounters a harder formation and the MSE increases accordingly. The driller will then assume the efficiency is reduced and try to identify the source of inefficiency, while it may just be a stringer, and the MSE is still optimal. For the opposite scenario where the formation becomes softer, this could also cause a problem. For a softer formation, sticking to the same MSE and following the new-bit-MSE trend-line is not as efficient as possible, and a

potential opportunity to achieve increased ROP is missed, as the MSE trend line is deceptive.

Other simplifications that could have an impact on the total efficiency is the efficiency factor of the bit, and the efficiency factor of energy loss along the wellbore. Under perfect circumstances, the bit-efficiency factor should be evaluated by data given from the manufacturer. However, since MSE is used as a trending tool; this simplification can be considered adequate, because the value is constant throughout the operation. The exception being the bit-dullness factor that changes over time.

The friction-loss-factor on the other hand, should be of concern. The problem lies with the approximation of lost energy. As the well increases in length, and often also in both azimuth and inclination, the drillstring will experience a non-linear increase in lost energy. This means that for a section starting at 2000 meters, a constant simplified efficiency factor between 0 and 1 is not a good indicator when later drilling at 3500 meters, as the efficiency factor will in fact be of greater magnitude at this depth if downhole torque is kept constant. Thus, the simplified factor will have a too large margin of error to make any real assumptions of what the actual efficiency is at this point. This type of error could be eliminated by using downhole data, but for most operations, this type of data is not available.

Another weakness of the current concept is that it only takes into consideration the mechanical energy. This means that the entire aspect of hydraulic specific energy is lost to simplification. While hydraulic energy may not be of equal magnitude, and may not fluctuate as much as the input of mechanical energy, it is still not of a constant value, and should be considered when evaluating the total efficiency of the progress.

3 New MSE-model - ADE

Several weaknesses were identified while investigating MSE and the model presented in section 2. Therefore, before modelling and testing of a new and more accurate MSE model, three weaknesses needed to be addressed: Lost mechanical energy, Hydraulic energy and Formation hardness. They stood out as the most severe limitations, and thus became the focus during the improvement process.

The aim of this thesis was to create a new more functional model for the drilling process, i.e. for it to function optimally by paying more attention to the abovementioned parameters. A broad fundament in previously published knowledge and mathematical modelling formed the basis for the development of the new mathematical model. It was adjusted with the purpose of functioning with commonly available real-time drilling parameters. A prototype MATLAB-agent was therefore created in order to better illustrate and test the improvements of the model.

3.1 Hardness

MSE is defined as the ratio between input energy and volume of removed rock per unit time. One of the largest causes of error for this method is the lack of consideration given to the hardness of the rock. For MSE to be a fair measure of actual efficiency, a measure of formation hardness needed to be implemented. Since formation strength rarely is uniform, a continuous evaluation is necessary.

The first step in modifying the efficiency model is to implement an extension accounting for formation hardness, yielding the formula

$$\mathrm{MSE}_{\mathrm{mod}} = \frac{\text{Input energy}}{\text{Volume removed} \cdot \text{Hardness}} = \frac{\mathrm{MSE}}{\text{Hardness}} \tag{7}$$

An increase in hardness should result in an increase in MSE, but this does not necessarily mean that the efficiency is reduced, only that more energy is needed to crush the current rock faced. By including this term into the total formula for efficiency, the output yielded should be easier to interpret for the operator.

As will be described later, the penetration rate equation proposed by Bourgoyne and Young (1986) forms the basis of the formation hardness evaluation used by the model. This was investigated by Berg (2015), and will be cited partly in this section.

Sedimentary formations are mainly made up of shales and sandstones. Due to the variation in mineral composition and the cementing of the grains, they vary in hardness

(Kjerkreit 2015). Thin strings of harder rocks, such as limestone and calcite provide even more complexity into the hardness evaluation process. Classifying formation hardness is a challenge, so when targeting to improve the MSE model, a good approximating model is of the essence.

Different approaches for determining formation hardness have been proposed by several scientists and engineers. Many have come to agree that evaluating a formation's hardness correlates with formation drillability. Drillability is, as the term might suggest, a measure of how easy a formation is drilled. Generally, they are recognized as being inversely proportional with one another, i.e.

$$\text{Drillability} = \frac{1}{\text{Hardness}} \tag{8}$$

Quantification of formation drillability can be done using several methods, or even a combination of these.

A uniaxial compression strength test is, as suggested by Spaar et al. (1995), perhaps the most accurate method for determining formation drillability. It is also the most expensive, as it requires cores extracted directly from the wellbore walls, and thorough investigation in a laboratory. When performed properly, the test can give an accurate measure of the formation's strength, i.e. its uniaxial compression strength. This measure of strength is then referred to as Unconfined Compressive Strength. More correctly: UCS is the maximum axial compressive stress that a right-cylindrical sample of rock can withstand under unconfined conditions, i.e. the confining stress is zero (SLB Glossary, 2016a). An example of such an investigation is shown in Fig. 13.

UCS obtained from core samples is obviously not available as a source of real-time data. However, it may be available from adjacently drilled wells, if core samples have been collected there. Depending on the geological profile of the area, core samples from adjacent wells could provide information beneficial for the ongoing drilling process since it may be considered a reliable source of information for the hardness profile of the new well.

If this kind of information is unavailable, there are other ways of determining the UCS of the formation. Shrivastava, Javed and Pratap (2013) reported that sonic log, density log and gamma log could be used to adequately determine formation drillability, and, thus, formation hardness.

If lack of information prevents further determination of UCS, real-time penetration rate equations is an alternative.

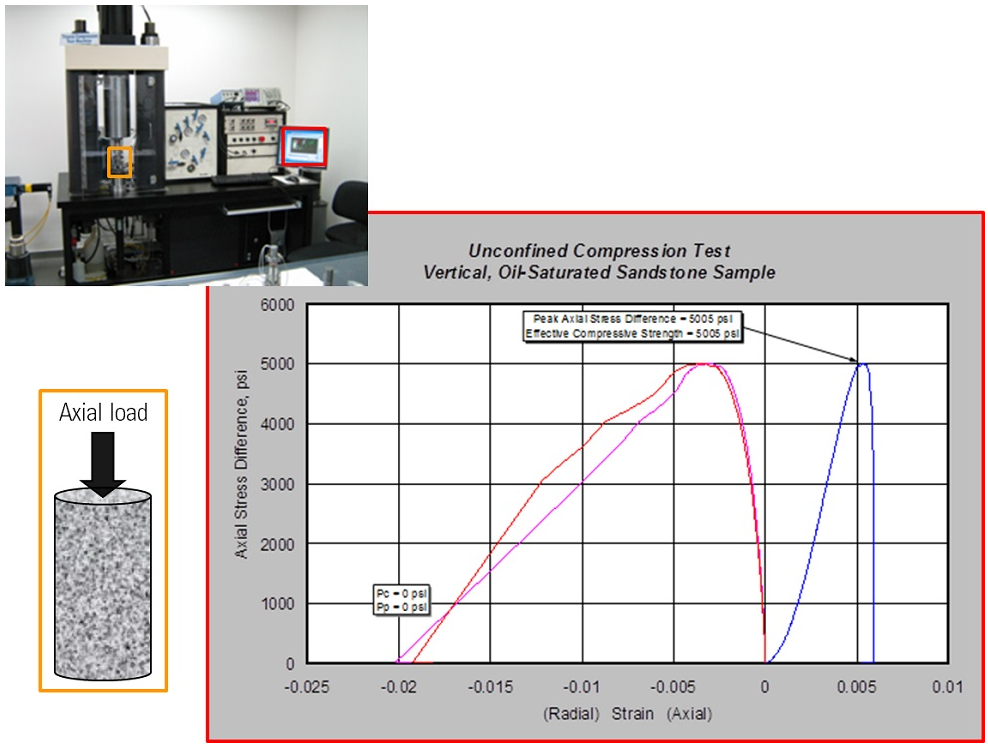

Figure 13: Uniaxial Compression Strength apparatus (top), core sample (left) and the corresponding measurements from the test, presented graphically (SLB Glossary 2016).

When describing formation characteristics with regard to penetration rate equations, the term abrasiveness is commonly used, in addition to drillability (Somerton, Esfandiari and Singhal, 1969; Bourgoyne, Chenevert and Millheim 1986). While drillability is a measure of how easy the formation can be drilled, abrasiveness is how fast the formation will wear the teeth of the drill bit. When drillability increases, the abrasiveness decreases, and vice versa. Thus, one might suspect a close relationship between abrasiveness and the formation's hardness. However, abrasiveness and bit dulling are accounted for by terms in the existing formulas, and will not be addressed further in present investigation.

The penetration rate equations primarily calculates drillability as a function of several drilling variables, e.g. compressive strength, which increases with depth, thus, decreasing drillability.

The complex interactions between the various drilling variables, and how they affect the ROP, are not fully understood today. An accurate mathematical model is therefore not possible to obtain (Bourgoyne, Chenevert and Millheim 1986). However, mathematical models that try to combine the already known relationships between the parameters,

exists.

These equations are usually on the form of

$$\text{ROP} = f_1 \cdot f_2 \cdot ... \cdot f_n, \tag{9}$$

where n is the number of terms in the equation.

The Bingham's model is an example of such penetration rate equation.

$$\text{ROP} = K \left(\frac{W}{d_b} \right)^{a_5} \tag{10}$$

ROP is the penetration rate, K is a constant of proportionality, which includes rock strength effects, W is weight on bit, d_b is bit diameter, and a_5 is a bit weight exponent. Due to the simplifications in the Bingham model, i.e. use of only a very few parameters, the model does not have a high degree of precision. The most complete model for penetration rate is, perhaps, the model proposed by Bourgoyne and Young (1974). This is the model used for calculating hardness used in the mathematical agent (section 4). It consists of eight functional relations:

$$\text{ROP} = f_1 \cdot f_2 \cdot ... \cdot f_8. \tag{11}$$

ROP is the penetration rate and f_i = 1,2,...,8 are functions of different drilling variables.

The penetration rate equation does not explicitly calculate the hardness, but it can be used to derive an expression for the drillability. The introduction of the inversely proportional relation between hardness and drillability yields an equation implicitly stating formation hardness.

Not all the terms in the equation have the same level of impact in the output. However, since some of the parameters are common for both the penetration rate equation and the original MSE-formula, Eq. 4, all the terms are given equal consideration.

The, in all, eight different terms, i.e., f_1 through f_8, are presented in appendix A.

The f_1 term accounts for the apparent formation drillability, and hence the equation must be rearranged with respect to f_1, yielding

$$f_1 = K = \frac{\text{ROP}}{f_2 \cdot f_3 \cdot ... \cdot f_8} \tag{12}$$

This is the form of the equation used by the agent.

The method allows for a continuous real-time evaluation of formation hardness. Since most of the input variables are identified during a normal drill-off test, the model can be operational early in the process. Another strength of this model, is the independency between the terms, meaning that it will function to a certain degree even though some of the variables are unavailable. The hardness evaluation can also be used for other purposes, such as bit selection, identification of hard stringers, and overall formation evaluation, if presented separately.

The weakness of using this formula in combination with MSE analysis is that the method is based on some of the same input variables, making its output values less independent from the MSE method than preferred. Still, there are enough variation in parameters used by the models to ensure some independency between the two.

Since the real-time drilling data is registered in SI-units, some conversion was needed for them to be compatible with the penetration rate equation. As mentioned above, the penetration rate equation is the third choice for determining hardness, but an adequate option if only real-time time data is available for hardness evaluation.

3.2 Hydraulic Mechanical Specific Energy (HMSE)

While the majority of progress during drilling is a result of mechanical energy exerted by the bit, it is also clear that the hydraulic energy in the drilling fluid plays an important role. In addition to transporting cuttings away from the path of the bit, the fluid exerts a jetting impact force on the formation as it is flushed through the bit nozzles. By introducing an additional term for hydraulic energy to the MSE model, more accuracy is added to the efficiency evaluation process.

While investigating different models of drilling efficiency, it became clear that most methods have neglected the hydraulic term completely, and little research had been done on the matter. However, two sources of reliable research were acquired. Cui Meng et.al. (2010) investigated the impact hydraulic energy has on the total energy output of the system. They intended to improve the optimization algorithm system known as Navigation Optimization (NAVO) by including the hydraulic energy aspect of the operation. Through this work, they created a new system introduced as DrillNAV, used for identifying downhole vibrations, and increasing ROP.

Mohan et al. (2009) investigated a method to further improve the accuracy of specific energy. In an attempt to better model downhole drilling, a model that does not only

calculate the energy used to crush the rock, but also the energy needed to transport the accumulated cuttings from beneath the bit is needed. The concept of Hydraulic Mechanical Specific Energy (HMSE) was developed in order to implement this hydraulic specific energy. Testing showed that the hydraulic specific energy accounted for an average of close to 15 percent of total energy input. HMSE is described in detail in this section.

The MSE expression is based on two terms; one accounting for the axial forces, and another accounting for the rotational forces. Hydraulic energy represents a third term in the HMSE formula.

$$\text{HMSE} = \frac{W_{\text{hyd}} + W_{\text{axi}} + W_{\text{rot}}}{\text{Volume of rock removed}} \tag{13}$$

W_{hyd} is the work done by the jetting force of the fluid onto the formation, W_{axi} is the work done by the WOB, and W_{rot} is the work done by the rotational motion of the bit onto the formation.

The hydraulic energy, E_h expended at the bit is given as the product of the pressure loss across the bit ΔP_b and the flow rate Q, i.e.

$$E_h = \Delta P_b Q \tag{14}$$

Of the total energy, only a fraction reaches the bottom of the hole (Mohan et. al 2009), and contributes to further progress. This fraction lies in the range of 25-40 percent. The efficiency reduction factor, η, is defined by bit- and nozzle-specifics, and is based on the two dimensionless variables A_v and M.

A certain volumetric flow, Q, is displaced through the bit nozzles during drilling. Given that close to no fluid is lost to the formation below the bit, the same volume flows through the annular space on its way up. The relation between volumetric flow, velocity, v, and cross-sectional area, A, is given as

$$Q = vA, \tag{15}$$

yielding the following expression for velocity.

$$v = \frac{Q}{A} \tag{16}$$

Since flow is constant, the increase in cross-sectional area subsequently leads to a decrease in velocity, i.e. the velocity in the annulus is lower than that through the nozzles. A_v is defined as ratio between these two velocities. Bit nozzle area is the average area of each nozzle times the number of nozzles, while the cross-sectional area of the annulus for a roller cone bit is approximately 15 percent of total bit area (Mohan et al. 2009).

$$A_v = \frac{V_n}{V_f} = \frac{0.15 d_b^2}{n d_n^2} \tag{17}$$

V_n is the velocity through the nozzles, V_f is the velocity through the annulus space, d_b is the diameter of the bit, d_n is the average diameter of the nozzles and n is the number of nozzles.

An efficiency loss factor, M_h, is added to account for the loss of energy between the nozzles and the formation. M is dependent on the distance between the formation and the nozzles, and nozzle specifics such as angle of the jet and diameter at release.

$$M_h = \frac{d_n + 2L\tan(\theta_j/2)}{d_n + s\tan(\theta_j/2)} \tag{18}$$

L is the length of potential core, s is the distance between the nozzles and the formation and θ_j is the angle of axially symmetric jet.

The total factor for hydraulic energy reduction:

$$\eta = \frac{1 - A_v^{-k}}{M_h^2} \tag{19}$$

k is assumed to be 0.122 (Warren, 1987).

Consequently the term for the hydraulic energy becomes:

$$W_{hyd} = \eta \Delta P_b Q \tag{20}$$

The hydraulic pump force also has an effect on the axial force, described as a pump-off effect. The force exerted by the fluid onto the formation, will have an opposite working force on the bit in accordance with Newton's third law, reducing the effective WOB onto the formation. The pump-off force is equal to the impact force F_j. The expression

for the effective axial force applied to the formation is therefore redefined.

$$\mathrm{WOB_e} = \mathrm{WOB} - \eta F_j \tag{21}$$

where

$$F_j = 0.000516 \rho_m Q V_n \tag{22}$$

ρ_m is the density of the mud.

The total expression for HMSE given in consistent units of psi:

$$\mathrm{HMSE} = \frac{\mathrm{WOB_e}}{A_b} + \frac{120\pi NT + C\eta \Delta P_b Q}{A_b \cdot \mathrm{ROP}} \tag{23}$$

C is a field unit conversion factor. N is the number of rotations per time, i.e. rpm, T is torque and A_b is the cross-sectional area of the bit.

The reason for choosing this method was due to its compatibility to the already established MSE method, and its mathematical simplicity. It was also an important factor that the selected model could be based on commonly available drilling parameters, such as flowrate and bit-specifics.

The method requires some intermediate calculations. With regard to the MATLAB-agent, these calculations require little extra computational time, as many of the variables are constant for the entire section. Regardless, these calculations entail negligible effects for the operator, apart from increased output accuracy.

The weakness of this paper becomes evident when evaluating the actual efficiency. Redoing their calculations, it was clear that the bit efficiency factor of 0.35 was neglected for the mechanical energy, meaning that the values presented as results are much larger than what is actually exerted at the bit. The authors still created and included a dummy factor, η to account for hydraulic energy reduction. This creates an imbalance between the output being presented for the mechanical- and the hydraulic energy.

While the axial force is based on WOB, and is therefore given as downhole information, the rotational force is given as torque, with no mention of where this parameter was measured. Given that the torque scales up to 27 kNm, it is a fair assumption that this value is measured at surface, meaning loss along the trajectory of the well is also

included.

When scaling the mechanical energy properly, results in the hydraulic energy accounting for more than twice the fraction presented in the paper, this error will be even more if the torque stated is measured as surface torque as suspected.

3.3 Energy loss

To search for and deplete new reservoirs, the petroleum industry has to drill further and deeper than ever before. Highly deviated wells stretching over several thousands of meters introduces new risks and challenges. One of these challenges is the loss of energy along the long and winding trajectory of the well. For situations where measurements are not available down-hole, parameter readings may deviate from the actually experienced parameters downhole. These deviations tend to increase with depth of the well. This section will take a closer look at each of the three energy inputs, evaluating how the energy measured downhole deviates from the energy measured at surface, and what adjustments should be made. This chapter will also evaluate the energy lost in the contact between bit and formation.

For MSE calculations, the most common procedure for dealing with loss along the drillstring is the efficiency-loss factor. Depending on the well path, this factor is set on a scale from 0 to 1, and usually kept constant for the entire section. As mentioned in section 2.2.6, this may cause problems, as it does not consider the additional loss due to the increasing well length and path change. For the model proposed in this paper, a more detailed approach has been implemented.

Among the factors that account for the largest energy loss along the drillstring are vibrations and axial and rotational friction. Friction is straightforward to estimate, while vibrations is more a matter of recording when it occurs. Energy loss due to vibrations is considered a cause of founder, but is, in terms of MSE, identified as a cause first after the problem appears. Continuous calculations regarding vibrations are therefore not implemented in the actual formula.

3.3.1 Rotational energy at bit

Manipulable parameters, e.g. RPM and block position, are usually measured and controlled at the surface, meaning that they may differ from the actual parameters downhole. Responding parameters, on the other hand, are often recorded downhole, and can be considered as RTDD compatible with the MSE-model. In order for manipulable parameters to be considered representative as downhole RTDD, they need to be adjusted with regard to the changes are subject to downhole.

The responding parameter torque is usually recorded as surface data. This means that the values given in RTDD does not consider the energy lost along the drillstring, and is therefore not representative for the actual torque experienced at the bit. This yields the following relation between top and bit torque:

$$T_{\text{bit}} = T_{\text{surface}} - T_{\text{loss}} \tag{24}$$

Considering the significance of torque in the MSE formula, the error resulting from not performing this adjustment would cause the output to be unreliable. The focus was therefore to approximate a value for the downhole torque exerted at the bit, by calculating the energy lost through friction along the drillstring, and subtracting it from the readings at surface.

The first step was to identify the trajectory of the well path. This means acquiring information regarding inclination and azimuth angle for each part of the well. This will be addressed in section 4.1.2. This information is needed to calculate the forces acting on the drillstring along the wellbore.

When the angle at each part of the well path is available, either as measured data, or through modelling, the torque can be closely estimated. Four different models were investigated in order to most properly calculate the energy lost during drilling.

The first method was presented by Boonsri (2014), and is based on the general form of force equilibrium and the use of Frenet-Serret local coordinates. The method includes six scalar products based on two equations.

The second method is a full stiff-string formulation presented by Mitchell (2008). By using this method, the author claims to remove some of the inaccuracies associated with loss of torque experienced with normal models. He states that some of the problem comes from using the minimum curvature method to calculate the well path, so an analytical drillstring solution is suggested as a better approach. These models were considered somewhat complicated for the purpose of this thesis, and therefore discarded.

A simpler method based on the formula of torque was also considered.

$$T_x = T_{x-1} + W_x \cdot r + \mu \tag{25}$$

T is torque, W is weight, r is radius of the drillstring and μ is a fricion factor. The indices x and $x-1$ represent the current and previous depth-element respectively.

The weight of the drillstring was calculated for each increment based on the following equation.

$$W_x = W_{\text{DS}} \cdot \beta \cdot \theta \cdot g \tag{26}$$

W_x is the submerged weight of the segment of the drillstring, W_{DS} is weight of the drillstring segment, β is buoyancy, θ is inclination angle and g is the gravitational acceleration.

Two simplifications needed to be made in order to use this method. The first is that the wellbore keeps a constant azimuth angle. The second is that the drillstring rests on the lower side of the wellbore at all times. This implies that the axial force from the rest of the drillstring does not affect each increment of the drillstring. Assuming a friction factor of 0.2, this will only be true for an inclination of more than 76.7 degrees (Sangesland 2014). For less inclination, the string will experience a drag force from the weight of the lower parts of the drillstring. During an angle reduction, this force will create additional normal force against the lower side of the wellbore. During a build-up, depending on the strength of the force, the drillpipe (DP) may be pushed against the upper side of the wellbore, as illustrated in Fig. 14. During these two scenarios, the normal force calculated by the weight of the increment alone is not sufficient, and a more complex formula is required.

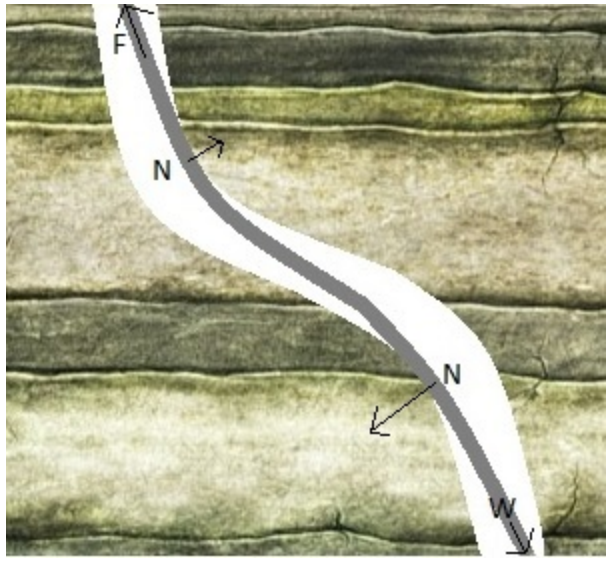

Figure 14: Normal force acting on the wellbore walls, due to the curvature of the well path.

The final concept is known as the discrete method (Sangesland 2014). This method

works well with continuous recordings of change in both inclination and azimuth angle, and has been known to give good results when used with RTDD (Brechan 2016). This method also considers the added frictional loss caused by side forces through bends. The drillstring above its neutral point is always in tension. Fig. 15 shows the forces and torque acting on the drillstring.

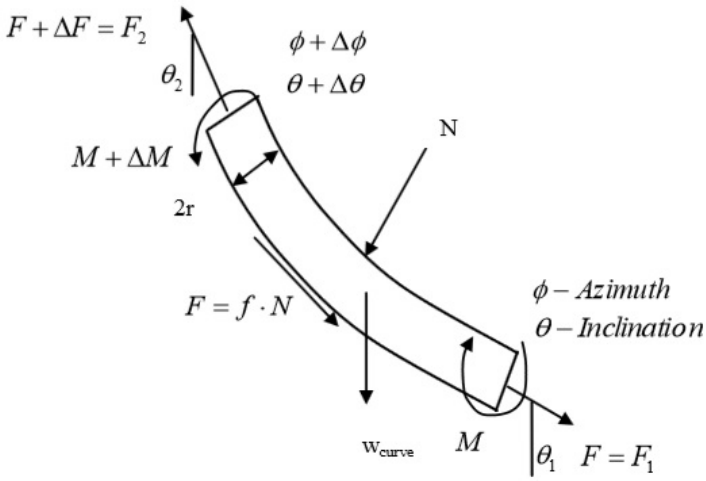

Figure 15: Forces and torque acting on the drillstring in a curved part of the wellbore (Sangesland 2014).

Torque is calculated from the bit and up, using the following equations.

$$M_x = M_{x-1} + \mu \cdot r \cdot |N_f| \tag{27}$$

M is the torque on bit, μ is the friction factor, and N_f is the normal force.

$$N = \sqrt{\left(F_x \cdot \Delta\phi \cdot \sin\bar{\theta}\right)^2 + \left(w_{\text{curve}} \cdot \sin\bar{\theta} + F_x \cdot \Delta\theta\right)^2} \tag{28}$$

$$F_x = F_{x-1} + w_{\text{curve}} \cdot \cos\bar{\theta} \pm \mu \cdot |N_f| \tag{29}$$

F_x is the axial force, F_1 being the negative force from WOB during drilling, w_{curve} is the weight of the drillstring segment submerged in fluid, $\bar{\theta}$ is the average angle of inclination of the curve and $\Delta\phi$ and $\Delta\theta$ is change in azimuth and inclination respectively. The plus-minus-sign accounts for pulling and lowering the pipe respectively.

During drilling, the pipe is subject to a dynamic force. This means that it is in a constant state between being pulled and lowered (Brechan 2016). A neutral weight is therefore selected, being the average between these two forces. Formula Eq. 29 may then be rewritten as

$$F_x = F_{x-1} + w_{\text{curve}} \cdot \cos\bar{\theta} \tag{30}$$

The formula works under the assumption that bit-torque is a known variable, and the surface torque is the unknown. When calculating the force, F_x, at every point of the well, this formula could be recompleted by some simple modifications, to fit the purpose of this paper, where bit-torque is the unknown factor.

$$M_{x-1} = M_x - \mu \cdot r \cdot |N_f| \tag{31}$$

While this model works well with RTDD and continuous drilling, some simplifications have been made. The first one is that at zero degree inclination, there is no contact between the drillstring and the surrounding wellbore, and no frictional forces are therefore experienced. The wellbore, with and without casing, is also assumed a perfect pipe, meaning a smooth surface with no change in well radius like tightness or cavities causing extra friction between the drillstring and the wellbore. Finally, the wellpath is considered smooth.

3.3.2 Axial energy at bit

For the axial force, RTDD given as weight experienced at bit is more common. Since downhole measuring of WOB is not often prioritized, this data is most commonly calculated based on hook load measured at surface. This means that depending on the procedure used to calculate WOB, the accuracy of the given value might be inaccurate. Substituting torque with weight in Eq. 24, WOB might be calculated based on hookload using Eqs. 28 and 29.

3.3.3 Hydraulic energy at bit

The SPP added at surface is lost during circulation along the DP, the bit and the annulus at different fractions (Skalle, 2014). As seen in Eq. 20, ΔP_b is given as the energy loss over the bit, meaning that the energy lost during transfer is already excluded. By including this term, the formula is already given as the energy as experienced at bit.

3.3.4 Energy loss at bit

When loss along the drillstring is already accounted for, the efficiency factors need to be revaluated. Until now the total-efficiency-factor as seen in Eq. 6 contained an inefficiency factor accounting for transmission losses along the well path, and a bit-efficiency-factor to account for energy lost during transfer from bit to formation. On account of the changes addressed in sections 3.3.1 to 3.3.3, all input energy is now given as downhole data, and the first term may be dismissed.

The latter term is added to account for non-optimal sliding-friction and additional torque. This loss of energy affects the rotational energy, but not the axial energy, as the force exerted by WOB is directly transferred to the formation below the bit. An adjustment is therefore suggested, to exclude this factor from the axial part of the expression.

For the hydraulic energy, the dummy factor, η, is already included to account for loss at bit, as stated in Eq. 20.

3.4 The complete expression

Since the new method introduced in this paper no longer only considers the mechanical specific energy, the specific energy input will be referred to as Total Specific Energy (TSE), which in correlation with formation hardness will be used to evaluate Actual Drilling Efficiency (ADE).

The equation for MSE formulated by Teale (1965) is as stated in Eq. 2.

$$\text{MSE} = \frac{E_{\text{axi,s}} + E_{\text{rot,s}}}{\text{Volume removed}}$$

and

$$\text{MSE}_{\text{eff}} = \frac{E_{\text{axi,s}} + E_{\text{rot,s}}}{\text{Volume removed}} \cdot (\text{Total efficiency factor})_{\text{s}} \tag{32}$$

s indicates that the parameter is recorded on surface, and Total efficiency factor includes bit efficiency and loss along the drillstring.

From this formula, and the theories presented in the previous three subchapters, the following adjustments were made to more accurately evaluate the drilling efficiency, and

form the basis of the MATLAB-agent presented in section 4.

$$\text{ADE} = \frac{E_{\text{axi,c}} + E_{\text{rot,c}} + E_{\text{hyd}}}{\text{Volume removed}} \cdot \frac{1}{\text{Hardness}} \tag{33}$$

c indicates that the factor is corrected.

The axial input energy is corrected in accordance to hydraulic pump-off force as shown in Eq. 21. If given as surface data, downhole values are calculated based on Eq. 21 and Eq. 30.

$$E_{\text{axi,c}} = E_{\text{axi,s}} - \text{Hydraulic recoil} - \text{Axial friction} \tag{34}$$

The torsional input energy is adjusted with regard to loss along the wellbore, in accordance to the adjustments illustrated in Eq. 31.

$$E_{\text{rot,c}} = (E_{\text{rot,s}} - \text{Rotational friction}) \cdot B_{\text{eff}} \tag{35}$$

B_{eff} is a bit efficiency factor. The hydraulic term E_{hyd} is added to account for hydraulic energy through the bit nozzles, and flushing away the crushed cuttings. The complete term for TSE is as follows.

$$\text{TSE} = \frac{E_{\text{axi,c}} + E_{\text{rot,c}} + E_{\text{hyd}}}{\text{Volume removed}} \tag{36}$$

Eq. 36 illustrates the energy needed to remove a specific volume of rock. To evaluate ADE, TSE must be evaluated against formation hardness.

$$\text{ADE} = \text{TSE} \cdot \frac{1}{\text{Hardness}} \tag{37}$$

Where hardness is given as UCS in pascal. Expressed with common drilling parameters, the equation is reformulated as:

$$\text{ADE} = \left(\frac{\text{WOB} - \eta F_j}{A_b} + \frac{120\pi N \left(T_{\text{surface}} - T_{\text{loss}}\right) \cdot B_{\text{eff}} + C\eta \Delta P_b Q}{A_b \cdot \text{ROP}} \right) \cdot \frac{1}{\text{UCS}} \tag{38}$$

Table 2 illustrates the similarities and differences between the adjusted method and the original method.

Table 2: The adjustments made by the ADE-method compared to the original.

	Original method	**Adjusted method**
Energy delivered from rig	+ Axial input energy + Rotational input energy	+ Axial input energy + Rotational input energy + Hydraulic input energy
− **Energy loss along wellbore**	x Loss efficiency factor	− Axial friction − Rotational friction − Pressure loss (ΔP_{DS}, $\Delta P_{\text{annulus}}$)
− **Energy loss at bit**	x Bit efficiency factor (0.35)	− Axial energy loss − Rotational energy loss (x 0.35) − Hydraulic pressure loss (η)
= **Energy used for progression**	= $\mathbf{MSE_{eff}}$	= **TSE**
/ **Formation hardness** = **Drilling efficiency**		/ Formation hardness (UCS) = **ADE**

4 Agent for determining ADE

The mathematical MSE-tool, until now referred to as the agent, was developed in order to do two things; to check the effects of the new improved MSE method, i.e. the ADE-method, and to help determine whether or not the effects could be monitored real-time. The agent was programmed using the mathematical program MATLAB, and tested on historical drilling data from well 147.

This chapter will give a thorough review of the development- and testing phase of the agent, along with a short presentation of both the software and the drilling data.

4.1 Mathematical model

The purpose of the agent is to monitor the drilling efficiency in terms of ADE, and to determine whether mechanical energy input is optimal or not. This is achieved through use of the carefully selected mathematical models, described in the previous chapter.

The models included in the agent, are as follows:

MSE original

- Axial specific energy
- Rotational specific energy

Actual drilling efficiency

- Total specific energy
  - Axial specific energy (Corrected)
  - Rotational specific energy (Corrected)
  - Hydraulic specific energy
- Formation hardness

The main concern while implementing the models in the script was to make them all compatible with one another, and to make them handle a continuous flow of time-based parameters. The latter proved to be an especially delicate matter with regard to the friction-loss calculations.

The following chapters include adaptations and implementations performed for the mathematical agent.

4.1.1 MSE, the basic model

Since the original MSE model proposed by Teale is the baseline of the new model, it was chosen as a basis of comparison when our potential improvements were to be evaluated.

Without further adjustments, the formula used as basis, is Eq. 4.

$$\text{MSE} = \frac{\text{WOB}}{\text{Area}} + \frac{2\pi \cdot \text{RPM} \cdot \text{Torque}}{\text{Area} \cdot \text{ROP}}$$

4.1.2 First extension; mechanical friction-loss of torque

One of the extensions and improvements suggested by the new model, is the effect of energy lost along the drillstring due to drag and friction. To estimate the loss along the drillstring, data regarding well-path must be available.

Adjusted model of well path

In the data provided, there were no well path coordinates available, which could have been used to more correctly calculated mechanical friction-loss. This proved to be a problem as both azimuth and inclination angles are needed to calculate loss of torque. The following model was implemented in order to approximate the inclination of the well path.

The method is based on simple trigonometric formulas, and the concept that a tiny part of a large curve will appear to be a flat line segment. For drilling operations, this means that even for a line with a somewhat large dogleg angle, e.g. 6 degrees per 30 meters, a distance of 0.1 meters will only change by 0.02 degrees, and therefore appear flat. Only by looking at several hundred meters of the drillstring will the curved shape appear. A mathematical simplification is then created by dividing the path of the well into smaller increments, modelling the continuous curve as the sum of shorter straight lines, as is illustrated in Fig. 16.

The degree of precision of this model depends on the length of each increment, and the angle of the curve. For a well path, this model should be quite reliable, as large change in angle over short distances is rare.

By denoting the change in measured depth ΔMD for a small segment of the well as the hypotenuse, and the change in vertical depth ΔTVD as one side, the angle between the two becomes the angle of inclination in a right-angled triangle, as shown in Fig. 17.

The angle of this segment of the well can be calculated using simple trigonometric

Figure 16: The modelled curve compared to the actual curve.

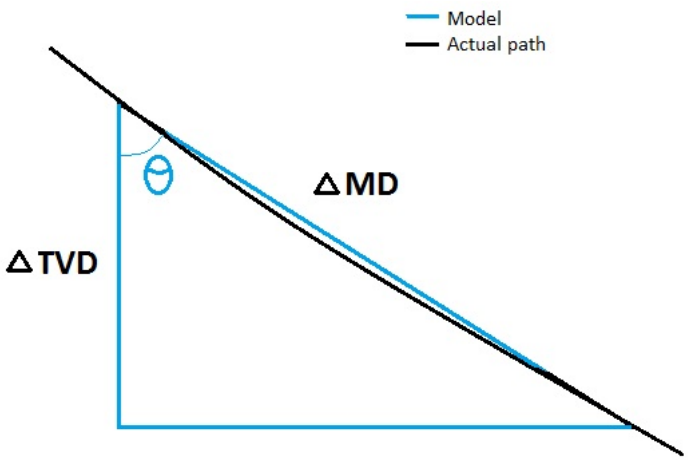

Figure 17: A right-angled triangle sharing one angle with the inclination angle.

functions, e.g.

$$\text{Inclination angle} = \theta = \arccos\left(\frac{\Delta\text{TVD}}{\Delta\text{MD}}\right) \tag{39}$$

The second principle is that the average angle over a continuous curve is the average of the angle at the beginning and at the end, i.e.

$$\text{Average inclination angle} = \bar{\theta} = \frac{\theta_2 - \theta_1}{2} \tag{40}$$

By then assuming that over a short distance the curvature will be somewhat smooth,

the angle, calculated from formula Eq. 39, can be considered constant for this increment of the well.

Modelling a well-path

The method modelling well-path as explained above, is needed to calculate loss of torque along the drillstring. Since this method only works for the sections of the well with continuous MD and TVD data, information about previously drilled sections had to be stored as historical drilling data. Since this data was not available, a simple model was created to give approximate values for inclination vs. MD/TVD. This model is based on the assumption that the well starts off with a vertical section, and then builds angle at a constant rate until the start of the current section, as illustrated in Fig. 18. The length of the vertical section is individually evaluated for each well. Angle at start of current section is calculated at start of drilling by formula Eq. 41. If not specified, no change in azimuth angle is assumed.

$$\theta_{\text{dogleg}} = \theta_s - \theta_v = \theta_s \tag{41}$$

Dogleg angles are often given in terms of degrees per 30 meters, which yields

$$\frac{\Delta\theta}{30\ m} = \frac{\theta_{\text{dogleg}}}{\text{MD}_s - L_v} \cdot \frac{30\ m}{30\ m} = \frac{30 \cdot \theta_{\text{dogleg}}}{\frac{\text{MD}_s - L_v}{m}} \cdot \frac{1}{30\ m} \tag{42}$$

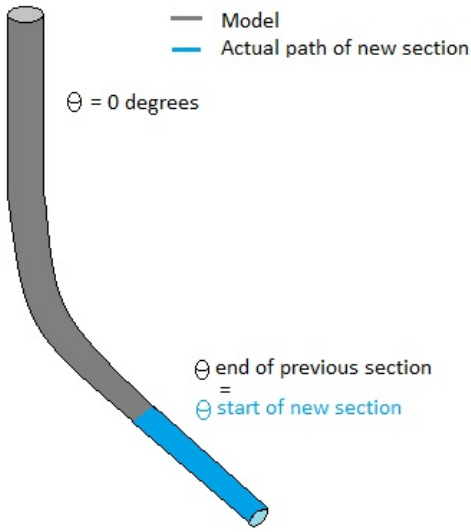

Figure 18: Modelled path of previous sections.

After making all the necessary adjustment and gathering all information needed, e.g. information about the drillstring components, the agent was tested on the 8 ½"-section.

4.1.3 Second extension; flush below bit and HMSE

The flushing effect exerted at the bit causes a contribution to the ROP to some degree. This is mainly due to improved cleaning of generated cuttings below the bit, but also partly due to abrasion of the formation by the fluid. Considering Newton's third law, the force exerted by the flushing fluid also works on the BHA, causing the WOB to decrease. To account for these two effects, a so-called hydraulic term is added to the MSE-equation, yielding a new MSE expression, i.e. HMSE (Hydraulic-mechanical specific energy, as described in section 3.2.

$$\text{HMSE} = \frac{\text{WOB}_\text{e}}{A_b} + \frac{120\pi NT + C\eta\Delta P_b Q}{A_b \cdot \text{ROP}}$$

4.1.4 Third extension; hardness of formation

As mentioned earlier, formation hardness can be quantified in several different ways. UCS obtained from adjacent wells or through GR-, neutron- and acoustic-logs is preferable, but not always available. Real-time evaluation through use of penetration rate equations is therefore a suitable option.

The penetration rate equation proposed by Bourgoyne and Young (1974) has formed the basis which this agent's hardness evaluation is based on. The equation is shown in its entirety in appendix A. As investigated by Berg (2015), WOB and RPM are the most significant factors in the penetration rate equation. Since these two parameters are also input parameters in the MSE equation, additional parameters need to be introduced in order to differentiate between MSE and hardness. Addition of extra terms also enables the agent to properly quantify the hardness of the formation.

With this in mind, the penetration rate equation yields the following expression for hardness:

$$\text{Hardness} = \frac{1}{K} = \frac{f_2 \cdot ... \cdot f_8}{\text{ROP}} \tag{43}$$

K is drillability and f_2 through f_8 are the different parameters affecting ROP, described in detail in appendix C.

4.2 Drilling data

Although one of the main purposes of the agent is to function with real-time drilling data, no data of such kind was available during the development of it, and thus, it has only been tested on historical drilling data. These data are described in detail in some other section. Compatibility with RTDD is a natural further extension of the agent. That, and other possible improvements, are described in section 6.5.

Drilling data obtained in the field will usually contain several discrepancies. Some of these anomalies will have negligible effects and cause no further problems for the calculations executed by the agent. However, others may lead to erroneous results, and have to be dealt with or removed before further calculations can be made. The measures done to prevent incorrect results are described in section 4.4.3.

One of the more regularly occurring discrepancies are abnormal fluctuations in measured depth. Logically the measured depth cannot decrease, only remain the same or increase. These anomalies may be caused by buckling of the drillstring or re-calibration of the depth monitoring system.

With exception of recorded ROP which is recorded according to pre-set depth intervals, all the variables in the historical drilling data were recorded as time dependent. The time unit is serial date numbers, which means that time is registered as days since January 1 year 0. Date numbers are a bit difficult to comprehend as they are in the magnitude of 736,000. However, by designating a certain value for time in each recording, few extra operations are needed in order to use time as an input variable, compared to if recorded as a calendar date.

4.3 Software

The platform used to develop the agent is MATLAB, a numerical computing environment optimized for solving engineering problems. The drilling data files were made compatible with MATLAB beforehand, which made the development faster and smoother.

In addition to MATLAB, Verdande Analytics, a software which presents the drilling data graphically, was used. Both softwares were utilized simultaneously to gain full comprehension of each of the cases, and to investigate and detect both trends and anomalies in the data.

4.4 The agent development

4.4.1 Pre-programming

The agent is based on the hardness detection agent developed by Berg (2015). It is compatible with historical drilling data and evaluates formation hardness using common drilling variables available in the dataset used during development of the ADE-agent.

Most of the required parameters were recorded in the historical drilling data, but some of the variables had to be found elsewhere. Among these are the pore pressure-gradient and various information about the drillstring components, such as drill-collar weight and bit-specifics. These were read off of EOW-reports, or directly from the manufacturers' sites. What proved the most difficult, was gathering correct data regarding bit-specifics. While information about bit nozzle diameter and count was available in the given EOW-repport, potential core length, s, distance between nozzles and bottom of the well, L, and nozzle angle, θ, were estimated based on the data given in the paper by Mohan et al. (2009), and bit specifics acquired from Crawford (2001). Pressure loss, ΔP_b was approximated to 0.5 times SPP (Skalle 2014).

The agent was developed to handle the drilled well section-wise, which makes it well suited for the available datasets. The 17 ½"-, 12 ¼"-section of well 147 were subject to the first round of development and testing. The following subsections will address these two in particular to exemplify aspects of the script and the development process.

Lastly the 8 ½"-section in the same well was subject to investigation and implemented in the agent, with good results.

4.4.2 Programming

Flowchart

The flowchart seen in Fig. 19 shows the key operations in the script. The blue rectangles are operations, e.g. calculations, the white rectangles are sub-operations and the yellow and green shapes are output plots, green being the main result.

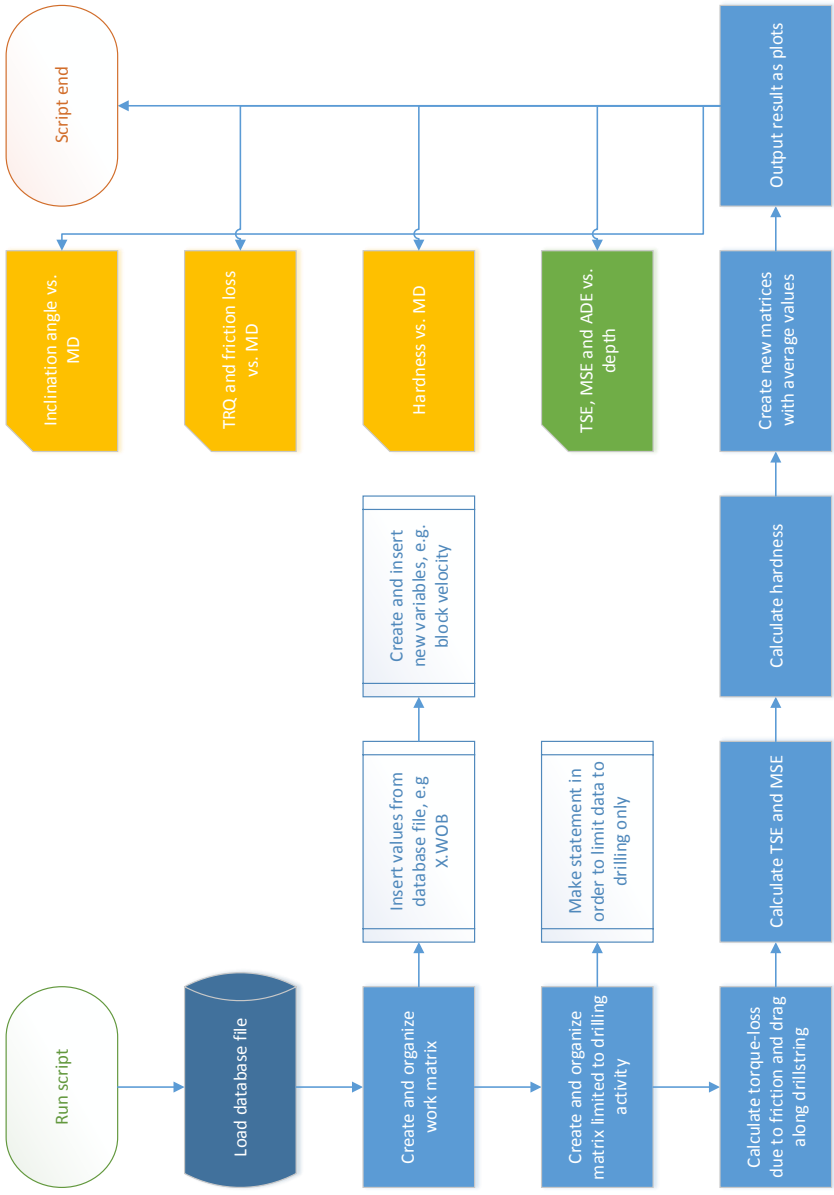

Figure 19: Flow chart showing the key operations of the agent.

Script setup

As mentioned above, the script is customized to handle drilling data section-wise. Therefore, the script starts by loading a set of drilling data from a preselected section of a well.

Secondly, the script measures the size of the dataset. It does this by counting the number of elements of the time variable, denoted "X.Time" in the particular cases of the abovementioned well sections. It then denotes this value "Size".

The third operation the script performs is to create a matrix, "A" , the size of Size x 20. The number of columns is rather arbitrary, but chosen to allow space for future extensions of the agent. Neither is this number fixed, meaning that a simple editing of the input in the matrix-command can change it.

Subsequently the matrix is filled with values from the different variables, each of which are assigned to designated columns. Table 3 shows the layout matrix A and some of its columns.

Table 3: Matrix A. The layout of matrix A with a selection of columns. The elements, i.e. rows, and the corresponding numbering, are indicated in the column on the left-hand side.

	Time	**DMEA**	**dbit**	**RPM**
1	Time(1)	DMEA(1)	dbit(1)	RPM(1)
...	...	...	...	...
i	Time(i)	...		
...	...	...		
Size	Time(Size)	...		

The majority of columns are filled with drilling data, e.g. WOB and RPM, but some of the columns are filled with "support-variables", i.e. products of several drilling-variables. For instance, the dbit-parameter is the difference in height between the bit-depth, DBTM, and the measured hole-depth, DMEA. This results in the new parameter, Δbit, hence the name delta bit.

Since drilling data often contains discrepancies, for instance missing recordings or irregularities such as abnormal readings, the script calls for a series of functions whose goal is to eliminate these anomalies. The functions, or for-loops, rather, will be addressed in the testing-section.

The next task is to isolate data originating from drilling, and thus discard the data recorded during other activities, i.e. tripping, reaming etc. This is achieved by making an if-expression and executing a statement if the conditions in the if-expression is met.

The following conditions had to be true in order for the script to interpret the activity as "drilling":

- Bit must be at the bottom of the well
- Rotation has to be above 25 rpm
- WOB has to be above 1 metric ton
- Mud flow (MFI) has to be above 500 lpm
- ROP has to be zero m/h or above

The agent checks if the conditions are met row-wise, from top to bottom of the A-matrix. It counts how many rows of A that meets these requirements, and denotes that number, "Size2". Subsequently, another matrix, "C" , is created, dimensioned by the number Size2, resulting in a Size2 x 30 matrix. The number of columns matches the number of parameters used in total by the script.

Then, the agent runs the same procedure again, i.e. checking which rows of matrix A that meet drilling-conditions. For those who do, all the cells of that row are copied into a new matrix, C, which should eventually only contain data from drilling.

The output of the agent are several plots used to interpret the correlation between TSE and the formation hardness. Therefore, lastly, before calculating the ADE, hardness etc., the agent calculates average values for some of the most critical variables. This ensures that no odd values are present during the calculations, which could otherwise cause large spikes to appear on the plots, rendering them unreadable for the operator of the agent. The method used for the calculation of average values is called "Simple Moving Average (SMA)".

In a data set, SMA is obtained by calculating the average for a subset of a given size, within the data set, and then shifting the subset forward, in order to calculate the average value for the next subset. This is repeated throughout the entire data set.

SMA for element n in a data set may be calculated based on subsets ranging from element n through element $n + k$, yielding the following equation

$$\text{Element } n = \frac{1}{k} \sum_{i=n}^{n+k} \text{Element}_i \tag{44}$$

The next subset would then range from element $n + 1$ through $n + k + 1$, yielding the SMA value for element $n + 1$.

The range from 1 through k may otherwise be defined as $n - k$ through $n + k$ or $n - k$ through n, the range of k, i.e. the size of the subset, being chosen with regard to the size of the data set, or desired "smoothness" of the elements. In this agent, the subset were defined to include the current element and the previous nine elements, i.e. SMA of 10 elements.

The first elements in the data set may be calculated using a smaller subset, for instance.

Torque-loss along drillstring
Torque lost along the drillstring due to friction is calculated first. Specifications of pipe weight, pipe radius and friction are found in EOW report, reliable websites, and some are obtained from the manufacturers. For this thesis, tool joint radius was used for DP. This means that all contact is predicted to happen in the interaction between tool-joint and wellbore, also in the open-hole section. This simplification was made as it is typical for harder formations. A friction factor of 0.16 was selected for steel versus steel, when calculating friction force between drillstring and casing. A friction factor of 0.2 was selected for steel versus stone, when calculating contact between drillstring and formation. Both factors are for greased surfaces, as the EOW-report stated that the mud in use was an oil-based mixture. For future use, this input is standardized for each section, and would have to be adjusted accordingly if seen necessary by the user.

The torque-loss is calculated using the formula presented in section 4.1, and the result is used to calculate an accurate value for both MSE, TSE and ADE.

ADE and TSE
Both ADE and TSE are calculated using the formulas described in section 4.1.

Hardness
Hardness is calculated based on the penetration rate-equation by Bourgoyne and Young, which have been thoroughly described section 3.1.

Plot
The results are most easily interpreted when printed as plots of the functions' graphs. The most relevant result, i.e. the TSE-plot, displays the contribution form axial-, rotational- and hydraulically specific energy as separate graphs. Another important output is the ratio between TSE and hardness, ADE. The operator can easily change the plots in order to display the desired information. The number of plots is also unlimited, meaning that meta data regarding the results can be displayed in separate plots.

In order for the plot to appear more smoothly, and to remove the effects of remaining discrepancies in the drilling data, the agent calculates average values for a number of variables in matrix C. The resulting values are copied from matrix C to a new matrix, "C2" , and then again, to another new matrix, "C3" , corresponding to each of the two average-calculations. This results in a 1:25 ratio between matrix C and C3.

Gamma correction is used in order for spikes to be removed from the plots (Toverud 2016). The ratio, R, between two points in a data set, a and b, is basically

$$R = \frac{a}{b}, \tag{45}$$

where $a > b$. If the dataset is raised to the power of n, this ratio will become

$$R^n = \frac{a^n}{b^n} = \left(\frac{a}{b}\right)^n \tag{46}$$

The ratio between R^n and R yields the following expression.

$$\frac{R^n}{R} = \frac{\left(\frac{a}{b}\right)^n}{\left(\frac{a}{b}\right)} = \left(\frac{a}{b}\right)^{n-1} \tag{47}$$

If $n = 1$, obviously no change will appear when the data set is plotted. If $n > 1$ the relation between a and b will increase, thus magnifying the spikes on the plot. If $n < 1$, however, the spikes on the plot will diminish, and the plot will appear smoother. The key is to find a value for n, which will dampen the spikes, thus making the plot easier to interpret, but still keep the characteristics of the plot. This is achieved by using $n = 0.1$ in the plotting of the results from the agent. 0.1 is a somewhat arbitrary value selected after some trial and error.

4.4.3 Testing and troubleshooting

Block velocity instead of ROP

Due to the recorded ROP being recorded based on depth, i.e. it is recorded as an average of the lastly drilled meter; it causes deviations in the hardness, MSE and ADE calculation, which otherwise uses variables recorded every 4.5 second. Therefore, instead of using the ROP from the drilling data, more accurate results can be achieved using block velocity as input instead (Skalle 2015; Swahn 2015).

Fig. 20 shows a plot of both the recorded ROP and the calculated block velocity. The two graphs match well. Still, there are noticeable differences. The block velocity fluctuates more than the ROP, probably because it is based on a larger number of

elements.

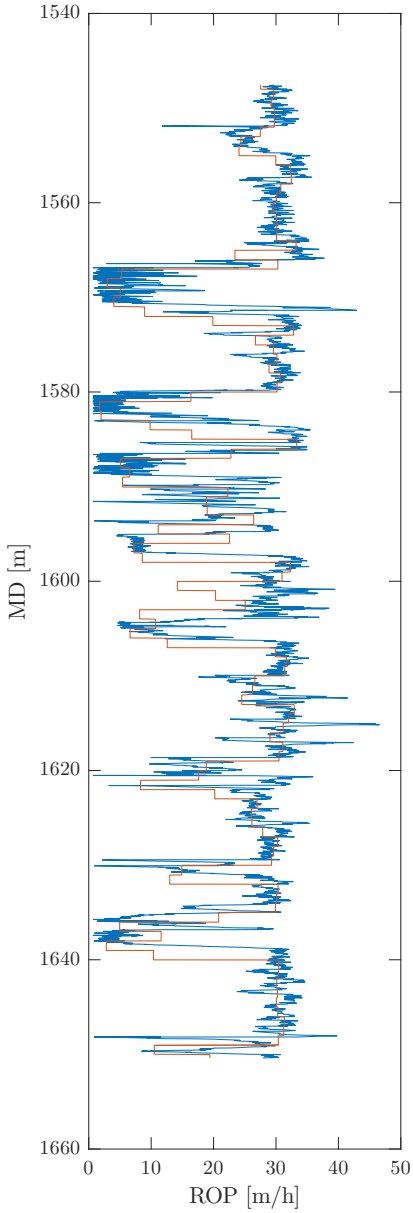

Figure 20: ROP (orange) and block velocity vs. depth. This hundred-meter interval in section 17 $^1/_2$", shows that the two graphs match well, but that block velocity clearly fluctuates more. It is also possible to identify a lag in ROP.

Removal of discrepancies in drilling data

Real-time drilling data will usually contain various types of discrepancies. These can be minor deviations from the preset interval between recordings, or anomalies, e.g. missing recordings and abnormal values of certain variables.

As the time between each recording is 4.5 seconds, an occasional deviation of up to one second proved to entail a small, or even negligible, effect on the calculations. These deviations happen often and inconsistent, and follow no fixed pattern. Calculating the moving average for the most critical variables ensures that the time-related discrepancies can be considered insignificant with regard to the accuracy demanded by the mathematical models.

Anomalies caused by missing data, on the other hand, may have, and had, for some instances, considerable effects on the calculations. They may be caused by an interruption in the communication between the BHA and the surface.

For instance, when calculating the hardness of the formation, ROP is one of the parameters used, and is calculated based on block position and time, i.e.,

$$\text{ROP} = \text{Block velocity} = -C_t \cdot \frac{\text{BPOS}_\text{i} - \text{BPOS}_\text{i-1}}{\text{Time}_\text{i} - \text{Time}_\text{i-1}} \tag{48}$$

BPOS [m] is the block position, i is the current element in the drilling data, and thus, $i-1$ is the previous element. C_t is a factor used to convert time from date numbers to hours, and the minus sign is implemented in order for the ROP to have positive value downwards.

Time-related variables in general and position variables in specific, need to be recorded continuously, as inconsistent recording may have a considerable impact on the values of the variables.

This type of anomaly proved to be a problem for especially one case in the 8 ½"-section of well 147. As can be seen in Fig. 21, data recording of both measured depth (DMEA) and block position (BPOS) halted for some time. When resumed, the actual increase in hole-depth and change in block position appeared to happen instantaneously.

The sudden change of 7.3 meters appears to have happened over a period of 4.5 seconds, which, using Eq. 48, would yield an approximate ROP of:

$$\text{ROP} = \frac{7.3\ m}{4.5\ s \cdot 1\ h/3600\ s} = 5.8 \frac{\text{km}}{\text{h}} \tag{49}$$

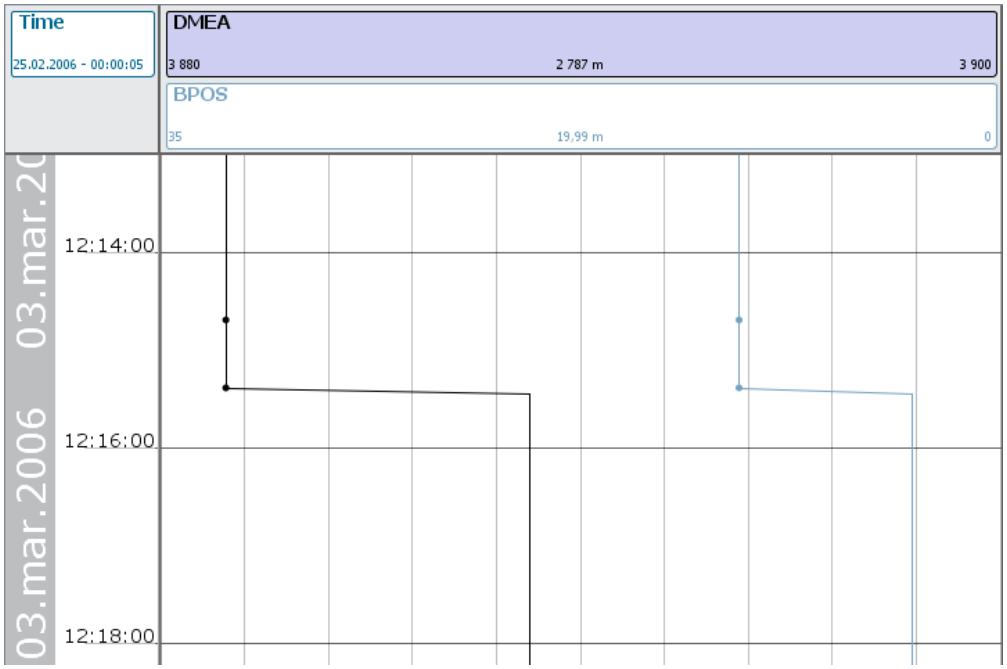

Figure 21: Instant change in measured depth (DMEA) and block position (BPOS) because of inconsistent recording. On March 3, 2006, the recording of some variables halted for a period of 55 minutes. When resumed, a sudden change in depth and position appeared (Verdande Analytics).

This caused an erroneous value for ROP, as it was in fact 7.96 meters.

Considering the formula for hardness, based on Eq. 12,

$$\text{Drillability} = K = \frac{1}{\text{Hardness}} = \frac{R}{DWN} \tag{50}$$

D, W and N being TVD, WOB and RPM respectively, and the fact that the constants in the denominator approximates 1, an ROP of 5.8 km/h would cause the drillability to sky rocket and thus, the hardness to plummet. This is obviously unrealistic, and removal of such anomalies is necessary before further calculations can be made.

The agent requires data from drilling only, and the script has an expression implemented in order to isolate this data. The problem is that the conditions that need to be met are true for the data even though anomalies such as these are present, i.e. they occur during drilling. As of now, the best solution is to manually remove these parts of the data, and focus on data without this type of anomalies. Further discussion on this topic can be read in the section about further development.

A third common discrepancy in the drilling data is the recording of odd values. They

typically appear as abnormal fluctuations in measured depth, but are present in other parameters as well, e.g. negative RPM. These discrepancies may have considerable impact on the calculations, but are easily removed using a simple expression in the script.

An example is the removal of unrealistic fluctuations in measured depth. The depth of a drilled hole can obviously not decrease, only increase or remain the same over time. The exception being during a cementing operation. In spite of this, there are several observations of depth reduction in the MD-graph. Demanding that a MD-element in the drilling data smaller than the previous element is equal to the previous element, i.e., in MATLAB-code:

```
% Preventing DMEA(i+1) to be less than DMEA(i)
for i= 2:Size
    if B(i,2) < B(i-1,2)
        B(i,2) = B(i-1,2);
    end
end
```

Removal of data from other activities

As mentioned above, the only activity relevant for an efficiency and hardness study is drilling. Therefore, data from activities, such as tripping, reaming, etc., must be removed. This is achieved using a series of conditions, all true only during drilling. The conditions are covered in its entirety in section 4.4.2.

Originally, there were three conditions involved; Δbit, WOB and RPM. They proved to be inadequate in terms of filtering out data from drilling. I.e., data leading to erroneous values for ADE and hardness were still being carried on. A couple of conditions involving MFI and ROP had to be added to ensure that this did not happen. This was a result of analysis of the sorted drilling data after the erroneous results from the ADE- and hardness-calculations.

The condition regarding MFI was added to involve yet another factor present during drilling. The ROP-condition is in fact made up of two separate conditions, one stating that ROP must be larger than or equal to 0, and another one stating that the moving average of ROP has to be larger than 0.1 m/h. These six conditions adequately filtrate out all other activities than drilling.

Sorting of data

An anomaly in the drilling data from the 17-5.m-file was found during the development

and testing of the agent. The file is supposed to range chronologically over a period. The data from section 17 ½" was however somehow cut in half, causing the recording with the smallest serial date number to appear as element 466,394. Fig. 22 illustrates this. A fix of the 17-5-file was later presented (Swahn 2015). Nevertheless, the script

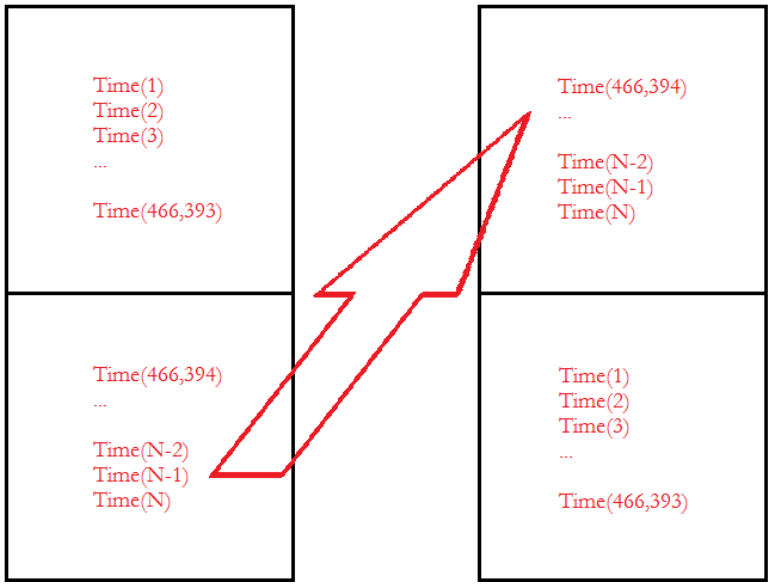

Figure 22: The shuffling of elements experienced in the 17 ½"-file. The column to the left illustrates how the list elements should be arranged; the smallest serial date number first, increasing downwards. The column to the right shows how file 17-5 was in fact arranged. The arrow indicates the placement of the out-of-place data before the fix.

sorts this issue out by use of the command "sortrow". A new matrix, "A2" , is the product of this sorting action. It contains all the elements from A, sorted with respect to time, hence ensuring chronological arrangement of all the list elements.

Implementation of new method for matrix-creation with RTDD

The fundament of the agent is the creation and operation of matrices of predetermined sizes. This is clearly a tidy arrangement when using historical drilling data, and has proved to be an easy way to manage all the drilling data. Nevertheless, when using RTDD, predetermined sizes of the matrices is not possible, as the sizes are not set.

While this was somewhat irrelevant in the case of this agent, an attempt was made to create a matrix of small size, and implementing a new line, a vector, so to speak, for every new element in the drilling data. This was carried out in the part considering loss of torque along the drillstring.

When the BHA exits the casing during drilling of the very first meters of a new section, the friction has to be calculated individually for casing and open hole. As the BHA moves out of the casing, increasingly more of the BHA experiences friction from the rock formation, and hence the friction from the casing becomes less. A clever way of calculating the interaction of these two frictional forces was implemented, and proves to function optimally.

Hardness and ADE both dependent on ROP

Investigation of the final formula for ADE, i.e. formula Eq. 38, versus the Bourgoyne and Young method selected for this agent, showed that ROP is a common factor for both ADE and hardness. Combining Eqs. 12 and 37, would result in ROP being removed from the term accounting for rotational- and hydraulic specific energy. ROP is then only represented as a factor in the axial specific energy term, which as will be discussed further in section 5.7.2 accounts for approximately 1.5 percent of total MSE.

Implementing the current hardness term directly into the ADE formula is therefore regarded as inexpedient. First of all because hardness, as a parameter, is meant to give an indication of drilling efficiency, but also because UCS is the preferred measure for hardness for equation Eq. 38.

Since ROP is a significant common factor for both equations, the most convenient presentation of hardness is as a separate graph plotted next to TSE. The ratio between the two is equal to the total ADE. This also proves useful for further analysis in the following chapters when presenting results, and investigating the trends of the two curves in relation to each other.

This change to the agent only applies if hardness is calculated based on drilling parameters, not for UCS. UCS would be a mere scalar, and could be implemented directly into the ADE model.

5 Results

This section shows the results of the conducted testing of the improved MSE model, i.e. the ADE model, also referred to as the "adjusted" model. The results will be presented shortly and in a clear form, and plots from the agent will be used to illustrate important aspects. Most plots are represented as specific energy, meaning the amount of input energy needed to remove one volume of rock per unit of time. All plots are based on data gathered from the three sections of well 147. The range of the graphs are individually selected for each of the plots in order to most easily be able to identify their features. This means that they differ from figure to figure.

5.1 Modelled torque-loss and well-path

Fig. 23 illustrate the well path inclination modelled by Eqs. 39 and 40, for the 8 ½"-section. Figures for the 12 ¼"- and 17 ½"-section are found in appendix B, Figs. B.1 and B.2 respectively. The approximated well path inclination forms the basis on which the calculated torque loss is calculated based on Eqs. 30 and 31. These losses together with total torque measured at surface for the 8 ½"-section, are illustrated in Fig. 24. The difference between the two is the calculated torque exerted at bit. Figures for the 12 ¼"- and 17 ½"-section are found in appendix B; Figs. B.3 and B.4 respectively.

5.2 Adjusted rotational energy

Fig. 25 illustrates the difference between the new method for calculating torque loss illustrated in Fig. 24, and the original method used for MSE_{eff}. The additional line shows the estimated torque loss along the drillstring, based on a constant loss factor estimated at start of the section. Figures for the 12 ¼"- and 17 ½"-section are found in appendix B; Figs. B.5 and B.6 respectively. Fig. 26 illustrates the difference in rotational specific energy when applying the torque estimated at bit, using the original method versus the method used for this paper.

5.3 Adjusted axial energy

Fig. 27 shows the axial specific energy as given in the original MSE formula by Teale. Fig. 28 shows the hydraulic specific push-off energy inflicted on the drillstring due to recoil from the flushing through the bit. The adjusted axial energy is the difference between those two.

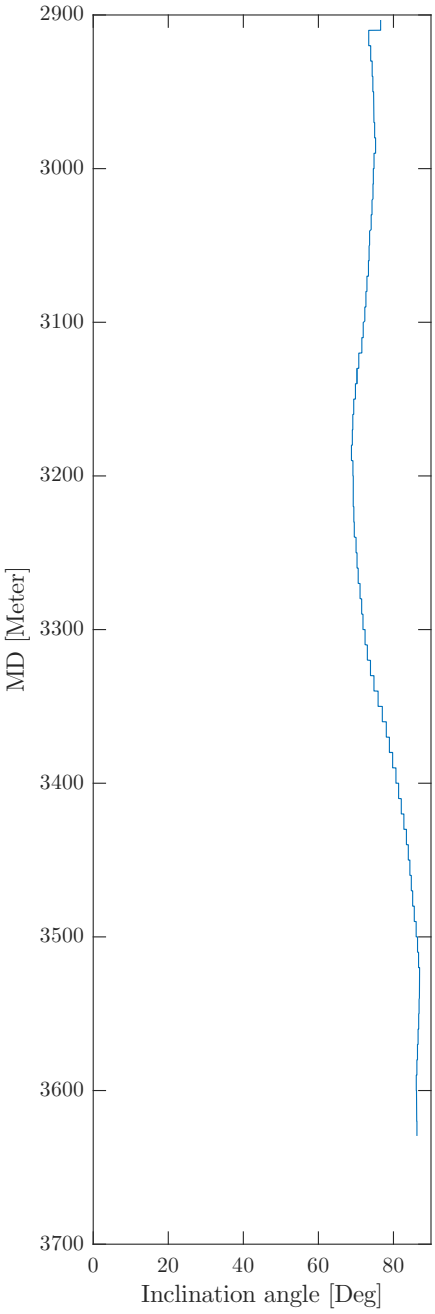

Figure 23: Inclination angle vs. MD in the 8 $^1/_2$"-section.

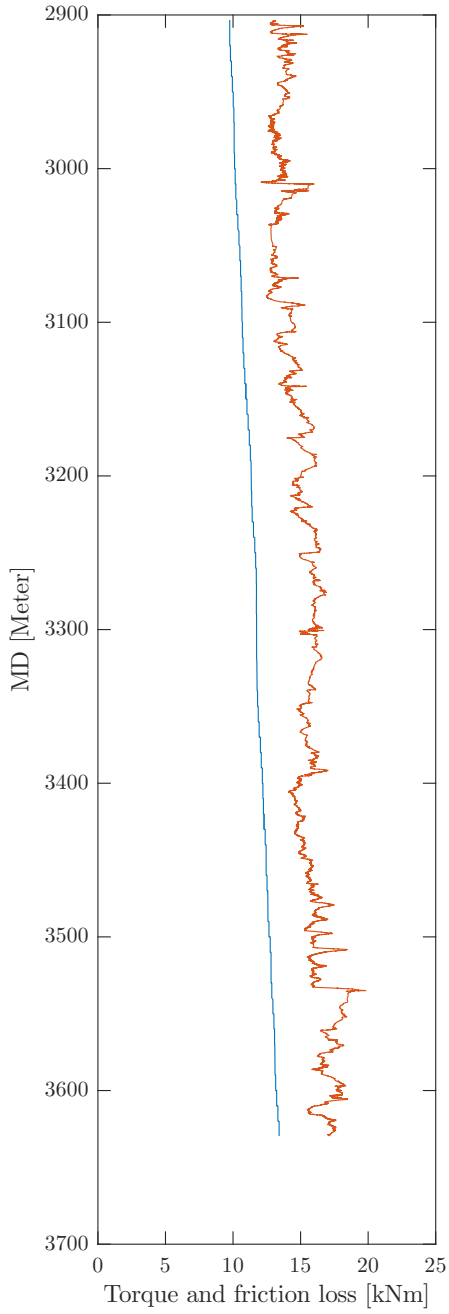

Figure 24: Measured torque (red) and calculated friction loss vs. MD in the 8 $^1/_2$"-section.

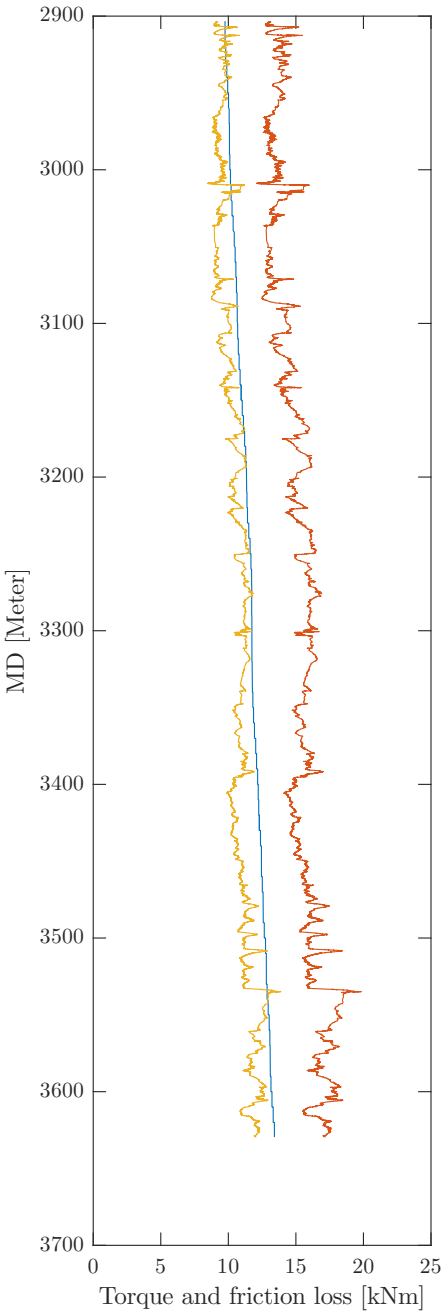

Figure 25: Torque measured at surface (red), calculated friction loss based on the new adjusted method (blue) and estimated friction loss in accordance with original method (yellow) vs. MD in the 8 1/2"-section.

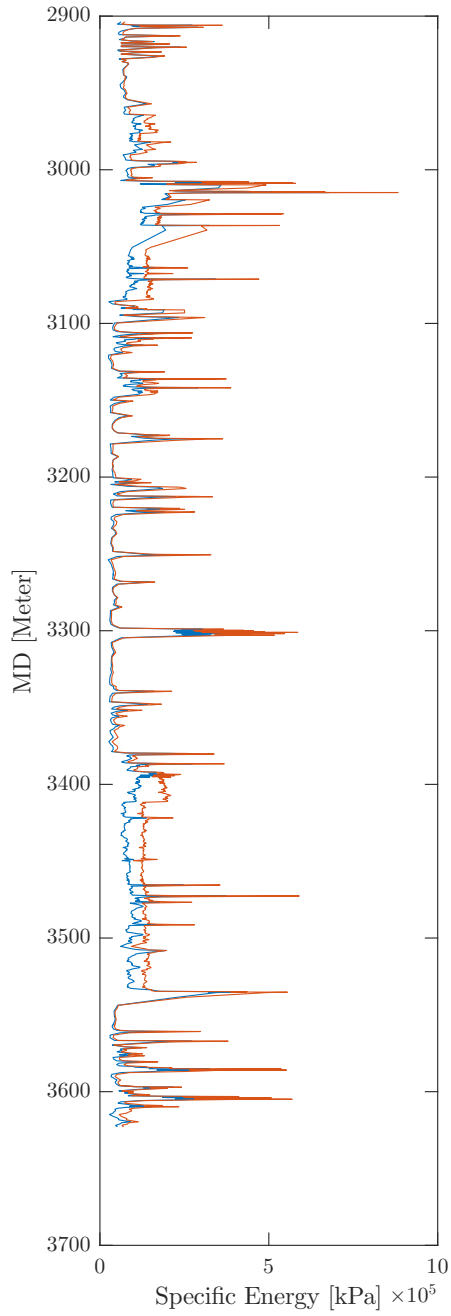

Figure 26: Rotational Specific Energy; based on friction loss factor from the original formula (red) and calculated friction loss based on the new adjusted method (blue) vs. MD in the 8 1/2"-section.

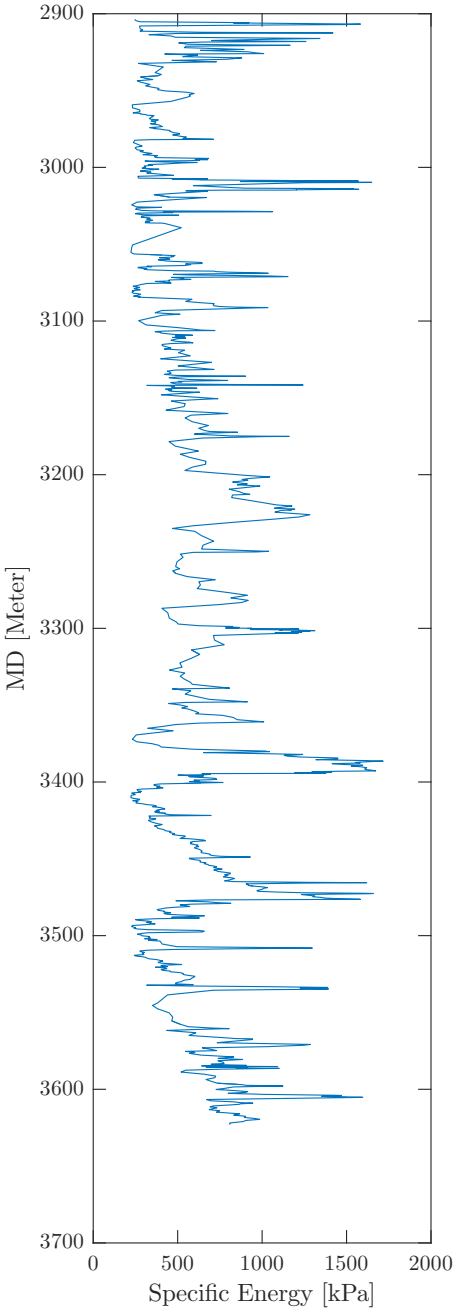

Figure 27: Axial Specific Energy vs. MD in the 8 1/2"-section.

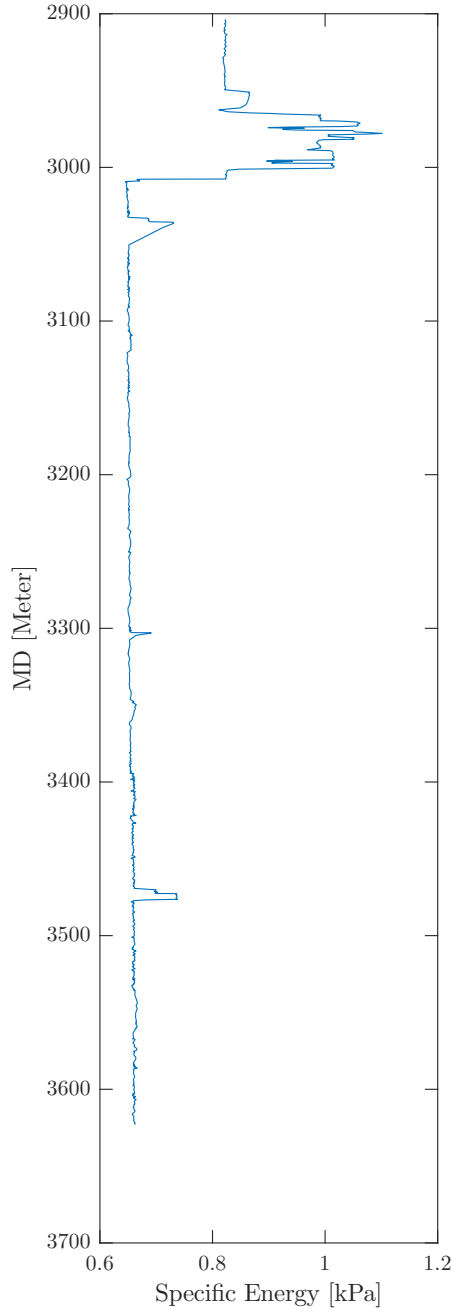

Figure 28: Axial push-off force as Specific Energy vs. MD in the 8 1/2"-section. Notice the difference in magnitude, indicated by the scale on the horizontal axis.

5.4 Hydraulic energy

As suggested by the HMSE formula, Eq. 23, the hydraulic energy can be calculated separately. The hydraulic energy is shown in Fig. 29.

5.5 Actual Drilling Energy

Plots of specific energies for the 8 1/2"-section, as suggested by Eq. 38, are shown in Fig. 30. The span between each line represents each of the three specific energies, axial, rotational and hydraulic from left to right accordingly. These three combined make up the TSE. Formation hardness is deliberately left out, due to the close relationship to ROP for both the TSE- and the hardness method. Figures for the 12 1/4"-section and 17 1/2"-section are found in appendix B; Figs. B.7 and B.8 respectively.

To allow for easier interpretation of the results, Fig. 31, Fig. B.9 and Fig. B.10 represents the same results as above, adjusted with gamma correction with regard to dampening of the spikes on the graphs in the plots. This adjustment also allows for easier interpretation of the magnitude of the axial specific energy.

The difference between the output specific energy of the new method and the original MSE method is shown in Fig. 32. Hardness is also here neglected for the ADE-method. Figures for the 12 1/4"- and 17 1/2"-section are found in appendix B; Figs. B.11 and B.12 respectively.

5.6 Actual drilling efficiency

As explained in section 3.4, ADE is given as the ratio between TSE and formation hardness. Due to the degree of correlation between the input variables of drilling energy and formation hardness in this script, plotting these two separately is regarded more illustrative. Fig. 33 shows total drilling energy based on Eq. 36, and Fig. 34 illustrates formation hardness based on Eq. 12 for the 8 1/2"-section. Figures for the 12 1/4"-section and 17 1/2"-section are found in appendix B; figs. B.13 to B.16 respectively.

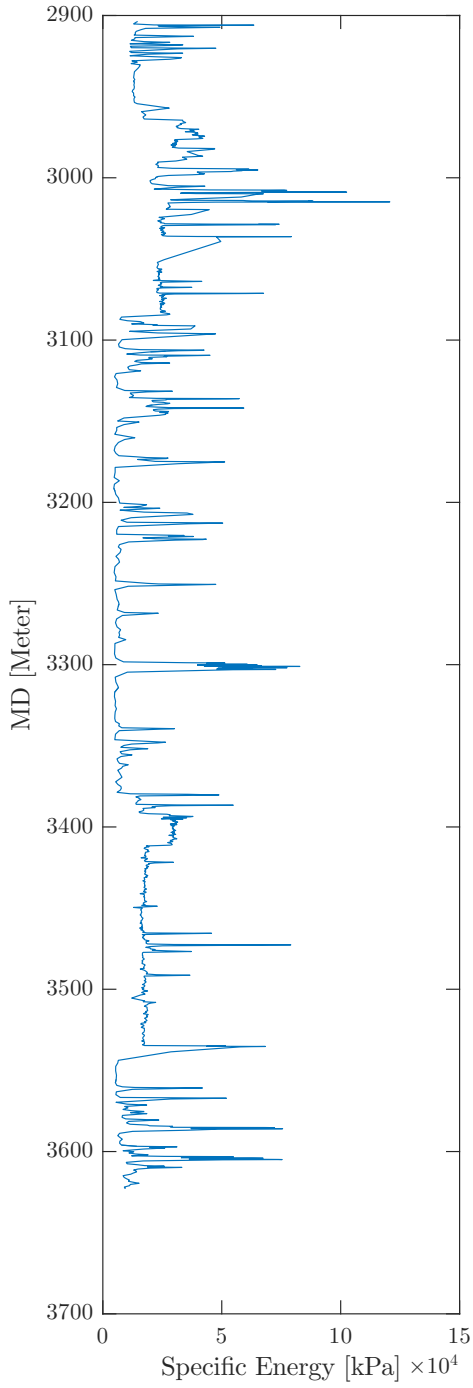

Figure 29: Hydraulic Specific Energy (of TSE) vs. MD in the 8 ½"-section.

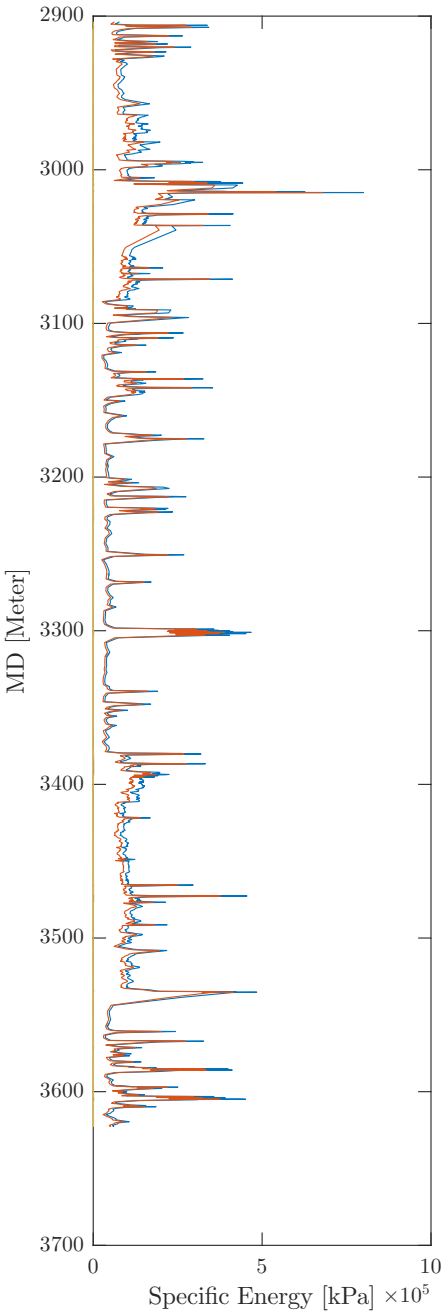

Figure 30: Specific Energy vs. MD in the 8 $^1/_2$"-section. Axial Energy (yellow), Axial and Rotational (red) and Axial, Rotational and Hydraulic (TSE) (blue).

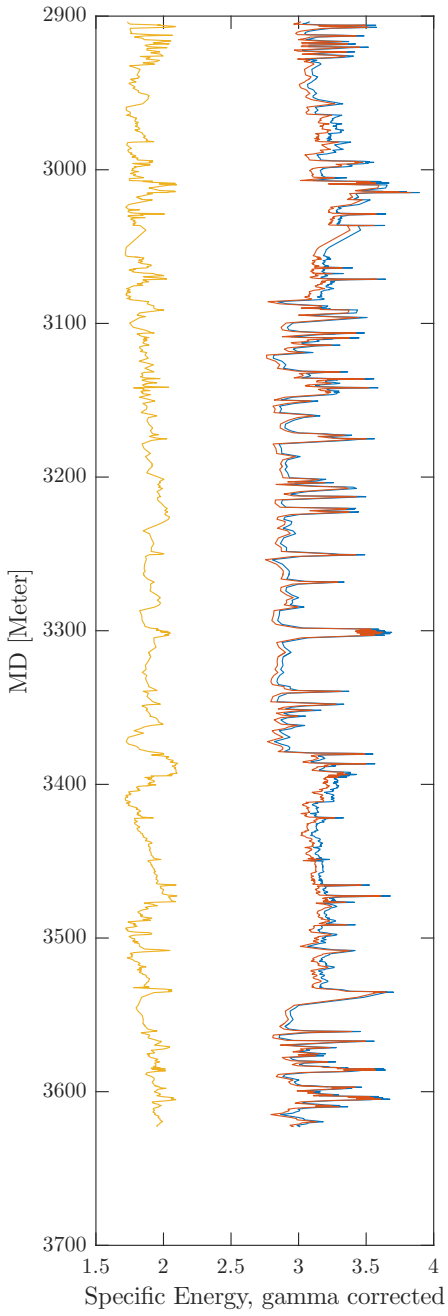

Figure 31: Specific Energy vs. MD in the 8 $^1/_2$"-section, adjusted with gamma correction, as shown by Eq. 47. Axial Energy (yellow), Axial and Rotational (red) and Axial, Rotational and Hydraulic (TSE) (blue).

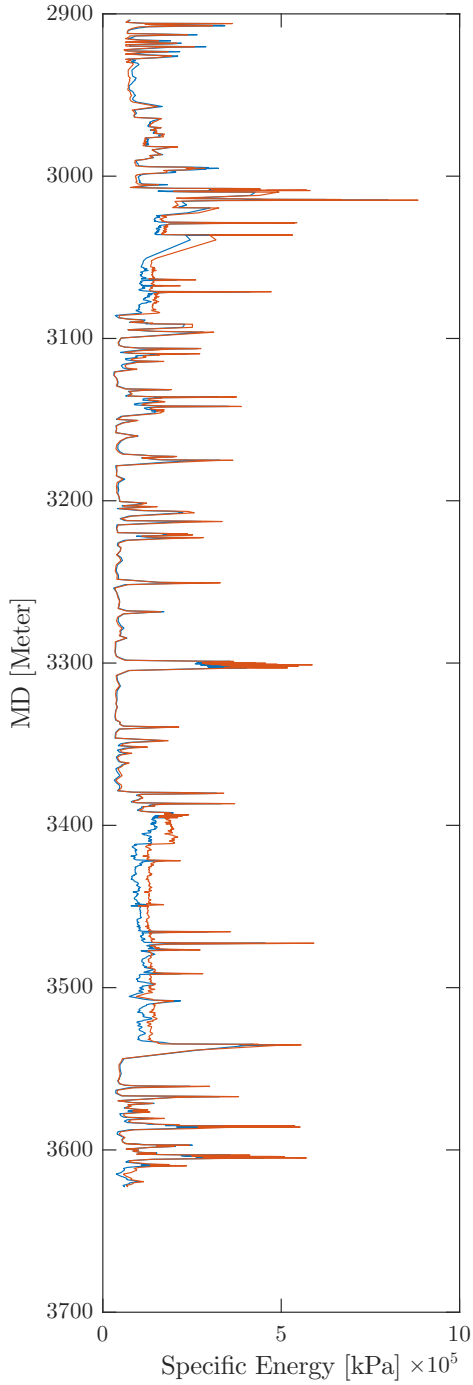

Figure 32: Total Specific Energy (blue) and Mechanical Specific Energy (red) vs. MD in the 8 $^1/_2$"-section.

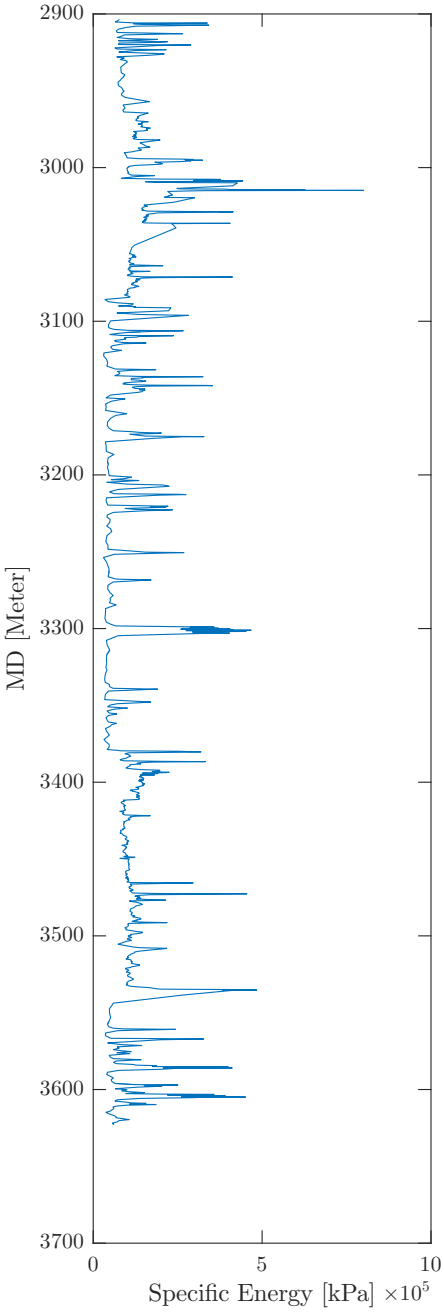

Figure 33: Total Specific Energy vs. MD in the 8 $^1/_2$"-section.

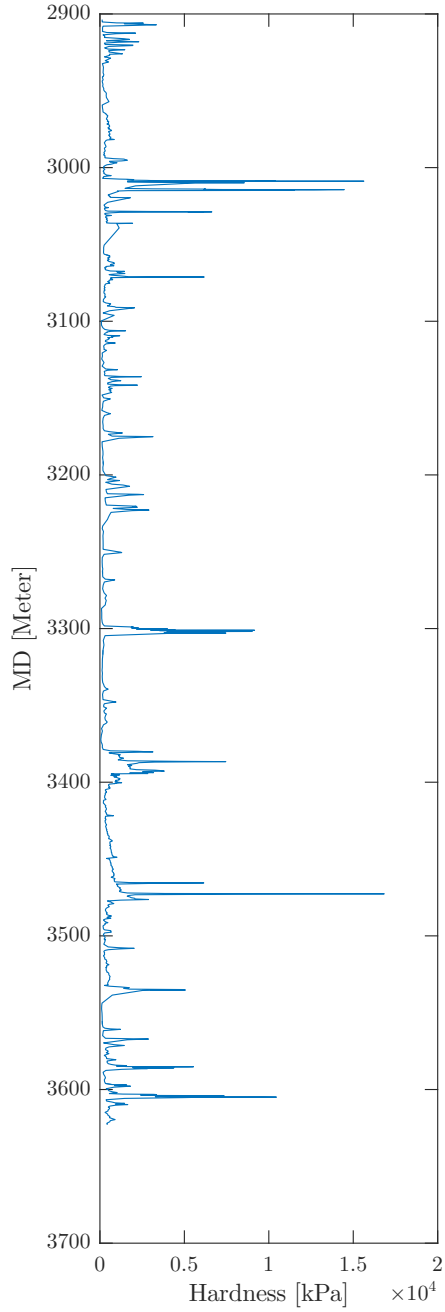

Figure 34: Formation Hardness vs. MD in the 8 $^1/_2$"-section.

5.7 Evaluation of results

5.7.1 Well-path

The well path estimation was performed, mainly to simulate well path as RTDD compatible with the mathematical agent. This would require a method with continuous estimations, based on already existing drilling data. It was also important the implemented method could be used for real-time measurements of well path, and be compatible with both azimuth and inclination variation.

The assumption that azimuth remained unchanged during drilling of well C-47 was made due to lack of information in the database file, i.e. azimuth was unavailable as a real-time drilling parameter. However, the survey of the well showed that this was not the case, as is shown in table 4.

Table 4: Clippings from the survey of well C-47. Listings under azimuth (Azi) shows that it does not remain unchanged.

Well	MD [m]	Inc [deg]	Azi [deg]	TVD [m]	N/S [m]	E/W [m]	DL [deg/30m]	Ver [m]	Instr
147	414,0	2,99	27,33	413,8	43,6	8,3	1,35	-5,9	Gyro
147	441,5	2,60	20,39	441,3	44,8	8,9	0,56	-6,5	Gyro
147	454,5	2,43	16,81	454,3	45,4	9,1	0,53	-6,8	Gyro
147	482,5	1,74	0,80	482,3	46,4	9,2	0,96	-7,4	Gyro
147	510,0	0,69	19,17	509,8	46,9	9,3	1,21	-7,8	Gyro
147	524,5	0,22	20,92	524,3	47,0	9,4	0,97	-7,9	Gyro
147	537,0	0,32	163,92	536,8	47,0	9,4	1,23	-7,8	Gyro
147	565,0	1,19	162,66	564,8	46,7	9,5	0,93	-7,5	Gyro
147	580,0	1,30	136,21	579,8	46,4	9,6	1,16	-7,2	Gyro
147	608,0	3,15	133,87	607,7	45,7	10,4	1,98	-6,1	Gyro
147	608,0	3,15	133,87	607,7	45,7	10,4	1,98	1,5	Gyro
147	640,0	4,68	136,50	639,7	44,1	12,0	1,44	3,3	Gyro
147	670,0	8,63	137,36	669,5	41,6	14,3	3,95	6,0	Gyro
147	740,5	12,90	141,97	738,7	31,5	22,8	1,85	15,7	Gyro
147	777,0	15,66	141,67	774,1	24,4	28,3	2,27	22,6	mwd
147	804,5	18,40	141,49	800,3	18,1	33,3	2,99	30,5	mwd
147	832,2	20,76	141,19	826,4	10,8	39,1	2,56	39,7	mwd
147	859,9	22,85	141,02	852,1	2,8	45,6	2,27	49,9	mwd
147	886,5	25,12	140,50	876,4	-5,5	52,4	2,57	60,7	mwd
147	914,4	26,87	140,30	901,6	-15,0	60,2	1,88	72,8	mwd

Nevertheless, as described in section 3.3.1, the model used in the agent is compatible with azimuth input as well, as long as it is available as a parameter in the data set. The principle of lost torque is properly illustrated using inclination as input only.

5.7.2 Input energy

To find the exact effect for each of the three forces, the results presented in Fig. 30, Fig. B.7 and Fig. B.8 were conducted to integration over the entire section. As seen in these figures, the input energy is dominated by rotational specific energy, which during the total drilling of each section accounts for 82, 82 and 79 percent of total energy reaching the formation in the 8 ½"-, 12 ½"- and 17 ½"-section respectively. The remaining 20 percent are mostly dominated by hydraulic specific energy, leaving axial specific energy at 0.5-1.5 percent close to invisible when the plot is not modified with gamma correction. Due to the surprising nature of these results, the ratio between axial- and rotational energy was further investigated using standardized drilling parameters for both the original MSE- and the corrected TSE-method. Input values are shown below, and results in table 5.

WOB = 10 tons, flowrate = 3000 lpm, torque at bit = 5 kNm, RPM = 100 rpm, ROP = 15 m/h, SPP = 120 bar, diameter of bit = 0.311 m (12.25") and bit efficiency factor = 0.35.

Table 5: Specific energies based on common drilling parameters.

Term	**Magnitude** [kPa]	**Contribution**
Axial	1011	1.6%
Rotational	45429	75.8%
Hydraulic	13553	22.6%
Total Specific Energy	59993 kPa	100.0%

This ratio is also confirmed by similar findings using the original MSE-method.

As seen in the drill-off test illustrated Fig. 1, there is a clear correspondence between WOB and ROP, even at constant RPM. As mentioned in section 2.2.1, Hamrick (2011) developed a model for expressing torque as a function of WOB. The theory was based on the assumption that torque may be modelled as linear function of WOB within a normal processing range. During his research, this linear correlation was explored and identified for a number of tests, as shown in Fig. 35.

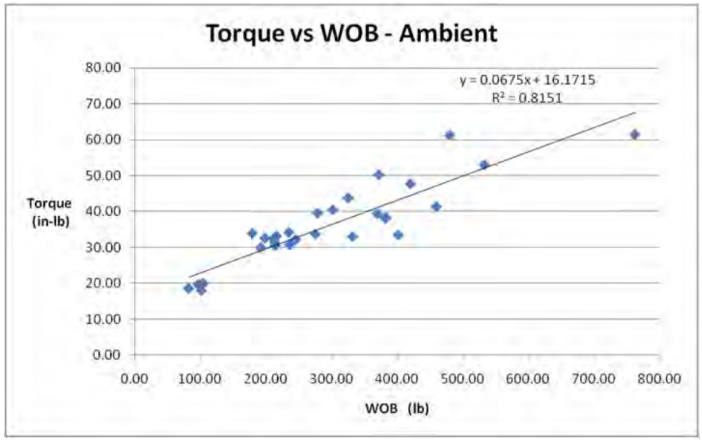

Figure 35: Torque as a linear function of WOB for ambient marble (Hamrick 2011).

$$\text{Torque} = f(\text{WOB}) = A_0 + A_1 \cdot \text{WOB} \tag{51}$$

When taking this into consideration, it is fair to assume that the contribution from the axial energy has a larger effect on the rotational energy, than as a stand-alone push force, when considering the drilling progress. While all three energy inputs included in this method is based on the basic definition of axial, rotational and hydraulic work, the three forces acting together might behave different than as three independent forces.

Axial energy

As seen in Figs. 27 and 28, the adjustments made to the axial energy on behalf of the hydraulic push-off force create a marginal difference from the original method. Due to the already small contribution from the axial energy as a whole, this adjustment does not affect the total energy, and could therefore be neglected in order to create a simpler expression.

Hydraulic energy

At close to 20 percent, the hydraulic energy clearly has a larger effect on drilling progression than the stand-alone push force given as the axial energy. As seen in Fig. 30, Fig. B.7 and Fig. B.8, the hydraulic energy is equal to 20, 18 and 18 percent of total energy for the 17 ½"-, 12 ¼"- and 8 ½"-section respectively. While this addition to the formula does make the model more complex, neglecting to include a variable factor of this magnitude would greatly reduce accuracy of ADE. The problem with this

method is that it is greatly dependant on exact values regarding bit parameters. Still, if proper bit-specifics are available, hydraulic energy should be included for all future use.

Rotational energy

As expected, the largest contribution for progress for a rotating drillstring was the rotational energy, accounting for close to 80 percent, depending on the manner of estimation. Adjustments made to this energy contribution are therefore close to proportional to the total output of both the TSE- and the ADE-formula.

For the original MSE_{eff} formula, a constant between 0 and 1 is implemented to account for vibrations and transmission losses along the wellbore in the entire section. Schlumberger demonstrates this in their case study, where instead of the normal bit-factor of 0.35 (Ahmadi et al. 2012), a factor of 0.125 was multiplied with the total expression to account for total losses. For the new method, the loss factor has been replaced; loss calculations are performed for each source of energy separately. The new method also separates calculations accounting for transmission losses along the drillstring, and at bit. For the rotational energy, the effect of this adjustment compared to the original method is illustrated in Figs. 26 and 27. The original MSE method uses a constant efficiency factor of 70 percent, calculated at start of the section, and fluctuates with an increasing trend compared to the improved method, which is constant.

While drilling forward, the original MSE method, always models as if 30 percent of the measured surface torque is experienced at the bit. As seen in Fig. 25, this simplification seems not to be too far off during drilling. For Figs. B.5 and B.6, this simplification seems to be a bit more inaccurate.

The problem with the original efficiency factor used in Eq. 5 occurs during scenarios where there is a change in torque compared to when the factor is calculated or estimated. This means, that if an increase in input torque at surface is performed at a specific depth to increase ROP, one could expect close to 100 percent of this additional energy to be transferred to the formation through the bit, as no additional loss to the wellbore is expected. The total increase in surface measured energy should therefore be considered as downhole torque. For the simple MSE method, 70 percent of this additional torque would be considered loss along the trajectory, and only 30 percent would be used. This would unjustly reduce the MSE-value, resulting in the efficiency appearing higher. The new method takes care of this problem with continuously calculating the actual loss to formation based on current data, rather than previous data, identifying which increase in torque was exerted at bit.

This type of situation can be detected at 3400-3500 mMD in the 8 ½”-section. As seen

in Fig. 37, this interval contains a tough formation followed by a softer formation. In response to this reduction in formation hardness, the surface torque is reduced as seen in Fig. 36. Assuming this reduction comes from the reduced torque between the bit

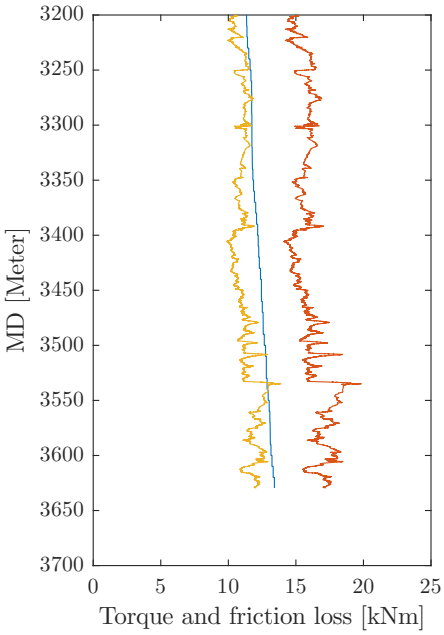

Figure 36: Torque at surface & Torque fr. loss vs. MD in the 8 1/2"-section. Clipping from Fig. 25.

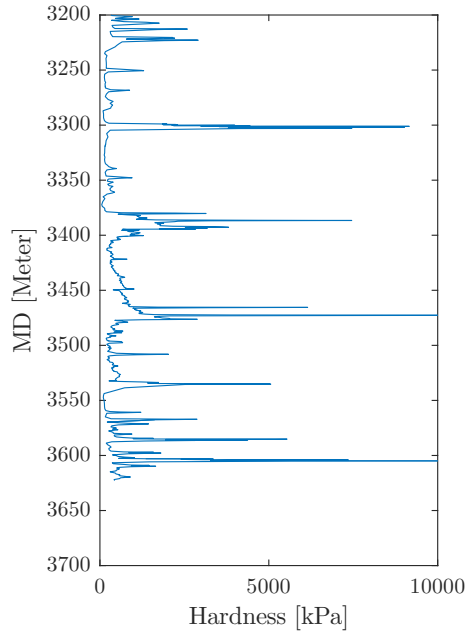

Figure 37: Hardness vs. MD in the 8 1/2"-section. Clipping from Fig. 34.

and the softer formation, the torque-loss between the drillstring and wellbore should be considered constant. As seen in Fig. 37, for the original MSE method, 70 percent of this reduction is modelled as reduced friction to the wellbore, leaving bit torque almost unaffected. Since no additional length or friction has been added to the wellbore, the new method calculates no change in loss along the wellbore, in accordance with Eqs. 24, 30 and 31. The entire loss is therefore modelled as lost bit torque. As seen in Fig. 36 at 3410 mMD, a small increase in formation toughness leaves the two methods differing on bit torque estimation at close to 100 percent. Since input rotational specific energy is proportional with bit-torque, this margin of error is directly transferred, which means that the inefficiency will appear a lot higher than what is actually the case.

Another problem occurs with increased measured depth, especially for longer sections. While it is clear that increased depth results in increased friction between wellbore and drillstring, it does not always increase torque experienced at the bit. With a constant loss-factor, an increase in measured surface torque will result in an equal ratio

of increased bit torque. This is well illustrated in Fig. 25. For the simplified model the estimated bit torque increases, while in reality the bit torque stays close to constant, or even decreases. This means that for drilling sections of greater length, the margin of error becomes larger.

As mentioned earlier, the rotational energy accounts for close to 80 percent of the total ADE value. Since calculated torque is directly proportional to the rotational input energy of the ADE, this source of error would create an approximately equal error on total estimated efficiency. This means that the adjustments made to more accurately estimate bit-torque has a vital effect on total accuracy.

5.7.3 ADE compared to formation hardness

As explained earlier, the plots illustrating TSE, does not take formation hardness in to account. Comparing Figs. 33 and 34, TSE and formation hardness seems to depend greatly on the same input values. While both methods are affected by WOB, RPM, flowrate and ROP, they also differ on factors like torque, ECD, pore pressure and vertical compaction of formation. When investigating the impact each of the input variables had on each method, it became clear that both methods were greatly dependent to ROP.

Fig. 38 is a plot of ROP^{-1} versus depth for the 8 ½"-section. Placing Fig. 33 and Fig. 34 next to Fig. 38 illustrates the correspondence between TSE, formation hardness and ROP^{-1}.

The similarities between the drilling efficiency formulas, and ROP^{-1}, further demonstrate the importance of evaluating the efficiency plot against formation toughness. Because Bourgoyne and Young's method was the only one applicable with the given data, it is difficult to draw any real conclusions on the actual drilling efficiency on basis of hardness from these plots.

A second weakness of the current hardness model was early identified; a problem that becomes clear when comparing the hardness plot for each of the three sections (Figs. B.13, B.16 and 34) with each other. Since no data from a drill-off test was available, some of the input variables needed in order to properly quantify formation hardness were unavailable. One of these was $(W/d_b)_t$, i.e. the threshold WOB at which the bit begins to drill, which means that bit diameter was not considered in the calculations. As a consequence of this, the impact from the WOB-term in the model differ from each other in the three sections. This is especially apparent in the 8 ½"-section. This further reinforces the suggestion that the trend of the curve is of greater significance than the exact value for the plots produced with these data.

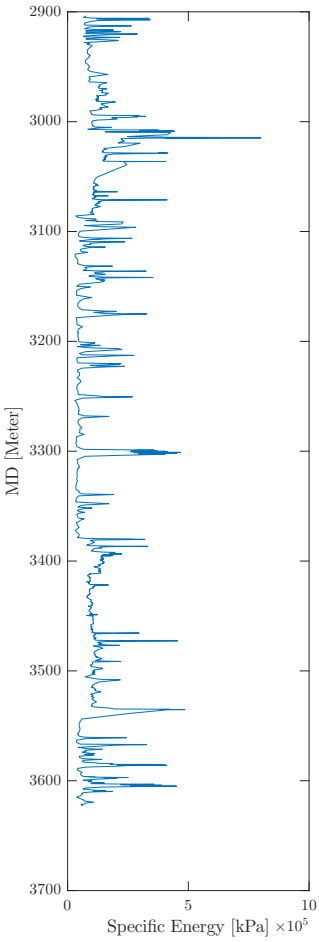

Figure 33: TSE vs. MD in the 8 1/2"-section.

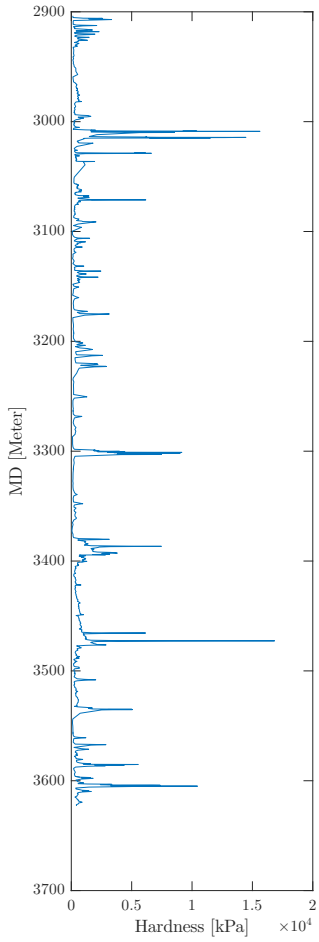

Figure 34: Formation Hardness vs. MD in the 8 1/2"-section.

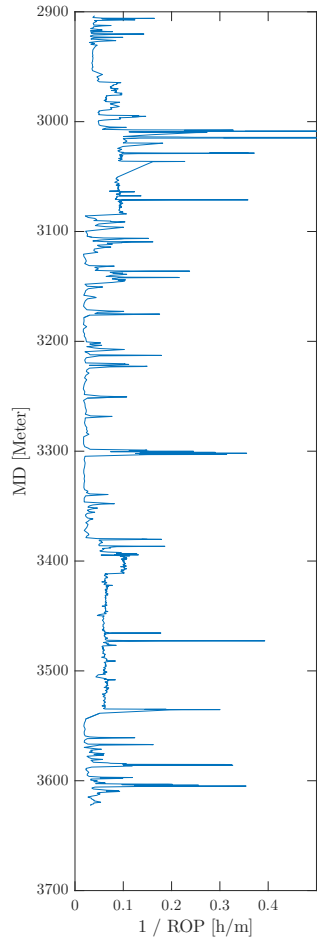

Figure 38: ROP^{-1} vs. MD in the 8 1/2"-section.

Still there are some examples where there is evident deviation between the two.

When looking at smaller increments, differences can be identified. Figs. 39 and 40 show different trends of section 12 1/4" from 2550 to 2700 meters.

On the hardness plot, spikes can be identified at 2580, 2610, 2635, 2675 and 2690 meters, without the same occurring to the same degree in the TSE-plot. To identify the source behind these spikes, Fig. 41 shows the axial specific energy from the TSE-plot.

These spikes occur due to an increase in WOB, and affect both the hardness and the axial input energy. Since the axial energy only affect the total energy by a factor of

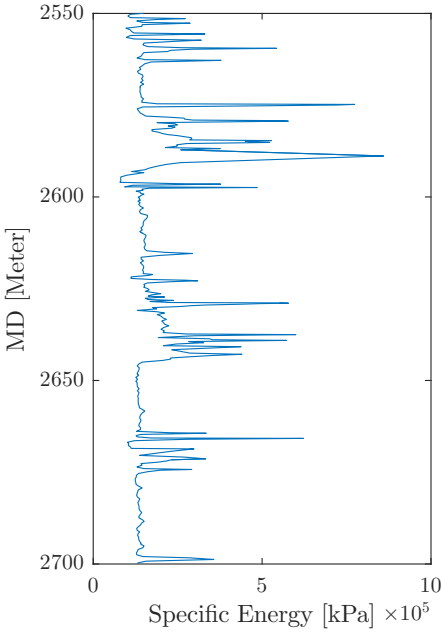

Figure 39: TSE vs. MD for the 12 1/4"-section. Clipping from Fig. B.13.

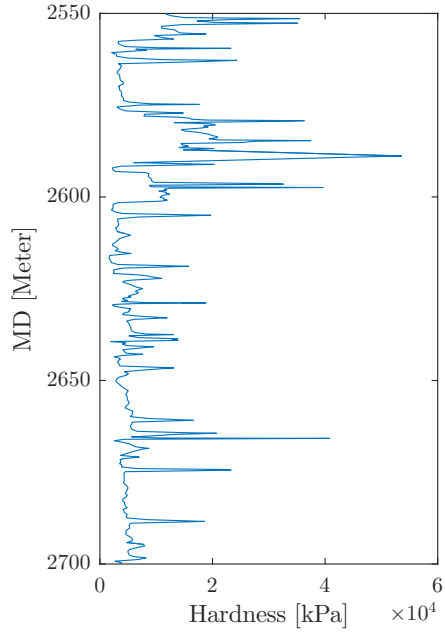

Figure 40: Hardness vs. MD for the 12 1/4"-section. Clipping from Fig. B.15.

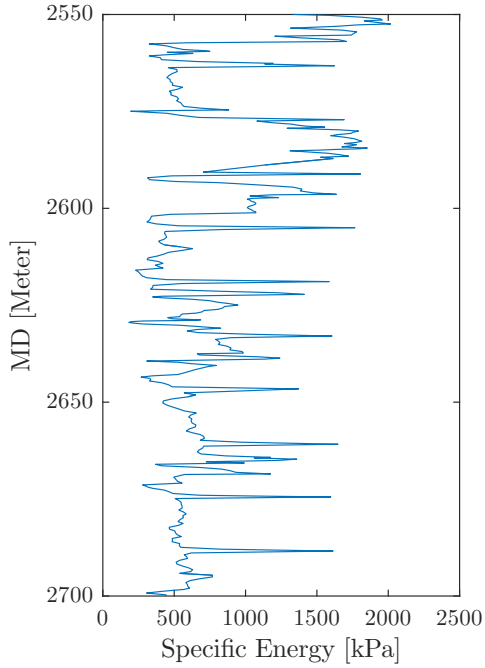

Figure 41: Axial Specific Energy vs. MD for the 12 1/4"-section.

1.5 percent, these spikes do not affect the total TSE energy to the same degree. This illustrates how the hardness formula by Borgoyne and Young, Eq. 12 is more affected by WOB than the efficiency formula.

Figs. 42 and 43 illustrate the TSE and formation hardness respectively, over a specific

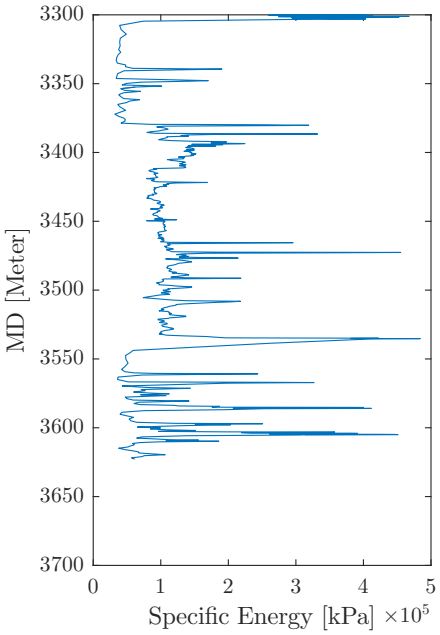

Figure 42: TSE vs. MD for the 8 1/2"-section. Clipping from Fig. 33.

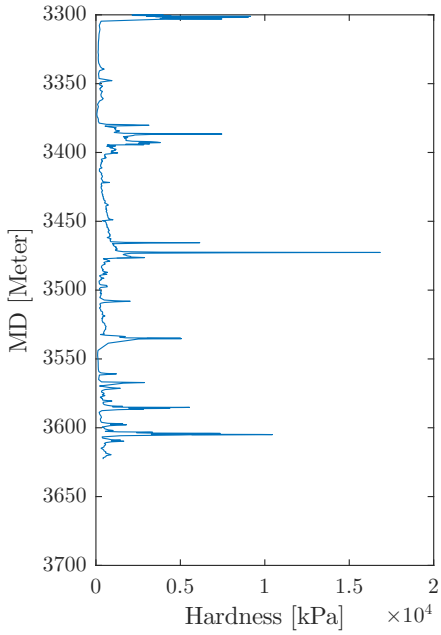

Figure 43: Hardness vs. MD for the 8 1/2"-section. Clipping from Fig. 34.

At approximately 3380 meters, the formation hardness increases and ADE increases accordingly. At 3400 to 3465 meters, the formation hardness decreases, while the input specific energy stays relatively high for the entire interval, indicating less efficient drilling than before and during the spike. The same problem occurs for the area following the spike in hardness at 3475 meters, where the following 50 meters are recognized by relatively high input energy compared to the formation hardness.

Figs. 44 and 45 illustrates the same phenomenon for the 17 1/2"-section.

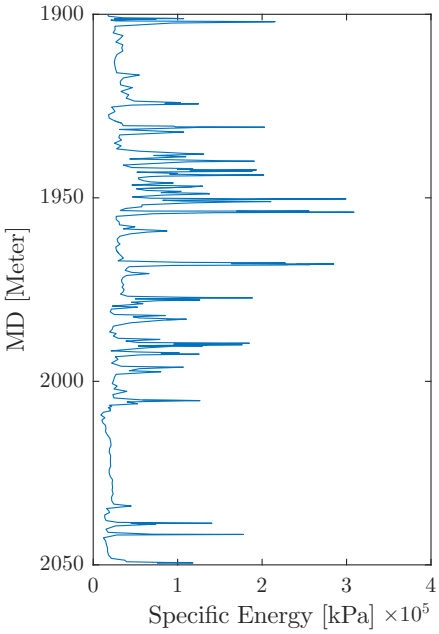

Figure 44: TSE vs. MD for the 17 1/2"-section. Clipping from Fig. B.14.

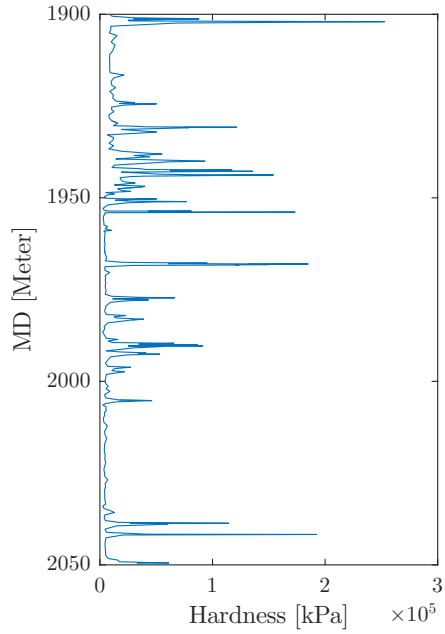

Figure 45: Hardness vs. MD for the 17 1/2"-section. Clipping from Fig. B.16.

Here, the formation hardness increases at 1940 meters, but returns to normal at 1950 meters. The specific energy input stays high and therefore inefficient for the next 60 meters.

As a hypothetical scenario, one could assume that this type of problem would occurred, as the driller identifies a tough formation due to reduction in ROP, and adjusted the input energy accordingly. Then due to lack of information the assumption was that the hard formation continued, so the input energy was kept constant for close to 150 meters, while the formation toughness varied, leaving the process inefficient for the larger part of the interval.

6 Self-assessment

An evaluation of own work will be covered in this chapter. Quality and shortcomings of the applied theory will be highlighted, as well as the strengths and weaknesses of the ADE-model and –agent. The reliability of the drilling data used during the testing and development of the agent, will be adressed, as well as other sources of error. Finally, future improvements and extensions of the work through solving or improving the shortcomings will be presented.

6.1 Applicability of the MSE-model

Teale's MSE-model, Eq. 4, showed that it was a proper way of defining drilling efficiency. Its applicability has since been approved times and times again. The idea is that drilling progression, i.e. ROP, can be maximized by optimizing a number of controllable drilling variables. The amount of energy put into the drilling process is somewhat fixed, as it is limited to rig- and DS-specifications, but by manipulating a set of drilling parameters, this fixed amount of energy can be exploited optimally. Expressed in terms of MSE; input energy per removed volume of rock is small when penetration rate is large, thus the drilling process is efficient.

The drilling parameters used as input variables in the MSE-model are often available as real-time drilling data. This means that the model is suitable as a basis for a real-time efficiency monitoring model and –agent.

However, the model from 1965 does have some shortcomings in terms of real-time monitoring. Firstly, the model does not consider formation strength when evaluating drilling efficiency. That means that a constant optimal MSE will have natural fluctuations, which corresponds to formation hardness. If the operator is unaware of this, unnecessary, even counterproductive, measures could be taken to counteract these fluctuations.

Secondly, the original method treats the efficiency factor as a constant. The corrected method on the other hand is based on continuous calculations, accounting for a number of real-time factors such as well-path, hydraulic energy, wellbore-friction etc.

Thirdly, the model does not account for the hydraulic force exerted at the bit. It is common knowledge for drilling engineers that the flushing of drilling fluid through the bit nozzles creates a considerable force in front of the bit. The energy in this fluid flow is an important factor for ROP, both in terms of hole cleaning and tearing the formation apart.

Lastly, one of the prime variables in the model, torque, is not straightforward to use as input during real-time monitoring. Torque is a surface monitored variable, meaning that the torque experienced at the bit differs from the monitors on the rig. Due to friction and drag, the torque down-hole is less than the readings on top suggests.

Calculation of the actual efficiency factor plus neutralization of the formation hardness are suggested in this paper.

In retrospect, the MSE method proved to have some oddities, e.g. the unexpected insignificance of axial energy, and should have been tested to a larger extent before implementing it into the ADE-model and the agent. The decision of running with the MSE-model unconditionally was made due to its widespread use in other investigations and projects.

6.2 Applicability of the ADE-model

The improved method is named ADE, Actual Drilling Efficiency, and it is based on Teale's MSE-model and improved with the abovementioned extensions. It was developed to serve as a tool for real-time monitoring of drilling efficiency.

The model is more representative for the drilling efficiency since it incorporates formation hardness. UCS is the best source of formation strength evaluation, but it can also be approximated using density-, neutron- and GR-logs, as well as a penetration rate model. The latter was investigated in particular in this paper as it is in compatible with RTDD.

UCS of the formations that are to be drilled is preferable, but not always available. The same goes for the density-, neutron- and GR-model. As will be further addressed in section 6.3, the penetration rate equation proposed by Bourgoyne and Young (1986) was presumed to be an adequate solution to that lack of information.

Applicability to the actual drilling processes is also one strength of the ADE-model, as it takes into account the difference between recorded and actual magnitude of certain drilling parameters. The best example is the thorough model used for approximating loss of rotational energy due to friction and drag, but WOB is also adjusted with regard to hydraulic recoil from the bit. The model used for calculating loss along the drillstring due to friction was selected due to its compatibility with a real-time system. It proved to correlate well with assumptions common in the industry today, i.e. that loss is equal to a certain percentage of torque reading at section start.

Contribution to drilling progression by hydraulic energy has been investigated numerous times. The so-called HMSE-model implements the hydraulic term into the MSE-model.

The difference in HMSE and MSE is small in some cases, but it allows for a more accurate evaluation of the drilling process.

Since the model is customized for real-time monitoring, it is a proper fundament for a real-time drilling efficiency agent. The qualities and weaknesses of the agent developed in this thesis is described in the following sub-sections.

6.3 The functionality of the agent

Even though the agent is meant for real-time drilling data, at this stage it is only functional with historical drilling data, i.e. database files of fixed size. This is mainly due to lack of RTDD during development and testing of the agent. Further development is required in order for it to handle RTDD.

The ADE-agent functions well in terms on measuring drilling efficiency, when applied to the historical drilling data from well C-47 sections 17 ½", 12 ¼" and 8 ½". Other information required by the agent, e.g. DS-component specifications, are acquired from producer's websites and similar. There is some degree of uncertainty linked to the hydraulic specifications, as the manufacturer claimed it was classified. Therefore, some assumptions about nozzle angle and distance were made, based on common sense and previously conducted investigation. Regardless, these are constants, meaning that they will not interfere with the trends in the same way as a changing variable.

The current output of the agent is plots, which will allow the operator to evaluate the drilling progression based on drilling efficiency. Large readings imply inefficient drilling, but corresponding large readings on the hardness plot may contradict that.

Due to the technical structure of the agent, i.e. chronologically based matrix-set up, the operator can easily customize the plots produced as output by the agent in the script. This involves both parameters and length of the well sections. The current output are plots of torque-loss, inclination, MSE, TSE, ADE and hardness.

The agent has a shortcoming due to the hardness model. Since UCS was unavailable, as were density-, neutron- and GR-logs, formation hardness had to be quantified using a penetration rate equation, namely Eq. 12. Because both the equation and the ADE-model uses four of the same input variables, i.e. ROP, WOB, RPM and mud flow, the hardness plot correlates with ADE to a certain degree. This is natural, since ADE increases as hardness increases, but due to the similarities in variables, they are a bit more correlated than preferred.

Regarding the code itself, a source of error may be the if-statement considering drilling,

i.e. the statement meant for isolating data from drilling only. The statement should be waterproof, and little, if any, information is lost because of it. Should, however, some of the conditions in the statement be untrue, due to some discrepancies in the drilling data for example, then bits of drilling information could be lost and thus create an insufficient result. Discrepancies in the drilling data may very well occur, but the script takes several measures to ensure that these discrepancies do not interfere with the output.

6.4 Difficulties

The agent is primarily designed to cope with drilling data, and to produce a plot showing drilling efficiency vs. depth. It does so, without too much finesse. Due to MATLAB being such a sophisticated scientific programming tool, it is difficult to gain complete comprehension of all the possible commands and functions. A more streamlined script could perhaps be obtained using commands and functions that are more advanced.

The script has only been tested on the available data, i.e. the three sections from well 147. An attempt was made to gather data from a database online, but as it turned out, very few of the required parameters were available.

The vast amount of variables in the data files used during testing and development lead to some unexpected challenges. E.g. is the rotational parameter sometimes recorded at the surface as RPM, other times downhole as RPMB. Getting the script to check the presence of these variables automatically proved to be difficult, and has yet to be sorted out. For now, they have to be identified manually before the script can be run properly.

The drilling data generally had some discrepancies, which is what should be expected of drilling data.

There was also lack of a proper drill-off test. This was unfortunate, as some of the parameters required for the complete hardness method are made available through this type of testing. Since It was also considered to scale the hardness plot equal to the ADE-plot at optimal efficiency identified by the drill-off test. This was a possible way to present the data and see how the plots would differentiate over time against the optimal efficiency. It would also be interesting to evaluate this data against the estimated efficiency factor of the ADE method.

While the mathematical expression given for the hydraulic term appears to be well established, it is greatly dependant on specific input parameters that were not available to us. More specifically the length of potential core given as L, the distance from hole

bottom to the nozzle given as s, and nozzle angle given as θ. While there was available information on typical values for these parameters, we cannot conclude that the values used in our script were correct for this case, although we can assume they were not too far off to give an indication of the hydraulic energy. When testing our model on the data provided by Mohan et al. (2009), the output does match the results given in their paper, giving some indication to the degree of certainty.

6.5 Possible future extensions and development of the agent

Making the agent compatible with RTDD will have to be the main objective. It is the prime target for the agent, but could not be achieved due to none being available. The technical restructuring required for this to be possible is already tested in the script; in the part regarding drillstring friction. To summarize, it can be achieved by writing new lines for every new recording of data, i.e. every 4.5 seconds or so, and adding them to a matrix.

If a drill-off test is available, implementing a function defining a new-bit trendline would be profitable for future use. This trendline would be set on basis of the optimal drilling efficiency achieved during the drill-off test, and would have to be adjusted according to factors that would change optimal efficiency over time. While changes in formation hardness and increased loss due to increased depth is already included, the new bit-trendline should include some scalar to account for bit-dulling to increase accuracy.

The if-statement aiming to isolate data from drilling could perhaps be re-defined, but no acute change is necessary.

As mentioned previously, the agent is perhaps not as streamlined as preferred. Commands that are more sophisticated could replace some of the code in the script, rendering it easier to operate and customize. Information about DS-components could also be made easier to implement.

Another extension could be for the agent to automatically check which variables that are present, and then to execute a function depending on the result. E.g. if UCS is unavailable, the agent checks if sonic-, neutron- and GR-logs are available, which can then be used to calculated hardness. Such a solution was implemented for the variables of the current hardness method, but was not possible to implement for the UCS, as data were not available for testing.

To cope with discrepancies and anomalies in the drilling data, additional functions

could be implemented in the future extension. These functions would be the result of thorough testing because some discrepancies may be distinctive for every single well.

6.6 Future development of model

The outline of the improved model has been established. However, since the scope of this paper is limited by the range of a master thesis, there are still considerable improvements that need to be made.

Among the most important improvements is the compatibility with SI-units. Currently, most of the model is compatible with SI-units, however, the hydraulic term of the ADE-model requires field units. For now, this is solved by a conversion factor. However, using solely SI-units will make it easier to evaluate the contributions from each of the parameters and terms.

Although the need of static factors accounting for loss of energy have been reduces by the ADE-model, some of the static factors are still required for the model to function. These factors are subjects for possible future improvements. Whether or not they are correctly estimated and if they succeed in accounting for all the resulting losses can only be ascertained through extensive testing. E.g, should the actual bit efficiency factors be calculated using models with bit-dulling and bit-specifics as input variables, instead of a static factor of approximately 0.35.

One source of uncertainty lies in the calculation of strain in the drillstring. The strain will affect the side-forces in the drillstring, but it was difficult to determine to what extent with the available data.

The downhole vibrations should be subject to extensive testing in order to determine their impact.

The method used for calculating formation hardness, i.e. the model based on Eq. 12, is rather simple and some has some potential for improvement. However, as specified in section 3.1, the selected method for determining formation hardness is regarded as the third most preferred method. Nevertheless, since the preferred methods are often unavailable due to lack of information, a proper model for real-time estimation of formation hardness should be established.

Further work with this model should also focus on proper identification of sources of inefficiencies, as this was not thoroughly addressed in present thesis. This should be performed in accordance with the system presented in table 1, and be implemented

as a real-time evaluation for the mathematical agent when changes in parameters corresponds with those of a specific inefficiency. This could also be one of the more important additions to the current agent.

In present version of the agent and the model, torque is approximated from surface reading and a mathematical model for loss along the drillstring. A future development would be to read off torque directly from the bit, a sort of down-hole torque, and test the current method against downhole data.

There should also be looked further into the ratio between axial and rotational energy, to see if this correlation is correct for the current method. If not adjustments should be made accordingly.

Further work should also include proper testing, as the current method have only been implemented on three sections of one well.

7 Conclusion

The report deals with the efficiency of drilling processes and how to accurately determine and monitor this efficiency. This is done by evaluating the input energy versus the output drilling progress. It gives a presentation of current methods used for efficiency determination, and factors that typically influence drilling efficiency, among those, MSE, which is a good measure for the efficiency of a drilling process. Real-time monitoring of MSE, when applied, could increase drilling efficiency as it will give the operator an option to make the necessary adjustments needed in order to maintain an optimal penetration rate. Due to obvious discrepancies with the existing efficiency model, the MSE model, a potentially improved method, the ADE-model, was suggested.

Three extensions were introduced in order for the original MSE-model potentially to be more accurate, especially with regard to real-time data; contribution from hydraulic energy, effect from hardness of formation and more accurate estimation of the energy reaching the formation.

- The first extension, hardness of formation, transforms the method from just evaluating input energy, to evaluating drilling efficiency

  The original method did not consider this at all. A large MSE-value can in some cases be explained by hard formation being drilled, thus yielding a more reliable MSE-model. The well sections investigated in this report shows correlations between hardness and MSE readings

- The second extension, hydraulic energy, accounts for approximately 20 percent of total input energy

  This should have a considerable effect on the accuracy of progression for the drilling process

- The third extension, more accurate bit torque determination through well path modelling, makes a considerable impact

  The improved method yields a more accurate output for actual torque. In some intervals, the two methods differed with up to 100 percent in terms of drilling efficiency

- The MATLAB-agent is functional with historical drilling data, and serves as a proper tool for investigating the effects of the suggested extensions

- More thorough testing is required to determine to which extent the effects of the extensions of the ADE-model optimize the MSE-model

Due to lack of data, the extensions could only be tested on three well sections, all as historical drilling data, not RTDD

- Future work on the agent involves making it compatible with real-time data, which will allow for monitoring of ADE/MSE during drilling
- The axial energy-term accounts for approximately 1.5 percent of total energy

  The real contribution from axial forces should be investigated further

- Further work with this model should also focus on proper identification of sources of inefficiencies

8 Nomenclature

8.1 Abbreviations

ADE	Actual Drilling Efficiency
BEF	Bit Efficiency
BHA	Bottom Hole Assembly
BPOS	Block Position
DBTM	Measured Bit Depth
DMEA	Measured Hole Depth
DOC	Depth Of Cut
DP	Drillpipe
DS	Drillstring
ECD	Equivalent Circulation Density
EOW	End Of Well
GR	Gamma Ray
HMSE	Hydraulic Mechanical Specific Energy
IPT	Department of Petroleum Engineering and Applied Geophysics at NTNU
MD	Measured Depth
MFI	Mud Flow In
MSE	Mechanical Specific Energy
NAVO	Navigation Optimization
NTNU	Norwegian University of Science and Technology
PDC	Polycrystalline Diamond Compact
ROP	Rate Of Penetration
RPM	Revolutions Per Minute
RTDD	Real-Time Drilling Data
SMA	Simple Moving Average
SPP	Standpipe Pressure
TSE	Total Specific Energy
TVD	True Vertical Depth
UCS	Unconfined Compression Strength or Uniaxial Compression Strength
WOB	Weight On Bit

8.2 Variables

β	Buoyancy factor
$\Delta\phi$	Change in azimuth
$\Delta\theta$	Change in inclination
Δh	Vertical change per time
ΔP_b	Pressure loss over bit
η	Factor for hydraulic energy reduction
θ_j	Angle of axially symmetric jet
θ	Angle of inclination
$\bar{\theta}$	Average angle of inclination
μ	Friction factor
ρ_c	ECD
ρ_m	Density of mud
A	Cross-sectional area
A_b	Cross-sectional area of bit
a_i	Exponent drilling constants, i=1,...,8
A_v	Ratio between velocities through bit and annulus
B_{eff}	Bit efficiency factor
BPOS_{i}	Block position at current time element
$\text{BPOS}_{\text{i-1}}$	Block position at previous time element
C	Unit conversion factor
D	TVD
d_b	Bit diameter
d_n	Nozzle diameter
$E_{\text{axi,s}}$	Axial energy recorded on surface
$E_{\text{rot,s}}$	Rotational energy recorded on surface
$E_{\text{axi,c}}$	Axial energy, corrected
$E_{\text{rot,c}}$	Rotational energy, corrected
E_h	Hydraulic energy
f_i	Term in the penetration rate equation, i=1,...,8

F_j	Hydraulic jetting/impact force beneath bit
F_x	Axial force in current depth element
F_{x-1}	Axial force in previous depth element
g	Gravitational acceleration
g_p	Pore pressure gradient
h	Fractional tooth dullness of bit
k	Exponent of hydraulic energy reduction
K	Constant of proportionality, or drillability
L	Length of potential core
M_h	Hydraulic energy loss factor
M	Torque on bit
$\mathrm{MSE}_{\mathrm{eff}}$	Effective MSE
n	Number of terms or nozzles
N	RPM
N_f	Normal force
Q	Volumetric flow rate
r	Radius of drillstring
s	Distance between nozzles and formation
T	Torque
T_x	Torque at current depth element
T_{x-1}	Torque at previous depth element
v	Velocity
V_f	Velocity through annulus
V_n	Velocity through nozzles
W	WOB
W_{DS}	Weight of drillstring segment
W_{axi}	Axial work
w_{curve}	Weight of drillstring segment submerged in fluid
W_{hyd}	Hydraulic work
W_{rot}	Rotational work

W_x	Weight at current length element
W_{x-1}	Weight at previous depth element
$\mathrm{WOB_e}$	Effective axial force
$(W/d_b)_t$	Threshold bit weight at which the bit begins to drill

9 References

Abbott, A. 2014. Mechanical Specific Energy. Houston, Texas. Statoil DPNA UOF DW D& W

Ahmadi, K. and Altintas, Y. 2013. Stability of lateral, torsional and axial vibrations in drilling, International Journal of Machine Tools and Manufacture 68: 63-74, doi:ISSN 0890-6955

Amadi, W. K., and Iyalla, I. 2012. Application of Mechanical Specific Energy Techniques in Reducing Drilling Cost in Deepwater Development. Presented at SPE Deepwater Drilling and Completions Conference, Texas, 20-21 June. SPE-156370-MS. doi:10.2118/156370-MS

Berg, P. V. 2015. M.Sc.-student, NTNU. paalveb@stud.ntnu.no, 92660677

Boonsri, K. 2014. Torque Simulation in the Well Planning Process. Presented at IADC/SPE Asia Pacific Drilling Technology Conference, Bangkok, Thailand, 25-27 August. SPE-170500-MS. doi:10.2118/170500-MS

Bourgoyne, A. T., Chenevert, M. E., Millhem, K. K. and Young, F. S. 2003. Applied Drilling Engineering, 9th edition. Richardson, TX: Society of Petroleum Engineers

Bourgoyne, A.T. and Young, F.S. 1974. A Multiple Regression Approach to Optimal Drilling and Abnormal Pressure Detection. *SPE Journal* 14 (4): 371-384. SPE-4238-PA. http://dx.doi.org/10.2118/4238-PA

Bourgoyne, A.T., Chenevert, M.E. and Millheim, K.K. 1986. Applied Drilling Engineering. Richardson, TX: Society of Petroleum Engineers

Brechan, B. A. 2016. PhD, Department of Petroleum Engineering and Applied Geophysics (IPS), Norwegian University of Science and Technology. Personal comments. Bjorn.brechan@ntnu.no, 73 59 49 18

Crawford, M. B. 2001. Apparatus and Method for a Roller Bit Using Collimated Jets Sweeping Separate Bottom-hole Tracks. US Patent No. 09/406,250

DrillingFormulas. 2014. What You Need to Know about Drilling Bit Balling Up and How to Trouble Shoot it. (14 October 2014) http://www.drillingformulas.com/what-you-need-to-know-about-drilling-bit-balling-up-and-how-to-troubleshooting-it/ (Accessed 06 February 2016)

Dupriest, F. E. 2006. Comprehensive Drill Rate Management Process To Maximize

ROP. Presented at SPE Annual Technical Conference, San Antonio, 24-27 September. SPE-102210-MS. doi:10.2118/102210-MS

Dupriest, F. E., and Koederitz, W. L. 2005. Maximizing Drill Rates with Real-Time Surveillance of Mechanical Specific Energy. Presented at SPE/IADC Drilling Conference, Amsterdam, 23-25 February. SPE-92194-MS. doi:10.2118/92194-MS

Guerrero, C. 2007. Drilling Optimization with Mechanical Specific Energy. Slideshare. 6 October 2012, http://www.slideshare.net/francoiskdevos/2007-drilling-drlg-sym-optimizing-bit-performance (Accessed 01 february 2016)

Hamrick, T. R. 2011. Optimization of Operating Parameters for Minimum Mechanical Specific Energy in Drilling. Doctor of Philosophy. West Virginia University, Morgantown, West Virginia (2011)

Kjerkreit, K. 2015. Geologist, Statoil. Kkjer@statoil.com, 938 36 161

Krueger, R. E. et al. 2012. Mechanical Specific Energy Drilling System. US Patent No. 13/442,642

Mamat, N.S., Ismail, I., Hashim, S., et al. 2013. The performance of polymer beads in water-based mud and its application in high-temperature well. Springerlink.com, 25 May 2013, http://link.springer.com/article/10.1007/s13202-013-0059-9 (Accessed 15 February 2016)

Meng, C., Mengci, S. and Jinwen, Z. et al. 2014. Maximizing Drilling Performance With Real-Time Surveillance System Based on Parameters Optimization Algorithm. CSCanada Advances in Petroleum Exploration and Development. 8 (1): 15-24, doi: http://dx.doi.org/10.3968/5537

Mitchell, R. F. 2008. Drillstring Solutions Improve the Torque-Drag Model. Society of Petroleum Engineers. Presented at IADC/SPE Drilling Conference, Orlando, Florida, USA, 4-6 March. SPE-112623-MS doi:10.2118/112623-MS

Mohan, K., Adil, F., and Samuel, R. 2009. Tracking Drilling Efficiency Using Hydro-Mechanical Specific Energy. Presented at SPE/IADC Drilling Conference, Amsterdam, 17-19 March. SPE-119421-MS. doi:10.2118/119421-MS

Pessier, R. C., and Fear, M. J. 1992. Quantifying Common Drilling Problems With Mechanical Specific Energy and a Bit-Specific Coefficient of Sliding Friction. Presented at SPE Annual Technical Conference, Washington D.C, October 4-7. SPE-24584-MS. doi:10.2118/24584-MS

PetroleumSupport. 2015. Drilling Bit Performance Guide. (28 September 2015) http://petroleumsupport.com/drilling-bit-performance-guide/ (Accessed 06 February 2016)

Remmert, S. M., Witt, J. W., and Dupriest, F. E. 2007. Implementation of ROP Management Process in Qatar North Field. Journal of Petroleum Technology, SPE 59 (12). doi:10.2118/105521-MS

Sangesland, S. 2014. TPG4215 High Deviation Drilling. Lecure Handhout as PDF. https://files.itslearning.com (Local file access)

Skalle, P. 2014. Exercises in Pressure Control During Drilling, 4th edition, Norway: http://www.Bookboon.com

Skalle, P. 2015. Supervisor and Professor of Department of Petroleum Engineering and Applied Geophysics (IPT), Norwegian University of Science and Technology. Personal comments. pal.skalle@ntnu.no, 73 59 49 29/918 97 303

SLB Glossary. 2016. Unconfined Compression Strength. http://www.glossary.oilfield.slb.com/Terms/u/unconfined_ compressive_ strength.aspx (Accessed 29 March 2016)

SLB. 2010. Drillstring Vibrations and Vibration Modeling. (1 January 2010) https://www.slb.com/~/media/Files/drilling/brochures/drilling_ opt/drillstring_ vib_ br.pdf (Accessed 09 February 2016)

Shrivastava, S. K., Javed, A., Pratap, K. K. 2013. Assessing Rock Compressive Strength and Predicting Formation Drillability using Sonic, Gamma & Density Logs. Presented at 10th Biennial International Conference & Exposition, Le Meridian, 23 November. http://www.spgindia.org/10_ biennial_ form/P412.pdf

Somerton, W.H., Esfandiari, F. and Singhal, A. 1969. Further Studies of the Relation of Physical Properties of Rock to Rock Drillability. Drilling and Rock Mechanics Symposium, Austin, 14-15 January. SPE-2390-MS. http://dx.doi.org/10.2118/2390-MS

Spaar, J. R., Ledgerwood, L. W., Goodman, H., Graff, R. L., & Moo, T. J. 1995. Formation Compressive Strength Estimates for Predicting Drillability and PDC Bit Selection. SPE/IADC Drilling Conference, 28 February-2 March, Amsterdam, SPE-29397-MS. doi:10.2118/29397-MS

Swahn, I. 2015. Co-supervisor and PhD Candidate, Department of Petroleum Engineering and Applied Geophysics (IPT), Norwegian University of Science and Technology. Personal comments. isak.m.swahn@ntnu.no, 454 84 506

Teale, R. 1965. The concept of specific energy in rock drilling. International Journal of Rock Mechanics and Mining Sciences & Geomechanics, Abstracts 2 (1): 57-73. doi: ISSN 0148-9062

Toverud, T. 2016. Dr.Ing. Personal comments. ttoveru@hotmail.com

Warren, T. M. 1987. Penetration Rate Performance of Roller Cone Bits. SPE Drilling Engineering, 2 (1): 9-18. doi:10.2118/13259-PA

Appendices

While trying to keep the report as short and consistent as possible, some information was considered too important to exclude completely. The following pages is therefore included as it might be of interest to the reader.

Appendix A Penetration rate equation

Appendix B Additional figures

Appendix C Well information and bit specifics

Appendix D The MATLAB-code

A Penetration rate equation

The terms and constants of the penetration rate equation by Bourgoyne and Young (1974).

$$f_1 = K = e^{2.303a_1} \tag{52}$$

The first term, f_1, predominantly represents the effects the formation strength and bit type has on the ROP. Also accounted for are other parameters, such as mud type and solids content.

$$f_2 = e^{2.303a_2(10{,}000-D)} \tag{53}$$

f_2 takes into account the increase in rock strength due to compaction as a function of depth, D [ft].

$$f_3 = e^{2.303a_3 D^{0.69}(g_p-9.0)} \tag{54}$$

The third term models under-compaction in formations with abnormal pressure. The variable g_p [lbm/gal] is the pore pressure gradient.

$$f_4 = e^{2.303a_3 D^{0.69}(g_p-\rho_c)} \tag{55}$$

Accounts for the effect of overbalance on ROP. The variable ρ_c [lbm/gal] is the Equivalent Circulation Density (ECD).

$$f_5 = \left[\frac{\left(\frac{W}{d_b}\right) - \left(\frac{W}{d_b}\right)_t}{4 - \left(\frac{W}{d_b}\right)_t}\right]^{a_5} \tag{56}$$

Models the effect of WOB. W [1,000 lbf] is the WOB, d_b [in] is the bit diameter and $(W/d_b)_t$ [1,000 lbf/in] is the threshold bit weight at which the bit begins to drill. It is often quite small, and is negligible in areas with soft formations. A drill-off test can determine the threshold value for more competent formations (Bourgoyne et al. 1986). Ignoring this term is possible as it is presumably insignificant in comparison to WOB.

The number 4, i.e. 4,000 lbf/in, is a reference value, when the f_5 term equals 1.

$$f_6 = \left(\frac{N}{60}\right)^{a_6} \tag{57}$$

Models the effect of rotary speed. N [min^{-1}] is the rotary speed, while 60 rpm is a reference value at which the f_6 term equals 1.

$$f_7 = e^{-a_7 h} \tag{58}$$

Accounts for the effects of tooth wear. The variable h is the fractional tooth dullness.

$$f_8 = \left(\frac{F_j}{1,000}\right)^{a_8} \tag{59}$$

Accounts for effect of bit hydraulics. The variable F_j [lbf] is hydraulic impact force beneath the bit. 1,000 lbf is a reference value.

The constants a_1 through a_8: By applying a multiple regression technique these constants can be computed using previously obtained drilling data from the same area (Buorgoyne and Young 1974).

The upper and lower recommended values for the drilling constants are presented in table A.1 (Buorgoyne et al. 2003).

Table A.1: Lower and upper values for the drilling constants in the Bourgoyne and Young penetration rate equation.

Constant	Lower limit	Upper limit
a_1	0.5	1.9
a_2	0.000001	0.0005
a_3	0.000001	0.0009
a_4	0.000001	0.0001
a_5	0.5	2.0
a_6	0.4	1.0
a_7	0.3	1.5
a_8	0.3	0.6

B Additional figures

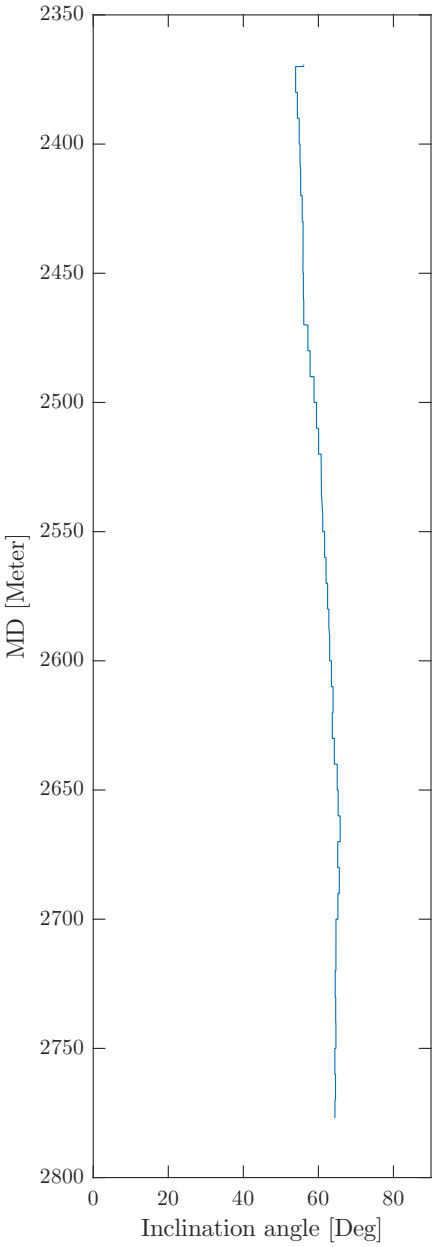

Figure B.1: Inclination angle vs. depth in the 12 $^1/_4$"-section.

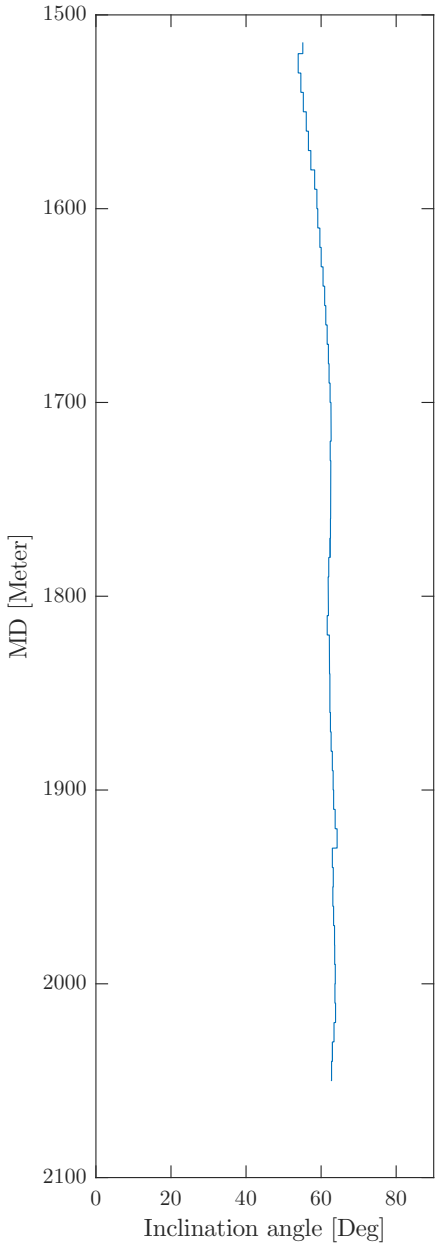

Figure B.2: Inclination angle vs. depth in the 17 $^1/_2$"-section.

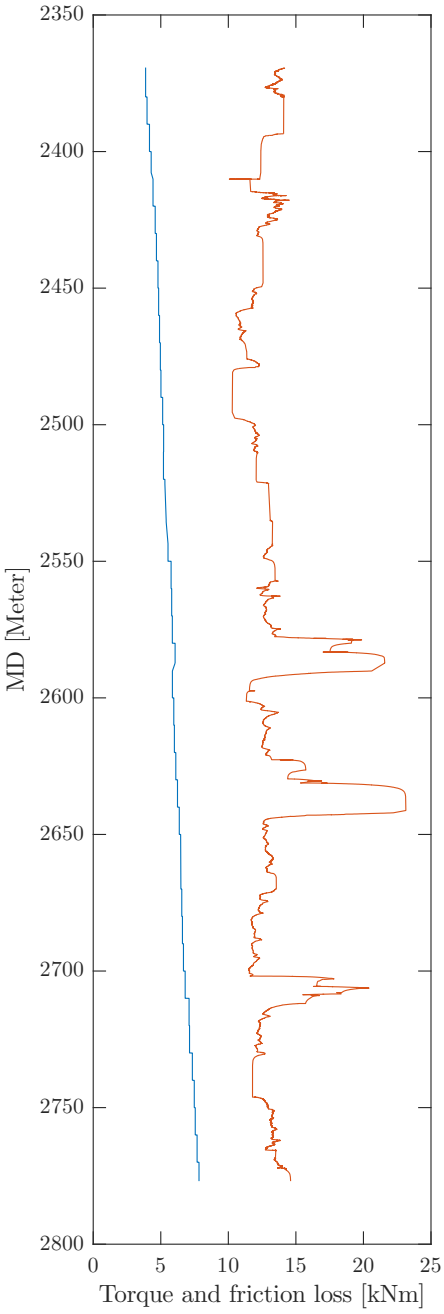

Figure B.3: Torque measured at surface (red) and estimated friction loss (blue) vs. depth in the 12 $^1/_4$"-section.

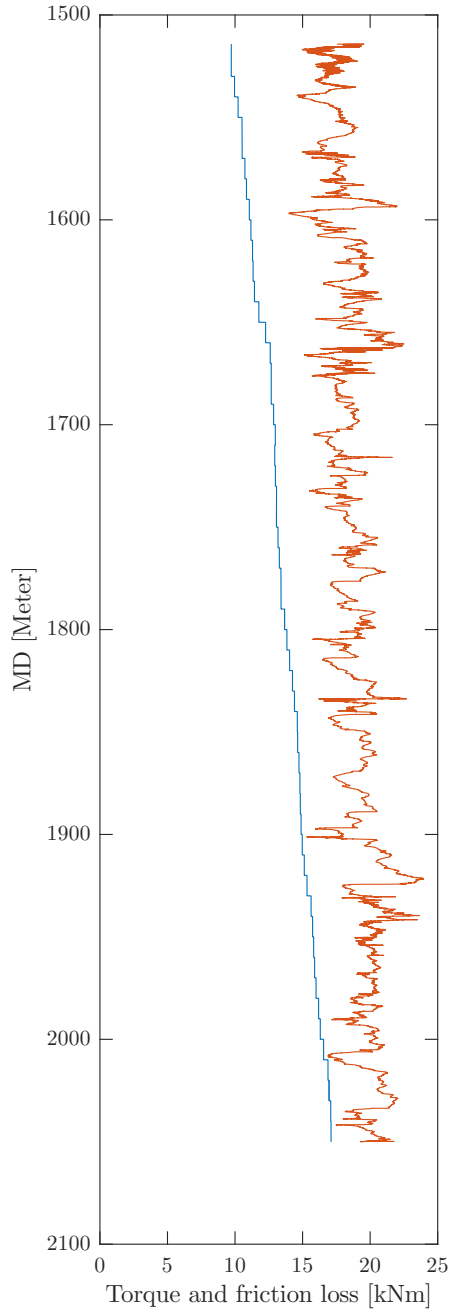

Figure B.4: Torque measured at surface (red) and estimated friction loss (blue) vs. depth in the 17 $^1/_2$"-section.

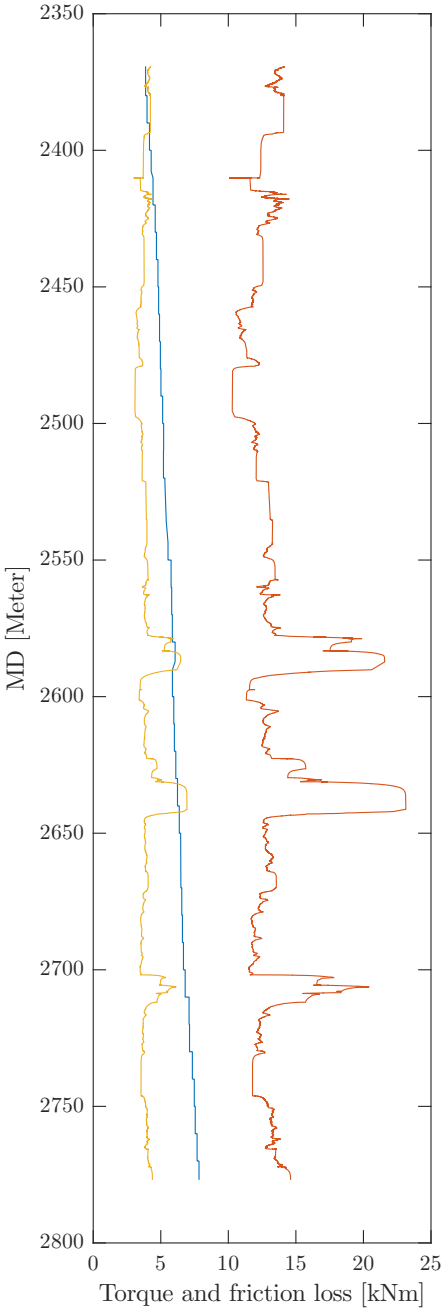

Figure B.5: Torque measured at surface (red), approximated friction loss from original formula (yellow) and estimated friction loss (blue) vs. depth in the 12 $^1/_4$"-section.

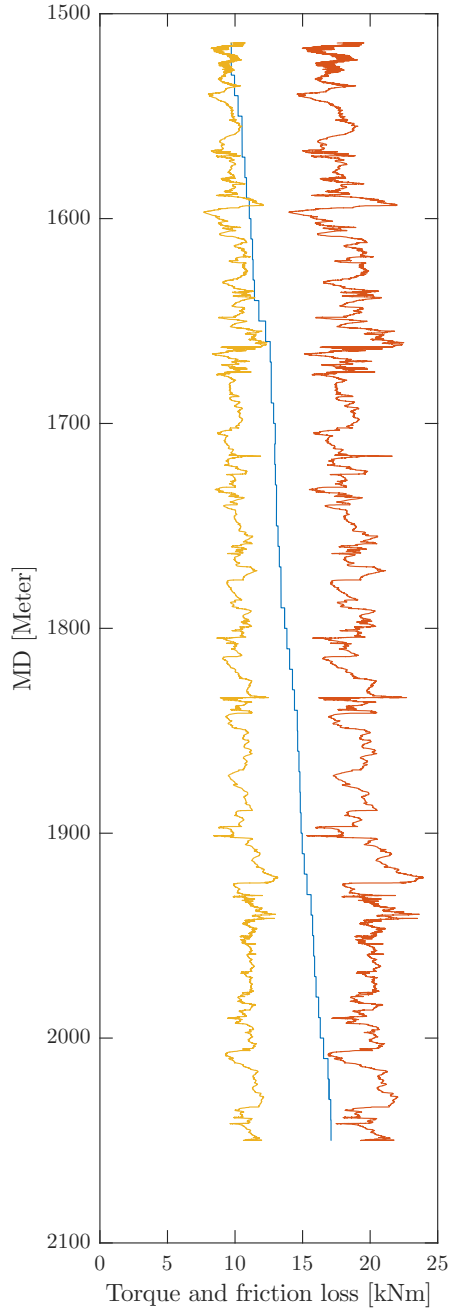

Figure B.6: Torque measured at surface (red), approximated friction loss from original formula (yellow) and estimated friction loss (blue) vs. depth in the 17 $^1/_2$"-section.

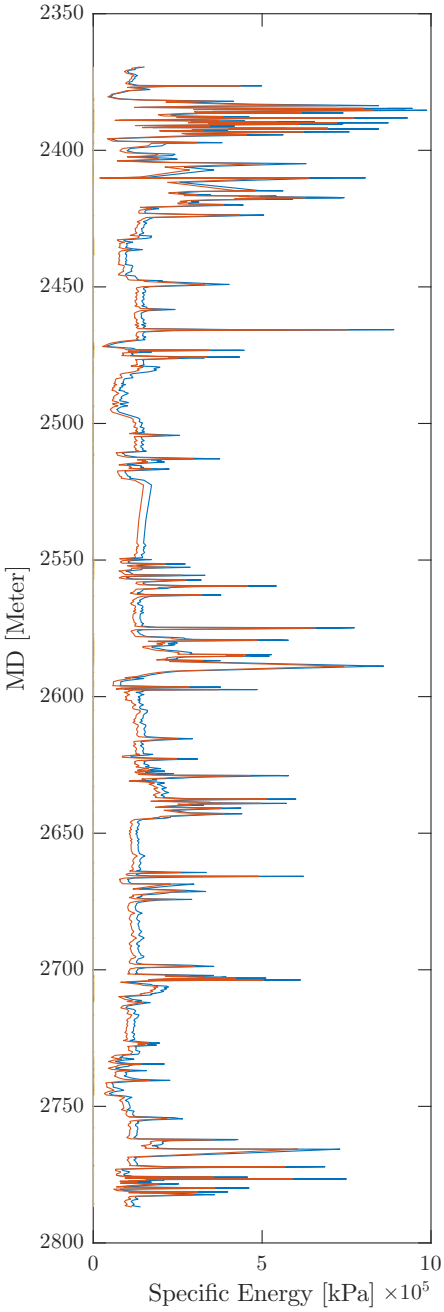

Figure B.7: Specific Energy vs. depth in the 12 $^1/_4$"-section. Axial Energy (yellow), Axial and Rotational (red) and Axial, Rotational and Hydraulic (TSE) (blue).

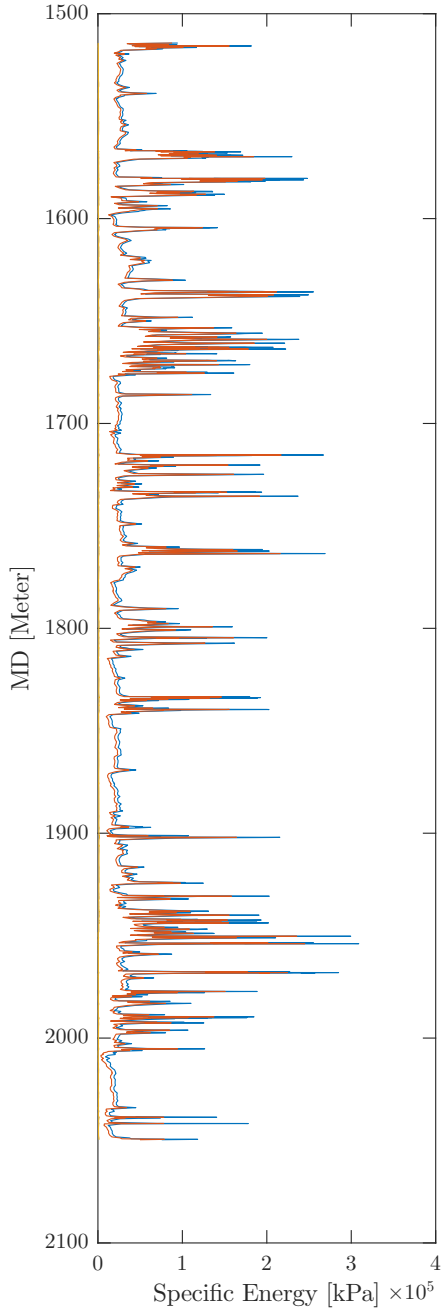

Figure B.8: Specific Energy vs. depth in the 17 $^1/_2$"-section. Axial Energy (yellow), Axial and Rotational (red) and Axial, Rotational and Hydraulic (TSE) (blue).

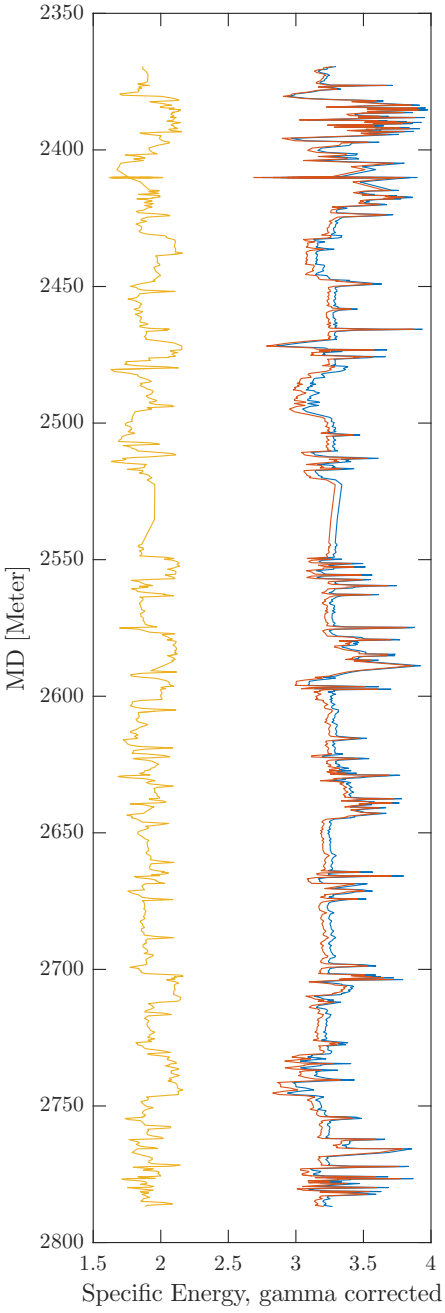

Figure B.9: Specific Energy vs. depth in the 12 $^1/_4$"-section, adjusted with gamma correction.

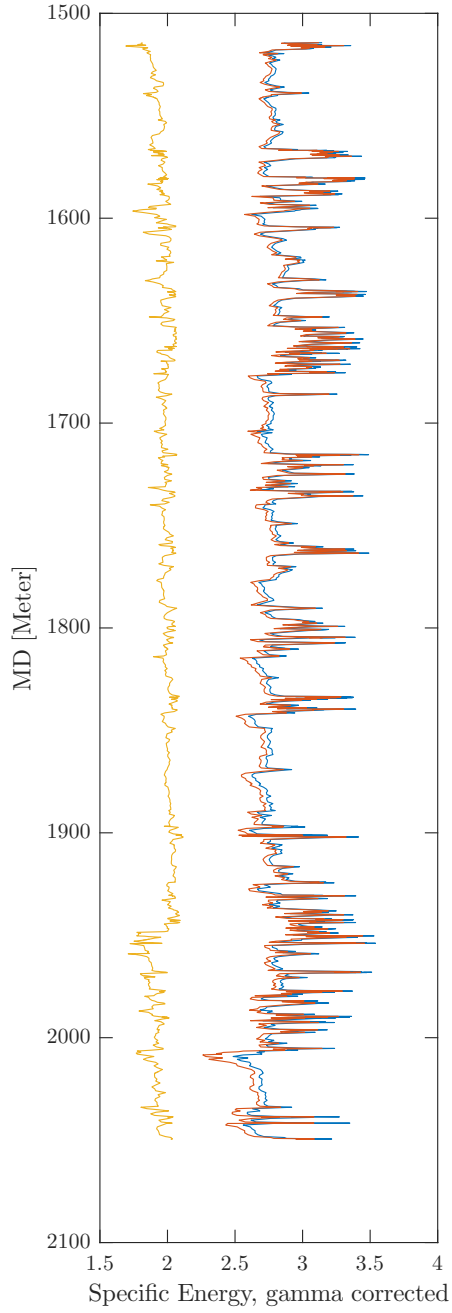

Figure B.10: Specific Energy vs. depth in the 17 $^1/_2$"-section, adjusted with gamma correction.

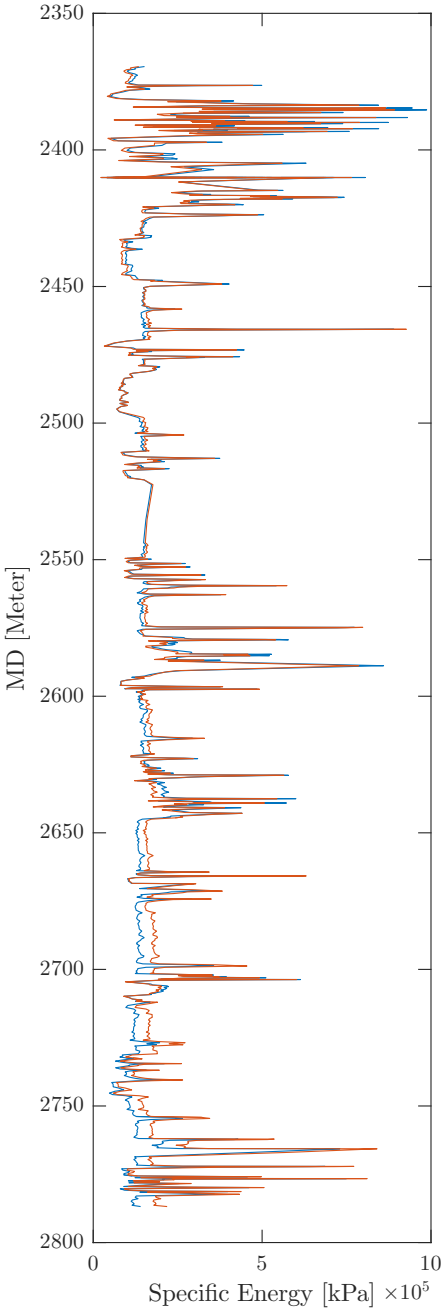

Figure B.11: Total Specific Energy (blue) and Mechanical Specific Energy (red) vs. depth in the 12 $^1/_4$"-section.

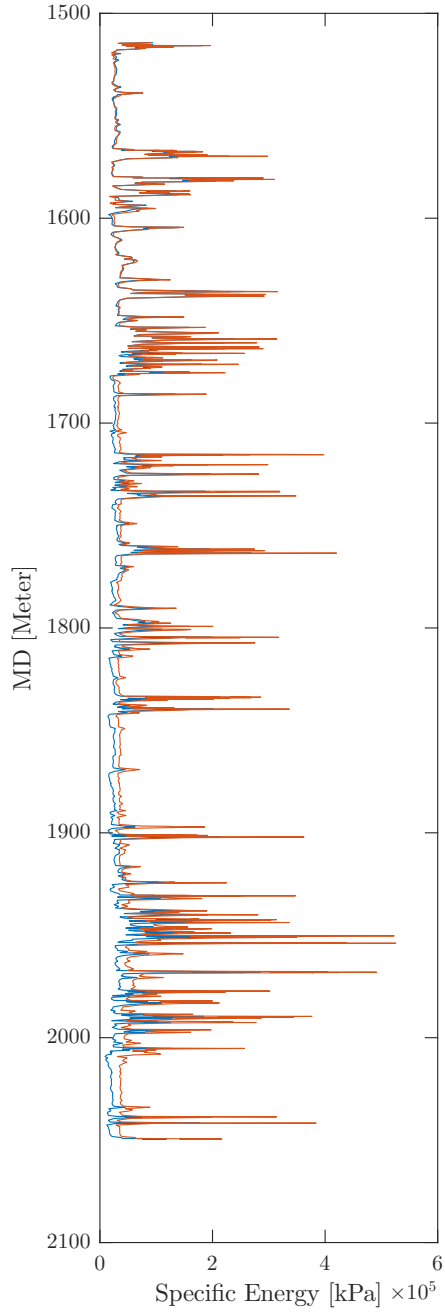

Figure B.12: Total Specific Energy (blue) and Mechanical Specific Energy (red) vs. depth in the 17 $^1/_2$"-section.

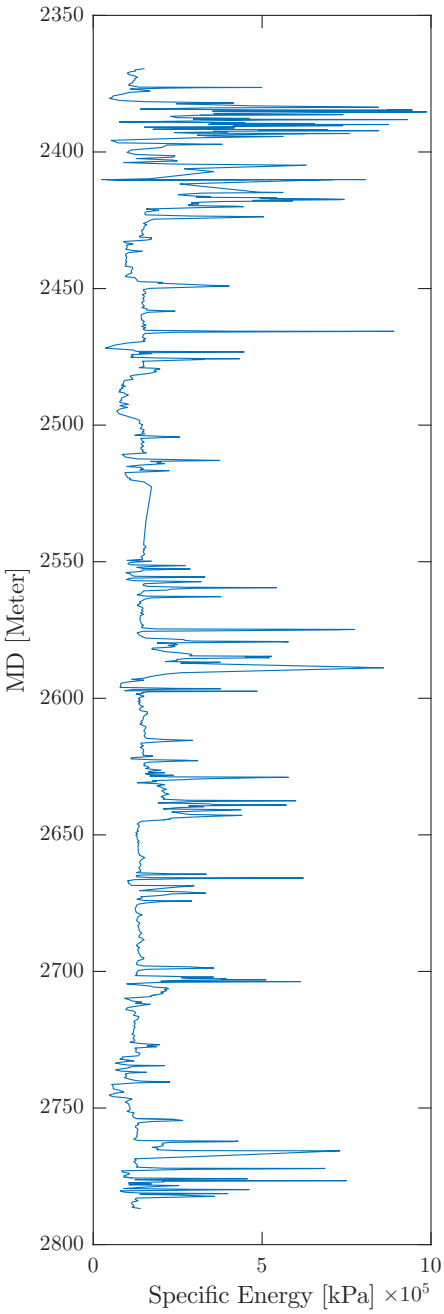

Figure B.13: Total Specific Energy vs. depth in the 12 $^1/_4$"-section.

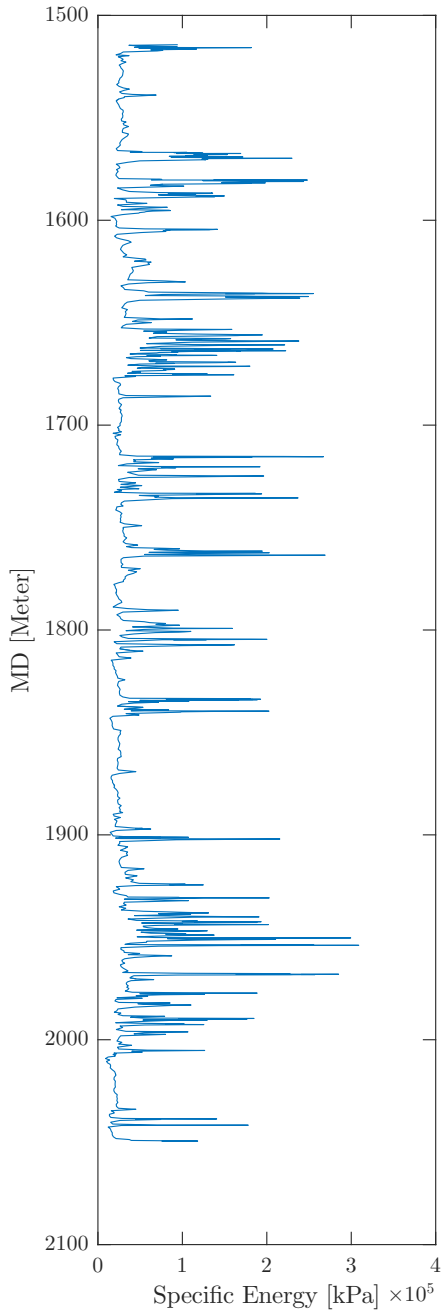

Figure B.14: Total Specific Energy vs. depth in the 17 $^1/_2$"-section.

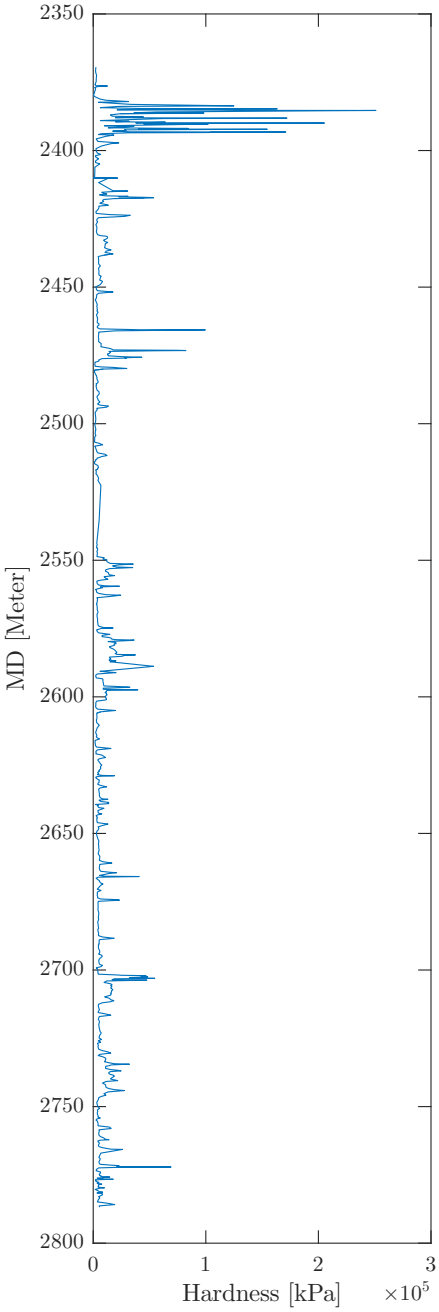

Figure B.15: Formation Hardness vs. depth in the 12 $^1/_4$"-section.

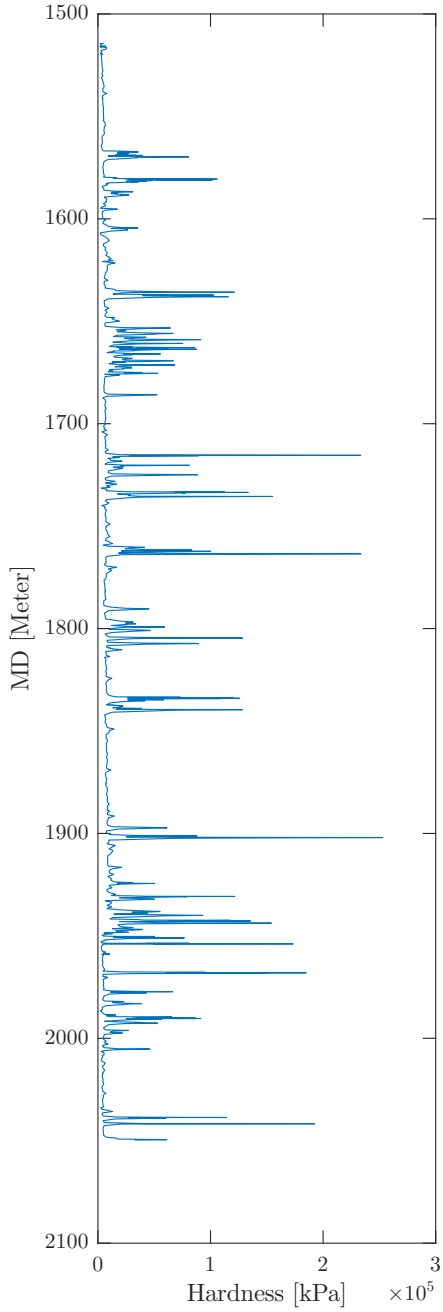

Figure B.16: Formation Hardness vs. depth in the 17 $^1/_2$"-section.

C Well information and bit specifics

Table C.1: Well trajectory, and bit and BHA specifics of section 17 $^1/_2$".

Well trajectory		
MD @ start	1508	m
MD @ end	2379	m
ΔMD	871	m
TVD @ start	1303	m
TVD @ end	1724	m
ΔTVD	421	m
Inlination @ start	60.6	°
Inclination @ end	60.6	°
ΔInclination	0	°
Azimuth @ start	134.5	°
Azimuth @ end	100	°
ΔAzimuth	-34.5	°
Bit and BHA specifics		
Number of nozzles	4	
Average nozzle diameter	21.75/32	in
Potential core length	105	in
Distance from nozzles to well bottom	8	in
Angle of axially symmetric jet	3	°
Length of BHA	192	m
Weight of BHA	22803	kg
Buoyancy factor (*)	0.8342	

(*) Buoyancy factor is 1-weight of mud/weight of steel, where weight of steel is 7840 kg/m^3.

Table C.2: Well trajectory, and bit and BHA specifics of section 12 $^1/_4$".

Well trajectory		
MD @ start	2379	m
MD @ end	2787	m
ΔMD	408	m
TVD @ start	1724	m
TVD @ end	1907	m
ΔTVD	183	m
Inlination @ start	60.6	°
Inclination @ end	63	°
ΔInclination	2.4	°
Azimuth @ start	100	°
Azimuth @ end	104.4	°
ΔAzimuth	4.4	°
Bit and BHA specifics		
Number of nozzles	3	
Average nozzle diameter	14.66/32	in
Potential core length	61.25	in
Distance from nozzles to well bottom	6	in
Angle of axially symmetric jet	3	°
Length of BHA	144	m
Weight of BHA	10919	kg
Buoyancy factor	0.7704	

Table C.3: Well trajectory, and bit and BHA specifics of section 8 $^1/_2$".

Well trajectory		
MD @ start	2787	m
MD @ end	4399	m
ΔMD	1612	m
TVD @ start	1907	m
TVD @ end	2104	m
ΔTVD	197	m
Inlination @ start	63	°
Inclination @ end	93	°
ΔInclination	30	°
Azimuth @ start	104,4	°
Azimuth @ end	179	°
ΔAzimuth	74,6	°
Bit and BHA specifics		
Number of nozzles	3	
Average nozzle diameter	20.66/32	in
Potential core length	42.5	in
Distance from nozzles to well bottom	4	in
Angle of axially symmetric jet	3	°
Length of BHA	128	m
Weight of BHA	8641	kg
Buoyancy factor	0.7832	

D MATLAB-code for 'Agent for determining ADE'

The MATLAB-code used with historical drilling data to determine ADE. Data from the 17 ½"-section are shown in this particular example. The code for the other sections are in general identical with exeption for the input variables, e.g. the drilling data and the bit specifics.

```
%% *MSE - Detecting MSE and hardness of formation*
%
% By:   Paal Vegar Berg, paalveb@stud.ntnu.no
%       ?yvind S?ther Tveit, oyvinst@stud.ntnu.no
% V:    2016-05-10
%
%--------------------------------------------------------------------------%
%% Load data
clear
format shortG

% Load data set
load 17-5.mat

%% Size of data set
Size = length( X.Time );

%% Create empty matrix, A
A = zeros( Size,20 );

%% Fill cells of A with values of variables
A(:,1) = X.Time;
A(:,2) = X.DMEA;

% New variable, X.DBTM_2 [m]; min value of bit depth and total
% depth, to prevent X.DBTM > X.DMEA
X.DBTM_2 = min( X.DMEA, X.DBTM );
A(:,3) = X.DBTM_2;

% New variable, dbit [m]; Difference in height between Bit Depth and
% Total Measured Depth (TMD)
A(:,4) = A(:,2)-A(:,3);

% Column 5: Value of RPM from either surface (RPM) or downhole (RPMB)
A(:,5) = max( X.RPM, X.RPMB );
A(:,6) = X.MFI;
A(:,7) = X.BPOS;
A(:,8) = X.TRQ;
A(:,9) = X.WOB;
A(:,10) = X.DVER;
A(:,12) = X.ECDB;
A(:,15) = X.SPP;
A(:,14) = X.ROP;

% Sorting matrix A chronologically
B = sortrows(A);

% Preventing DMEA(i+1) to be less than DMEA(i)
for i= 2:Size
```

```
    if B(i,2) < B(i-1,2)
        B(i,2) = B(i-1,2);
    end
end

% Preventing DVER(i+1) to be less than DVER(i)
for i= 2:Size
    if B(i,10) < B(i-1,10)
        B(i,10) = B(i-1,10);
    end
end

% Block velocity as sub for ROP
for i= 2:Size
    B(i,11) = -(B(i,7) - B(i-1,7))./((B(i,1) - B(i-1,1)) * 24);
    if B(i,11) > 60
        B(i,11) = 60;
    end
end

% Moving average Bvel / ROP
for i= 10:Size
    B(i,13) = sum(B(i-9:i,11))/10;
end

% Average for Bvel / ROP element 1:9
for i= 10:18
    B(i-9,13) = B(10,13);
end

% Eliminating negative values of TRQ
for i= 2:Size
    if B(i,8) < 0
        B(i,8) = 0;
    end
end

% Create new matrix C for drilling only
Size2=0;
for i= 1:Size
    if B(i,4) < 0.2 && B(i,5) > 25 && B(i,9) > 1 && B(i,6) > 500 ...
            && B(i,11) >= 0 && B(i,13) > 0.1
        Size2=Size2+1;
    end
end

C1 = zeros( Size2,36 );

% Defines area of interest
% 17-5 section:
st=1;               % TVD = 1311    MD = 1500
fi=28250;           % TVD = 1570    MD = 2050
fi2=5649;           % ^ for avg 3
fi3=2400;           % 1500-1700 MD
fi4=1130;           % 1500-1700 MD for 2. gj.snitt
fi5=1050;

% Removing other activities than drilling
k=1;
for i= 1:Size
    if B(i,4) < 0.2 && B(i,5) > 25 && B(i,9) > 1 && B(i,6) > 500 ...
```

```
                && B(i,11) >= 0 && B(i,13) > 0.1
            C1(k,1) = B(i,1);                   % Time
            C1(k,2) = B(i,2);                   % DMEA
            C1(k,3) = B(i,3);                   % DBTM
            C1(k,4) = B(i,4);                   % dbit
            C1(k,5) = B(i,5);                   % RPM
            C1(k,6) = B(i,6);                   % MFI
            C1(k,7) = B(i,7);                   % BPOS
            C1(k,8) = B(i,8);                   % TRQ
            C1(k,9) = B(i,9);                   % WOB
            C1(k,10) = B(i,10);                 % DVER
            C1(k,11) = B(i,11);                 % Bvel / ROP
            C1(k,12) = 0;                       % Bvel / ROP mov avg
            C1(k,13) = 0;                       % HMSE
            C1(k,14) = 0;                       % HMSE mov avg
            C1(k,15) = 0;                       % HMSE relative
            C1(k,16) = 0;                       % Drillability
            C1(k,17) = 0;                       % Hardness
            C1(k,18) = 0;                       % Drillability mov avg
            C1(k,19) = 0;                       % Hardness relative
            C1(k,20) = 0.94 + 0.4*...
             ((C1(k,10)-C1(st,10))/...
             (C1(fi,10)-C1(st,10)));            % Pore pressure
            C1(k,21) = B(i,12);                 % ECD
            C1(k,22) = 0;                       % f2
            C1(k,23) = 0;                       % f3
            C1(k,24) = 0;                       % f4
            C1(k,25) = 0;                       % f5
            C1(k,26) = 0;                       % f6
            C1(k,27) = 0;                       % f7
            C1(k,28) = 0;                       % f8
            C1(k,29) = 0;                       % Inc angle
            C1(k,30) = 0;                       % Loss of torque along DS
            C1(k,31) = B(i,15);                 % SPP
            C1(k,32) = 0;                       % MSE
            C1(k,33) = 0;                       % MSE mov avg
            C1(k,34) = B(i,14);                 % recorded ROP
            C1(k,35) = 0;                       % MSE aksiell
            C1(k,36) = 0;                       % MSE aksiell mov avg
            k=k+1;
        end
    end

    SizeC = Size2-1850;
    % Removing elements recorded during drilling of cement, i.e. 1:1850
    C = zeros( SizeC,40 );
    for i= 1:SizeC
        C(i,1:36) = C1(1849+i,1:36);
    end

    % Moving average Bvel / ROP
    for i= 10:SizeC
        C(i,12) = sum(C(i-9:i,11))/10;
    end

    % Average for Bvel / ROP element 1:9
    C(1:9,12) = C(10,12);

    % Moving average TRQ
    for i= 10:SizeC
        C(i,8) = sum(C(i-9:i,8))/10;
```

```
end

% Average for TRQ element 1:9
C(1:9,8) = C(10,8);

% ROP =/= 0
for i= 2:SizeC
    if C(i,12) == 0
        C(i,12) = C(i-1,12);
    end
end

% Moving average SPP
for i= 30:SizeC
    C(i,31) = sum(C(i-29:i,31))/30;
end

% Average for SPP element 1:9
C(1:29,31) = C(30,31);

%% Torque loss along drillstring
% Values from EoW report and DS specs
% Buoyancy
mw = 1300; % mud weight: 1.3 sg
sw = 7840; % steel weight
b = 1-mw/sw;
% BHA
l_BHA = 192; % meter
% DC
l_DC_8 = 53; % meter
l_DC_9 = 16; % meter
wpl_DC_8 = 148.01 * 1.488; % lb/ft -> kg/m
wpl_DC_9 = 214.41 * 1.488; % lb/ft -> kg/m
                    % from http://workstringsinternational.com/ ...
                    % equipment/spec_sheets/hwdp/
r_DC = 9 * 0.0254 / 2; % radius of DC, meter
% HWDP
l_HWDP = l_BHA - l_DC_8 - l_DC_9; % HWDP + tools + crossover
wpl_HWDP = 57.69 * 1.488; % from workstringsint...
r_HWDP = 8.5 * 0.0254 / 2; % radius of HWDPTJ, meter
% DP
l_DP = 0; % length of DP tbd
wpl_DP = 27.7 * 1.488 * b * 10 / 1000; % lb/ft -> 1000kg/10m + buoyancy
r_DP = 8.5 * 0.0254 / 2; % radius of DPTJ, meter
% tot weight BHA
w_BHA = b*(wpl_DC_8 * l_DC_8 + wpl_DC_9 * l_DC_9 + wpl_HWDP * l_HWDP);
% friction factors
f_ch = 0.16; % cased hole, metal on metal: 0.16
f_oh = 0.2; % open hole, metal on rock: 0.2 - 0.3

L_BHA = floor(l_BHA/10);
L = 0;
wpl_BHA = (w_BHA / L_BHA) / 1000; % 1000kg/10m

Casingl = C(1,2);   % min depth = casing depth, i.e. first element in C
CasingL = floor(Casingl/10); % convert to 10 m segments
% Approximated inclination out of casing
IncCasing = acosd((C(440,10)-C(1,10))/(C(440,2)-C(1,2)));
%Approximated dogleg-angle in casing
DL = IncCasing/CasingL;
g = 9.81; % Acceleration of gravity
```

```
TM = zeros(CasingL,6); % Matrix with values from cased hole torque

% Calculating torque for DP and BHA in casing
% Torque for 10m DP in casing
for i = 1:floor(CasingL/2)
    TM(i,1) = wpl_DP;  % Constant
    TM(i,2) = wpl_BHA; % Approximated constant by us
    TM(i,3) = 0; % Inc
    TM(i,4) = 0; % Inc
    TM(i,5) = 0; % Azimuth NA
    TM(i,6) = 0; % Azimuth NA
end
m = 0;
for i = ceil(CasingL/2):CasingL
    TM(i,1) = wpl_DP;
    TM(i,2) = wpl_BHA;
    TM(i,3) = m*DL; % Inc
    TM(i,4) = sum(TM(i-20:i,3))/20; % Inc
    TM(i,5) = 0; % Azimuth NA
    TM(i,6) = 0; % Azimuth NA
    m = m + 2;
end

C(1,29) = TM(CasingL,4);
%C(1,30) = sum(TM(1:(CasingL-L_BHA),1))+sum(TM((CasingL-L_BHA):CasingL,2));
% Calculating torque for DP and DC in open hole
RD = CasingL;    % Reached Depth / 10m
m = 0;
mm = 1;
NL = [wpl_DP wpl_BHA 0 0 0 0]; % New line in matrix
                    % Weight DP, Weight BHA, inc, azi, avg inc, avg azi
% Torque in open hole
for i = 2:SizeC
    if floor(C(i,2)/10) > RD
        RD = floor((C(i,2)/10));
        NL(1,3) = acosd((C(i,10)-C(i-m,10))/(C(i,2)-C(i-m,2)));
        if NL(1,3) == 90
           NL(1,3) = TM(RD-1,3);
        end
        NL(1,4) = (sum(TM(RD-19:RD-1,3))+NL(1,3))/20;  %  Moving Average
        NL(1,5) = 0; % Azimuth data N/A
        NL(1,6) = (sum(TM(RD-19:RD-1,5))+NL(1,5))/20;  %  Moving Average
        C(i,29) = NL(1,4);
        TM = [TM; NL];
        % Torque at given depth is calculated
        Fnew = -g * C(i,9); % F1 = WOB 1
        Mnew = 0; % M1 = Torque 1
        for j = 2:RD
            dAzi =(TM(RD+2-j,6)-TM(RD+1-j,6))*pi/180;  %Radians
            sAzi =(TM(RD+2-j,6)+TM(RD+1-j,6))/2;
            dInc =(TM(RD+2-j,4)-TM(RD+1-j,4))*pi/180;  %Radians
            sInc =(TM(RD+2-j,4)+TM(RD+1-j,4))/2;
            if j <= L_BHA
                Fnew = Fnew+g*TM(RD+2-j,2)*cos(sInc); % Using w and r of DC
                Nnew = sqrt((Fnew*dAzi*sin(sInc))^2 ...
                    +(g*TM(RD+2-j,2)*sin(sInc)+Fnew*dInc)^2);
                if RD+1-j > CasingL
                    Mnew = Mnew+f_oh*r_DC*Nnew;  % Friction of Open Hole
                else
                    Mnew = Mnew+f_ch*r_DC*Nnew;  % Friction of Cased Hole
```

```
                end
            else
                Fnew = Fnew+g*TM(RD+2-j,1)*cos(sInc); % Using w and r of DP
                Nnew = sqrt((Fnew*dAzi*sin(sInc))^2 ...
                    +(g*TM(RD+2-j,2)*sin(sInc)+Fnew*dInc)^2);
                if RD+1-j > CasingL
                    Mnew = Mnew+f_oh*r_DP*Nnew;  % Friction of Open Hole
                else
                    Mnew = Mnew+f_ch*r_DP*Nnew; % Friction of Cased Hole
                end
            end
        end
        C(i,30) = Mnew;
        m = 0;
    else
        if RD == CasingL
            mm = mm+1;
        end
        m = m+1;
        C(i,30) = C(i-1,30);
        C(i,29) = C(i-1,29);
    end
end

% Avoid 0 torque loss for the first points plotted.
C(1:mm,30) = C(mm+1,30);

%% MSE
bita = (X.BDIA(1)*0.0254)^2;
pb = 0.5; % Fraction of pressure loss over bit
nn = 4; % Number of nozzles
dn = 21.75/32; % avg nozzle diameter
Av = 0.15*X.BDIA(1)^2/(nn*dn^2); % Area of escape vs. area of nozzles
S = 8; % Distance from nozzles to bottom of hole
lpc = 6*X.BDIA(1); % Potential core length
theta = 3; % Angle of axially symmetric jet
M = (dn+2*lpc*tand(theta/2))/(dn+S*tand(theta/2));
K = 0.122; % Warren, 1987 <- Source
eta = (1-Av^(-K))/M^2;
CP = 6895; % psi to Pa
cpr = 14.5; % bar to psi
ltg = 0.2642; % lpm to gpm
mtf = 1/0.3048; % meter to ft
itf = 0.006944; % sq inch to sq ft
ktp = 0.008345; % kg/m3 to ppg
na = pi*nn*dn^2/4; % nozzle-area
mts = 60; % min to s
Ltm = 1/1000; % L to m3
gpm = 264.17; % gal per m3
q = 1; % q = Q, i.e. C(i,6)
Ltf = 0.035315/60; % lpm to ft3/s
Fj = 0.000516*(mw*ktp)*(q*ltg)*(q*Ltf)/(na*itf);
ltN = 0.004448; % lbf to kN
bef = 0.35; % bit efficiency
Ctot = CP/1000*1154*eta*pb*4/pi*ltg*cpr/mtf;

% Total Specific Energy
for i=1:SizeC
    C(i,13) = ... % Aksiell, WOB [kN] and eta*Fj [lbf]*[kN/lbf]
         (C(i,9)*g-eta*ltN*Fj*(C(i,6)^2))/bita + ...
        ... % Tangentiell
```

```
        bef*(120*pi*C(i,5)*(C(i,8)-C(i,30)))/(bita*C(i,12)) + ...
        ... % Hydraulic
        Ctot*(C(i,6)*C(i,31)/ ...
        ((X.BDIA(1)^2)*C(i,12))) ;
    % [kPa]
end

% MSE
for i=1:SizeC
    C(i,37) = bef * ...
        ... % Aksiell
        ( C(i,9)*g/bita + ...
        ... % Tangentiell
        (120*pi*C(i,5)*(C(i,8)*0.45))/(bita*C(i,12)));
    % [kPa]
end

% Rotational and Axial
for i=1:SizeC
    C(i,32) = ...
        ... % Aksiell
        ( (C(i,9)*g-eta*ltN*Fj*(C(i,6)^2))/bita + ...
        ... % Tangentiell
        bef*(120*pi*C(i,5)*(C(i,8)-C(i,30)))/(bita*C(i,12)));
    % [kPa]
end

% Axial
for i=1:SizeC
    C(i,35) =  (C(i,9)*g-eta*ltN*Fj*(C(i,6)^2))/bita; % aksiell
    % [kPa]
end

% Dampen spikes
meanhmse = 2.5*mean(C(1:28250,13));
meanmse = 2.5*mean(C(1:28250,32));
meanmsea = 2.5*mean(C(1:28250,35));
meanmseb = 2.5*mean(C(1:28250,37));

    % HMSE
for i= 1:SizeC
   if C(i,13) > meanhmse
       C(i,13) = (1/4)*(C(i,13) - meanhmse) + meanhmse;
   end
end

    % MSE
for i= 1:SizeC
   if C(i,32) > meanmse
       C(i,32) = (1/4)*(C(i,32) - meanmse) + meanmse;
   end
end

    % MSE axial
for i= 1:SizeC
   if C(i,35) > meanmsea
       C(i,35) = (1/4)*(C(i,35) - meanmsea) + meanmsea;
   end
end

    % MSE axial
```

```
for i= 1:SizeC
   if C(i,37) > meanmseb
       C(i,37) = (1/4)*(C(i,37) - meanmseb) + meanmseb;
   end
end

% Moving average
for i= 10:SizeC
    C(i,14) = sum(C(i-9:i,13))/10;
    C(i,33) = sum(C(i-9:i,32))/10;
    C(i,36) = sum(C(i-9:i,35))/10;
    C(i,38) = sum(C(i-9:i,37))/10;
end

% Average for element 1:9
C(1:9,14) = C(10,14);
C(1:9,33) = C(10,33);
C(1:9,36) = C(10,36);
C(1:9,38) = C(10,38);

% Min value of HMSE to determine ratio of MSE to optimal
HMSEmin = min( C(1:SizeC,14) );

% MSE in range of 0 to 1 where 1 is largest, i.e. relative HMSE
C(:,15) = C(:,14)/HMSEmin;

for i=1:SizeC
    if C(i,15) < 0
        C(i,15) = 0;
    end
end

%% Hardness detection
% Input for constants a(2,5,6)
a2 = 0.00001;    % 0.00001
a3 = 0.00009;    % 0.00009
a4 = 0.000001;   % 0.00001
a5 = 1.25;       % 1.25
a6 = 0.7;        % 0.7
a8 = 0.5;        % 0.5

% Conversion factors for SI to Field
cl = 1/0.3048;   % m to ft
cw = 2.2046;     % kg to lb
cp = 8.3454;     % kg/L to lb/gal

% Drillability, K
for i= 1:SizeC
    C(i,22) = exp(2.303*a2*cl*C(i,10));                          % f2
    C(i,23) = exp(2.303*a3*(cl*C(i,10))^0.69*(C(i,20)));         % f3
    C(i,24) = exp(2.303*a4*cl*C(i,10)*cp*(C(i,20)-C(i,21)));     % f4
    C(i,25) = (cw*C(i,9))^a5;                                    % f5
    C(i,26) = (C(i,5))^a6;                                       % f6
    C(i,28) = (C(i,6)^2*Fj)^a8;                                  % f8

    C(i,16) = C(i,12)/ ...
              (C(i,22)*C(i,23)*C(i,24)*C(i,25)*C(i,26)*C(i,28));
end

% Dampen spikes
meanK = 8*mean(C(1:28250,16));
```

```
for i= 1:SizeC
   if C(i,16) > meanK
       C(i,16) = (1/4)*(C(i,16) - meanK) + meanK;
   end
end

% Moving average drillability
for i= 10:SizeC
    C(i,18) = sum(C(i-9:i,16))/10;
end

% Average for K element 1:9
for i= 10:18
    C(i-9,18) = C(10,18);
end

% Hardness = 1/Drillability
for i= 1:SizeC
    C(i,17) = 1/C(i,18);
end

% Show hardness as portion of Hmax Kvalitativt f?rst og fremst
Havg = mean( C(:,18) );

% Detect spikes
[num] = max(C(:,4));
[r,c] = ind2sub(size(C),find(C==num));

% Hardness in range of 0 to 1 where 1 is hardest formation
C(:,19) = C(:,18)/Havg;

%% Kj?yr gj.snitt (av 5) for MSE og hardness
Size3 = floor(SizeC/5);
C2 = zeros(Size3,7);
j=1;

for i= 5:5:SizeC
        C2(j,1) = sum(C(i-4:i,2))/5;      % DMEA av
        C2(j,2) = sum(C(i-4:i,14))/5;     % Total m.a + avg
        C2(j,3) = sum(C(i-4:i,17))/5;     % Hardness m.a + avg
        C2(j,4) = sum(C(i-4:i,12))/5;     % ROP m.a + avg
        C2(j,5) = sum(C(i-4:i,33))/5;     % Rot+Axi m.a. + avg
        C2(j,6) = sum(C(i-4:i,36))/5;     % Aksiell m.a. + avg
        C2(j,7) = sum(C(i-4:i,38))/5;     %
        j=j+1;
end

%% Kj?yr gj.snitt igjen (av 5) for MSE og hardness
Size4 = floor(Size3/5);
C3 = zeros(Size4,7);
j=1;

for i= 5:5:Size3
        C3(j,1) = sum(C2(i-4:i,1))/5; % DMEA
        C3(j,2) = sum(C2(i-4:i,2))/5; % Total m.a + av
        C3(j,3) = sum(C2(i-4:i,3))/5; % Hardness m.a + av
        C3(j,4) = sum(C2(i-4:i,4))/5; % ROP m.a + av
        C3(j,5) = sum(C2(i-4:i,5))/5; % Rot+Axi m.a + av
        C3(j,6) = sum(C2(i-4:i,6))/5; % Aksiell m.a + av
        C3(j,7) = sum(C2(i-4:i,7))/5;
```

```
        j=j+1;
end

%% Matrix D shows a selection of data from C
D = C3(st:fi5,1:7);

%% Plot Hardness vs. MD (Fig. A16)
figure(1);
% Select plotted data
x1 = D(:,3);
y1 = D(:,1);
plot(x1,y1)

set(gca,...
'Units','normalized',...
'FontUnits','points',...
'FontWeight','normal',...
'FontSize',10)

% Format axes
%title('Hardness vs. MD');
ax = gca;

% X
xlabel('Hardness [kPa]');
%ax.XLim = [0 200000];

% Y
ylabel('MD [Meter]');
set(gca,'Ydir','reverse')
%ax.YLim = [1850 1900];

% Position on screen
hFig = figure(1);
set(hFig, 'OuterPosition', [610 20 300 1000]);
```